1965

Ultimate shear strength tests of full-sized prestressed concrete beams

H. Brecht

J. M. Hanson

C. L. Hulsbos

LEHIGH UNIVERSITY INSTITUTE OF RESEARCH

Prestressed Concrete Bridge Members
Progress Report No. 28

ULTIMATE SHEAR TESTS OF FULL-SIZED PRESTRESSED CONCRETE BEAMS

by
Howard E. Brecht
John M. Hanson
C. L. Hulsbos

Fritz Engineering Laboratory Report No. 223.28

PRESTRESSED CONCRETE BRIDGE MEMBERS

PROGRESS REPORT NO. 28

ULTIMATE SHEAR TESTS
OF
FULL-SIZED PRESTRESSED CONCRETE BEAMS

Howard E. Brecht

John M. Hanson

C. L. Hulsbos

Part of an Investigation Sponsored by:

PENNSYLVANIA DEPARTMENT OF HIGHWAYS
U. S. DEPARTMENT OF COMMERCE
BUREAU OF PUBLIC ROADS
REINFORCED CONCRETE RESEARCH COUNCIL

Fritz Engineering Laboratory
Department of Civil Engineering
Lehigh University
Bethlehem, Pennsylvania

December 1965

Fritz Engineering Laboratory Report No. 223.28

TABLE OF CONTENTS

1. INTRODUCTION

1.1 BACKGROUND AND PREVIOUS INVESTIGATIONS

The investigation of the strength and behavior of prestressed concrete bridge girders at Lehigh University began in 1951, when full-sized pretensioned and post-tensioned concrete beams were tested under simulated highway traffic.[1,2] This investigation was extended to develop fundamental information about prestressed concrete beams in the following three areas:

1. Bond characteristics of seven-wire prestressing strand
2. Fatigue resistance of strand and concrete
3. Ultimate strength under combined moment and shear.

The study of bond resulted in the establishment of criteria for assuring safety against bond failure when 7/16-in. diameter or smaller sized strand is used for prestressing.[3,4]

Investigations of the fatigue resistance of 7/16-in. diameter strand and concrete under a varying stress gradient resulted in the development of procedures for predicting the flexural fatigue life of prestressed beams.[5,6,7,8,9] Currently work is underway, by VanHorn and others, on the bond and fatigue characteristics of the ½-in. diameter strand.

The ultimate strength of prestressed concrete beams under combined moment and shear was first studied by Walther.[10] Walther and Warner[11] then tested 20 beams without web reinforcement, designated as the A and B Series, to study the behavior and mode of failure of beams with different amounts of prestress force. Further investigations of prestressed beams without web reinforcement were continued by McClarnon, Wakabayashi and Ekberg.[12] Their tests on 28 C and D Series beams were used to study the effect on shear strength of length of overhang at the reaction, existing inclined cracks, and loading through diaphragms.

Hanson and Hulsbos[13,14,15,16,17] extended the Lehigh research on ultimate strength under combined moment and shear to prestressed beams with web reinforcement. Sixteen E Series beams were tested statically

to study the overload behavior of the specimens. Two E Series beams were subjected to repeated loading which showed that an overload causing inclined diagonal tension cracking may cause a beam to be more critical in fatigue of the web reinforcement than in fatigue of the prestressing strand.

Thirty-eight tests were conducted on 23 I-beams, designated as the F Series, to evaluate the static ultimate shear strength of prestressed beams with vertical stirrups. All of the beams were doubly symmetric with a depth of 18-in., a flange width of 9-in., and a web width of 3-in. Concentrated loads were applied in 36 of the tests, in which the principal variables were amount of web reinforcement and length of shear span. Shear failures occurred in all but one test. The percentage of web reinforcement, based on the web width, ranged from 0.08 to 0.73 percent, and the shear span to effective depth ratios ranged from 2.12 to 7.76. Two beams, both with a percentage of web reinforcement equal to 0.13 percent, were subjected to uniform loads. These beams were loaded on span length to effective depth ratios of 10.6 and 14.8, and shear failures occurred in both tests.

Inclined cracking was classified as either diagonal tension or flexure shear. Diagonal tension cracking occurred in tests on shear span to effective depth (a/d) ratios less than approximately 4.5, and started from an interior point in the web due to high principal tensile stresses. Flexure shear cracking occurred in tests on a/d ratios greater than approximately 4.5, and was due to flexural cracking which either turned and became inclined in the direction of increasing moment or precipitated inclined cracking in the web above the flexural crack. In the concentrated load tests, the shear causing diagonal tension cracking was closely predicted as the shear causing a principal tensile stress of $(8 - 0.78\ a/d)\ \sqrt{f'_c}$ at the center of gravity of the section at the midpoint of the shear span. Flexure shear cracking was closely predicted as the shear causing a tensile stress in the bottom fibers of $9.5\sqrt{f'_c}$ at a distance $[a + 31.6 - 15.6(a/d) + 0.88(a/d)^2]$ in inches from the support.

In the uniform load tests, the shear causing inclined cracking at any section a distance x from the support was closely predicted as the least shear causing either a principal tensile stress of $(8 - 0.78\ x/d)\sqrt{f'_c}$ at the center of gravity of the section at x minus d/2, or a tensile stress in the extreme fibers in tension of $9.5\sqrt{f'_c}$ at x minus d.

Web crushing, stirrup fracture, and shear compression failures were observed in the tests on the F Series beams. Web crushing failures occurred in 14 tests, generally on the shorter a/d ratios. Fracture of the stirrups occurred in 15 tests, and shear compression failures occurred in 8 tests. Most of the web crushing failure started near the junction of the web and the compression flange. The shear compression failures generally occurred in a second test on a beam. The behavior of some of the beams subjected to concentrated loads was adversely affected when less than 0.15 percent web reinforcement was provided in the shear span.

It was determined that the ultimate shear strength of the E and F Series beams could be closely predicted as the sum of the shear causing significant inclined cracking plus the shear carried by the stirrups which were crossed by an idealized inclined crack. This idealized inclined crack was assumed to have an effective horizontal projection equal to the distance from the extreme fiber in compression to the lowest level at which the web reinforcement was effective. The stirrups crossed by the inclined crack were assumed stressed to their yield point.

Investigations of ultimate shear strength of prestressed concrete beams have also been carried out at other universities and research organizations. Several of these are listed in References 15 and 16. Particularly notable work which relates directly to this investigation was carried out at the University of Illinois and Portland Cement Association Research and Development Laboratories. Zwoyer and Siess[18] and Sozen, Zwoyer, and Siess[19] have reported the results of tests on 99 pretensioned beams having both rectangular and I-shaped cross-sections. Hernandez[20] conducted 37 tests on similarly shaped beams with web reinforcement, and MacGregor[21] continued this work by testing an additional 50 beams and analyzing the combined results of the 87 tests.

Principal variables in these tests were the amount, type, and spacing of the web reinforcement, and the profile of the longitudinal reinforcement. This latter variable was the subject of a paper by MacGregor, Sozen and Siess.[22] Recommendations for design of web reinforcement based on these tests were made by Hernandez, Sozen and Siess.[23] Mattock and Kaar[24] have reported the results of 14 tests on continuous composite pretensioned beams which were 1/2 scale models of AASHO-PCI Type III bridge girders. Their test program investigated the influence on ultimate shear strength of amount of vertical web reinforcement and location of the applied loads.

1.1.1 Specification for Design of Web Reinforcement

Based on research cited in the preceding section, it was recommended[16] that the following specification be used for the design of web reinforcement in prestressed concrete bridge girders:

> The area of web reinforcement placed perpendicular to the axis of the member at any section shall not be less than
>
> $$A_v = \frac{(V_u - \phi V_c)s}{f_y d} \qquad (1)$$
>
> nor less than
>
> $$A_v = \frac{\lambda V_u s}{f_y d} \qquad (2)$$
>
> nor more than
>
> $$A_v = \frac{7 b' s \sqrt{f'_c}}{f_y} \qquad (3)$$
>
> The shear, V_c, at inclined cracking shall be taken as the lesser of V_{cd} and V_{cf}. V_{cd} is the shear causing a principal tensile stress of f_t at the center of gravity of the cross-section resisting the live load. If the center of gravity is not in the web, f_t shall be computed at the intersection of the web and the flange. V_{cf} is the shear

causing a flexural tensile stress of f_r in the extreme fiber in tension at a distance in the direction of decreasing moment from the section under consideration equal to the effective depth of the member.

Web reinforcement shall not be spaced further apart than $d_s/2$, or 24 inches, whichever is smaller, and shall be anchored in both the tension and compression flanges of the member.

Web reinforcement between the support and the section a distance equal to the effective depth of the member from the support shall be the same as that required at that section.

Notation

A_v	=	cross-sectional area of one stirrup placed perpendicular to the longitudinal axis of the member
b'	=	width of web
d	=	distance from the extreme fiber in compression to the center of gravity of the prestressing steel, i.e., the effective depth of the member
d_s	=	distance from the extreme fiber in compression (in composite sections from the top of the girder alone) to the lowest level at which the stirrups are effective.
f'_c	=	ultimate compressive strength of concrete
f_t	=	$(6+0.6\frac{x}{d})\sqrt{f'_c}$, but not less than $2\sqrt{f'_c}$
f_r	=	$8\sqrt{f'_c}$
f_y	=	yield point of the web reinforcement, but not larger than 60,000 psi
s	=	spacing of stirrups
V_c	=	inclined cracking shear
V_{cd}	=	dead plus live load shear at inclined cracking caused by excessive principal tensile stress in the web
V_{cf}	=	dead plus live load shear at inclined cracking caused by flexural cracking
V_u	=	ultimate shear
x	=	distance from the section under consideration to the closest support
λ	=	0.15 for beams with single webs and 0.2 for beams with double webs

The ultimate shear strength of a prestressed concrete beam may be predicted from Eq. 1 by solving for V_u:

$$V_u = V_c + A_v f_y d_s / s \qquad (4)$$

Equation 4 has been used, without regard to the limitations on amount and spacing of the web reinforcement, to predict the ultimate shear strength of the Lehigh and Illinois test beams with web reinforcement which failed in shear. Figure 1 shows a comparison of the test to predicted ratios of shear strength of beams subjected to concentrated loads with the a/d ratio. There is good correlation between the Lehigh and Illinois tests, even though the average concrete strength of the Illinois tests is approximately 3500 psi, compared to an average concrete strength of approximately 6500 psi for the Lehigh tests.

The average test to predicted ratio of all of the tests represented in Fig. 1 is 1.21. It is greater than 1 because of the conservative calculation of the inclined cracking shear. The test to predicted ratios of shear strength are least in the neighborhood of an a/d ratio of 4, and increase with both increasing and decreasing values of a/d. The increase for the shorter shear spans, where diagonal tension inclined cracking occurs, reflects the increase in strength due to the closeness of the load point and the support. It would be difficult to take this added strength into account, and to do so is undesirable because the shear strength for short shear spans is greatly influenced by bond and anchorage conditions in the end of the beam. The increase for the longer shear spans, where flexure shear inclined cracking occurs, is due in part to the assumption that the critical flexural crack occurs at a distance equal to the effective depth of the member from the critical section which is adjacent to the load point, rather than at an increasing distance from the load point with increasing a/d ratio. It would also be undesirable to take this added strength into account, because the restraint on the flexure shear crack by the load point would be lost if the load point were a moving load.

1.2 OBJECT AND SCOPE

The objective of this investigation was to compare the behavior and shear strength of full-sized prestressed concrete bridge girders, selected from standard Pennsylvania Department of Highways cross-sections,[25] with the behavior and shear strength of the smaller Lehigh E and F Series I-beams which were described in Section 1.1. In particular, the investigation was intended to determine whether or not the recommended specification would predict the ultimate shear strength of full-sized bridge girders.

Precast prestressed concrete bridge girders currently used in Pennsylvania have either I or box-shaped cross-sections. The I-beams range in depth from 30 to 60-in. and are generally used at spacings ranging from 4.5 to 7.5-ft. They are designed compositely with a deck slab having an effective thickness of approximately 7-in. The box beams are either 36 or 48-in. wide and range in depth from 17 to 42-in. They are either placed adjacent to each other, in which case a composite slab or a bituminous surface course is placed on top of the beams, or they are used at spacings which commonly range from 7 to 9-ft, in which case they are designed compositely with a deck slab having an effective thickness of approximately 7-in.

Two I-beams and two box beams were tested in this investigation. Details of the beams are similar to their bridge girder counterparts, except for the amount of web reinforcement. The section selected for both I-beams is nominally described as an 18/36 I-beam, indicating that the width of the tension flange and the depth of the beam are 18 and 36-in., respectively. The section selected for both box beams is nominally described as a 36 x 36 box beam, indicating that the overall depth and width are 36-in. The prestressing strand in all 4 beams were straight throughout the length of the member. Concrete strength of all 4 beams ranged between 6600 and 8000 psi.

A total of 9 ultimate strength tests were conducted on shear span to effective depth ratios ranging from 2.92 to 5.84. There were 6 shear failures, 2 flexural failures, and one premature failure due to damage sustained from a prior test.

The behavior of the beams during testing is analyzed in this report, with particular emphasis placed on the loads causing flexural and inclined cracking and the modes of failure of the beams. The shear strength of the beams is compared to the shear strength predicted from Eq. (4). Information is presented on inclined crack widths. In addition, a study of the influence of type of cylinder mold and type of compaction on the ultimate compressive strength and the splitting tensile strength of the concrete is included.

2. TEST SPECIMENS

2.1 DESCRIPTION

The G Series test specimens were comprised of two 47-ft and two 29-ft pretensioned prestressed concrete bridge beams. One beam of each length had a 36-in. square box-shaped cross-section, and the other had a 36-in. deep I-shaped cross-section. These beams were fabricated in accordance with standards of the Pennsylvania Department of Highways,[25] except for the amount of vertical web reinforcement, which was less than normally required. Details of the beams are shown in Figs. 2 and 3.

The total length of each beam consisted of a test span and two anchorage regions of one foot length at each end. The test span was divided into three equal length regions, designated A, B, or C, in which different amounts of vertical web reinforcement were provided. Size and spacing of web reinforcement in the different regions are given in Fig. 2. The amount of vertical web reinforcement may be compared by the ratio $rf_y/100$.

The properties of the gross concrete cross-section are tabulated in Fig. 3. These properties are based on the nominal cross-sectional dimensions, and were used in all calculations. External dimensions of the beams were measured before testing. The width and depth of the I-beams were consistently 1/8 to 1/4-in. greater than the nominal dimension, and the strands were approximately 1/8 to 3/16-in. high. The width of the box beams was consistently 1/4-in. less than the nominal dimension at the top, and within 1/8-in. of the nominal dimension at the bottom. The depth of the box beams ranged from 36 to 36.5-in., and the strands were approximately 1/4-in. high and 1/4-in. laterally eccentric.

Internal dimension of the box beams were measured after testing. The box beams were broken open, generally at the failure section, and the cardboard void form removed. The web thickness varied by as much as 7/8-in. from the nominal dimension of 5-in., but the total thick-

ness at any cross-section was always close to 10-in. The thickness of the compression flange ranged between 2.5 and 3.25-in. Internal diaphragms and end blocks were bulged out approximately 2-in.

Prestress was provided by straight prestressing elements of 7/16-in. diameter 270 ksi strands. Sixteen strands were used in the I-beams, and twenty-six strands were used in the box beams, resulting in longitudinal reinforcement ratios of 0.46 and 0.52 percent, respectively. Each strand was pretensioned to a nominal initial force of 21.7 kips, providing a total design prestress force of 347.2 kips for the I-beams and 564.2 kips for the box beams. Assuming losses of 5 percent in the prestress force at release, the stress in the top and bottom fibers is 550 psi tension and 1840 psi compression, respectively, in the I-beams, and 550 psi tension and 2170 psi compression, respectively, in the box beams. The prestressing elements in both the I-beams and box beams were located such that if the member would fail in flexure, the strain in the strand would be greater than 1 percent and the neutral axis would lie in the compression flange.

2.2 MATERIALS

2.2.1 Concrete

The concrete was supplied by Schuylkill Products, Inc., Cressona, Pennsylvania. The mix contained 8.5 bags per cu yd of Type III cement manufactured by the Lone Star Cement Corporation. Proportions by weight of the cement to sand to coarse aggregate were 1 to 1.15 to 2.4. The sand was obtained by the supplier from the Refractory Sand Company, Andreas, Pennsylvania, and the coarse aggregate, which was crushed limestone, from Berks' Products, Reading, Pennsylvania. Coarse aggregate was obtained from two stockpiles of material; one was classified as aggregate 1-B, and the other as aggregate 2-B. Aggregate 1-B was graded to ½-in. maximum size, and aggregate 2-B was graded to 3/4-in. maximum size. These two aggregates were combined in the ratio 1 to 1.5, respectively. Gradation curves of the sand, both coarse aggregates, and the combined material are shown in Fig. 4. The fineness modulus of the sand was 2.8.

Slump for all of the mixes ranged between one and two inches. Plastiment was added to delay the setting of the concrete for a maximum period of 1 hr. The percentage of entrained air in the mix ranged from 4.5 to 7.2 percent.

Forty-two 6- by 12-in. standard cylinders were taken from the concrete used in each beam. Cardboard and metal molds were used to form the cylinders. Metal molds were either steel or cast iron. The cardboard molds were obtained from the Philadelphia Container Company and were constructed with 5/64-in. waxed cardboard walls and 33 gage metal bottoms. Three cardboard and 3 metal cylinders from each beam were rodded, and all others were internally vibrated with a 7/8-in. diameter 12,000 vpm vibrator.

Cylinder tests were conducted to determine the ultimate compressive strength of the concrete, f'_c, at the time of release of the prestress force and also at the time of test. Strains were measured on randomly selected cylinders with a compressometer to obtain the stress-strain curve and the modulus of elasticity, E_c, of the concrete. Typical results for the concrete in G-1 are shown in Fig. 5. Cylinder tests were also conducted to determine the splitting tensile strength of the concrete, f'_{sp}, at test. Strips of 1/8-in. plywood, 1-in. wide and 12-in. long were placed on the upper and lower bearing lines of the cylinder. All cylinders except the splitting tensile test specimens were capped with carbo-vitrobond material.

The results of all cylinder tests are tabulated in Table 1. The average f'_c in the test beams ranged from 5910 psi to 6820 psi at release and from 6660 psi to 7920 psi at test, as determined from vibrated cylinders cast in metal molds.

An analysis of the cylinder tests indicated that:

1. Values of f'_c at release and at test averaged 5.1 percent and 5.2 percent lower, respectively, for vibrated cylinders cast in waxed cardboard molds than for vibrated cylinders cast in metal molds.

2. Values of f'_c at test averaged 6.0 percent lower for rodded cylinders cast in waxed cardboard molds than for rodded cylinders cast in metal molds.

3. Values of f'_c at test for cylinders cast in metal molds averaged 1.2 percent higher for vibrated cylinders than for rodded cylinders.

4. Values of f'_c at test for cylinders cast in waxed cardboard molds averaged 2.1 percent higher for vibrated cylinders than for rodded cylinders.

5. Values of f'_{sp} at test averaged 2.2 percent lower for vibrated cylinders cast in waxed cardboard molds than for vibrated cylinders cast in metal molds.

6. Values of E_c obtained from tests on cylinders cast in metal molds averaged 1.6 percent higher than the values obtained from tests on cylinders cast in waxed cardboard molds.

2.2.2 Prestressing Steel

Uncoated stress relieved 270 ksi 7/16-in. diameter strand, meeting the requirements of ASTM A416-59 specifications, was used for the pretensioning elements. The strand was manufactured by John A. Roebling's Sons Division of The Colorado Fuel and Iron Corporation. The load-strain curve shown in Fig. 6 is a plot of the average values obtained from 3 strand tests conducted in the laboratory. Special Supreme Products Corporation No. 350 chucks were used during the testing of the strand; however, all 3 specimens failed in the grips at an average load of 31.9 kips and strain of 4.5 percent. Information provided by the manufacturer stated that the strand had an area of 0.1167-sq. in., and a minimum tension test breaking load of 31.0 kips. All of the strand used in the test beams were cut from the same roll of strand, the surface of which was free from rust and dirt.

2.2.3 Reinforcing Bars

Hot rolled deformed reinforcing bars of intermediate grade steel were used for non-prestressed reinforcement within the beams. The bars were clean and free from rust. Number 4, 5, and 6 bars were

used as tensile reinforcement in the top flange and as end reinforcement in the beams. The web reinforcement in the center or C region of each beam was made from deformed No. 5 bars. Web reinforcement in the A and B regions was made from No. 2 or No. 3 deformed bars. At least 4 specimens of each size bar were tested, and the results of one typical test on each size bar are shown in Fig. 7. The values listed in the accompanying table are average values of all specimens tested. The deformed No. 2 bars were taken from stock at the laboratory. All other reinforcing bars were taken from stock at the prestressing plant, which was obtained by the fabricator from Bethlehem Steel Company, Inc.

2.3 FABRICATION

The beams were fabricated by Schuylkill Products Inc., Cressona, Pennsylvania. This plant regularly produces similar beams for the Pennsylvania Department of Highways. Standard fabrication procedures were followed except to install instrumentation or to obtain readings from various control devices. The casting dates are given in Table 2.

The major operations in fabricating the I-beams and box beams were similar. The first operation was prestressing the strand. This was followed by installation of the non-prestressed mild steel reinforcement and the internal strain bar instrumentation. All of the non-prestressed steel and the instrumentation in the I-beams was installed prior to placing the concrete. Only the non-prestressed steel and instrumentation in the bottom flange of the box beams was installed before the concrete in the bottom flange was placed. Then the remainder of the non-prestressed steel and instrumentation were installed and the rest of the concrete was placed. After casting, the beams were steam-cured. Finally the prestress was released and the beams were removed from the bed. These operations are discussed in more detail in the following sections.

2.3.1 Prestressing

The strands were strung between the bulk-heads of a 76-ft column-type prestressing bed. Load cells were placed on 12 strands at

one end of the bed. Each strand was individually stressed with a hydraulic jack at the opposite end of the bed. Figure 8 shows a general view of the stressing operation. The load was measured during jacking by means of a 50 kip Chatillon strand dynamometer connected in the linkage between the strand and the hydraulic jack.

The strands had to be pulled to approximately 24 kips in order to have the design load of 21.7 kips after locking the chucks and releasing the jacking force. After all the strands had been stressed, the load on the 12 instrumented strands was checked by means of the load cells and adjustments made as required. The total prestress force in any beam, determined from the 12 instrumented strands, is given in Table 3. The force in any instrumented strand was within 5 percent of the design force, except for strands which sustained single wire failures.

Five single wire failures occurred while prestressing the strands. Three of these occurred in G-1, and the other two in G-2. One of the failures in G-1 occurred in the center region of the bed and the strand containing this wire was replaced. The remaining failures, two in G-1 and two in G-2, occurred in the chucks at the ends of the bed. Three of these failures were located at the jacking end. These strands were not replaced. The load cells indicated that a strand lost approximately 10 percent of its force at the time of a single wire failure.

2.3.2 Placement of Non-Prestressed Steel

In the I-beams, the web reinforcement and the longitudinal non-prestressed steel were made up into a cage at an auxiliary work area. Some of the stirrups were tack welded to the longitudinal steel to set up the cage, while the rest were tied with No. 16 gage wire ties.

The non-prestressed steel in the bottom flange and the end region of the box beams, shown in Fig. 9, was tied to the strands. The remaining non-prestressed steel was made up into a cage in the same manner as the I-beams. The cages were transferred to the bed after the concrete had been placed in the bottom flange and the void form was installed. The cage was held away from the void form by small grout blocks placed between the void form and the longitudinal steel.

Lifting hooks were installed in each end of the beams.

2.3.3 Placement of Instrumentation and Miscellaneous Items

Internal strain bars, described in the next section, were installed at the locations shown in Fig. 10. The electrical wires were taped to the vertical reinforcement and routed out of the top of the beam.

Water drains of 3/4-in. diameter plastic tubing and air vents of ¼-in. diameter copper tubing were installed in the top and bottom flanges, respectively, of the box beams so that one drain and one vent would be provided for each void.

Straps of 5/8-in. wide No. 25 gage steel were placed under some of the strands in the bottom of the box beams at approximately 5½-ft intervals. These straps were draped out and over the top of the forms, as can be seen in Fig. 9, and subsequently used to hold the void form in place.

2.3.4 Forming

Plywood was used to form the ends and the base of the beams. Triangular wedge-shaped strips were nailed to the sides of the base to form the chamfer. Standard prefabricated steel forms were used on the sides of the beams. All forms were cleaned and oiled prior to casting. The forms were braced externally at the base, and held together by spreaders at the top. The voids in the box beams were formed with cardboard. The surface of the cardboard void forms was waxed.

2.3.5 Casting

Ready-mix trucks delivered the dry concrete mix to the prestressing building. Here the materials were dry-mixed before water was added. The mix was transported from the trucks to the forms with a 1.75-cu yd bucket which was lowered to within 1-ft of the top of the forms before discharging the concrete.

The beams were cast in two lifts. The first lift in the I-beams was to the level of the junction of the bottom flange and web, while the first lift in the box beams was to the top of the bottom slab. The concrete was vibrated with two 1.38-in. diameter 12,000 vpm internal vibrators. Samples of concrete for slump tests, entrained air tests, and cylinder tests were taken from every bucket.

The void forms and reinforcement cage were installed in the box beams between the first and second lift. This operation required less than ½-hr. The surface was then finished with a steel trowel.

2.3.6 Curing

A double thickness of saturated burlap was placed over the top of each beam after casting. The cylinders were placed on top of the forms. The cylinders, beam, and forms were draped with another covering of saturated burlap which extended down to the floor of the bed. Tarpaulins were suspended around the beam so as to form a completely enclosed region.

After a period of not less than two hours, steam was injected into the region under the tarpaulin. The steam had a relative humidity of 100 percent and the temperature in the enclosure was maintained at 140 $\pm$ 10 degrees F. Steam curing was continued for at least 36 hours.

Six cylinders were tested to determine f'_c at the conclusion of the steam curing period. These cylinders were capped with carbo-vitrobond material and allowed to cool for 2 hrs. before being tested in a Forney model QC 225 compression testing machine at the fabricating plant. The ultimate compressive strength of all cylinders tested at this time surpassed the 4500 psi requirement for release of the prestress force. Steam was discontinued at the time of removal of the 6 test cylinders, but the beam was not uncovered until after the cylinders were tested. Six additional cylinders were taken to Fritz Engineering Laboratory and tested to determine f'_c and E_c.

2.3.7 Release

The forms were loosened prior to release of the prestress force, which was accomplished by simultaneously torch cutting individual strands at both ends. Each strand was heated over a length of several inches to obtain as much yielding as possible before cutting. After cutting the forms and tarpaulin were removed.

Internal strain bar readings and load cell readings on the 12 instrumented strands were taken before and after release. After release each beam was inspected for cracks. However, no cracking was found in any beams.

2.4 INSTRUMENTATION

Instrumentation consisted of strand load cells, internal strain bars, Whittemore targets, deflection gages, SR-4 electrical resistance gages, and miscellaneous items.

2.4.1 Strand Load Cells

Load cells were used to determine the prestress force prior to release, as discussed in Section 2.3.1. A description of the load cells can be found in a previous report.[8]

2.4.2 Internal Strain Bars

Internal strain bars were used primarily to determine the loss in the prestress force at release and until such time that Whittemore targets could be placed on the surface of the beams. A complete strain bar consisted of a 1-in. and a 36-in. length of No. 4 reinforcing bar with a strain gage attached to the center of each bar. The surface of each bar was ground smooth at the location of the gage, and a type AB-7 electrical resistance gage was attached with a resin compound. Both gages were waterproofed. Felt padding was wrapped around the short bar, and a rubber finger cot was placed over the felt and held against the lead wires with a rubber band. The short bar was attached at the right angle to the center of the long bar. The strain bars were embedded in the beams at the locations shown in Fig. 10. The long bar was

placed parallel to the strands. When both gages would be read simultaneously, the long bar gave the total strain change and the short bar gave the strain change due to change in temperature.

2.4.3 Whittemore Targets

Deformations and crack widths were measured with a 5-in. and a 10-in. Whittemore Strain Gage, and also a 0.001-in. extensometer. Brass plugs, 7/32-in. in diameter and 3/32-in. in thickness, were drilled with a No. 1 center drill and used for gage points, or targets, on the beam. The targets were cemented to the beams with Armstrong Adhesive A-6 epoxy resin. Figure 11 shows the location of all of the targets placed on the beams. Targets represented by a solid circle were installed on both sides of the beam at the prestressing plant after release, and initial readings were taken on these targets within 1 day. Targets represented by an open circle were installed on one side of the beam at the laboratory prior to testing. Targets on rows B and C were used for crack width measurements. Targets on row D are at the level of the cgs.

2.4.4 Deflection Gages

Deflection measurements were obtained by Ames dial gages placed under the beam along the longitudinal centerline. Deflection and support settlements were also obtained by level readings on scales graduated to 0.01-in.

2.4.5 SR-4 Electrical Strain Gages

Type A-9 electrical resistance strain gages were attached to the beam at the laboratory prior to the first test. Figure 11 gives the location of all gages placed on the beams.

2.4.6 Miscellaneous

The strands were cut about 3-in. from the end of the beam. Plastic tape was wrapped around each strand prior to testing. Measurements were taken from a reference point on the tape to the end of the beam before and after testing to determine if slip occurred.

2.5 PRESTRESS

The loss in the prestress force from the time that the strands were pretensioned until approximately 1 day after release was determined from readings on the internal strain bars. These readings were corrected for the effect of change in temperature by simultaneous readings of the temperature compensating gages. It was assumed that the strain distribution in the beams was planar, and therefore the strain bar readings could be used to calculate the change in the strain at the cgs.

Considerable difficulty was experienced in taking the strain bar readings. The extreme dampness in the prestressing plant caused shorts in the connections and affected the reliability of the strain indicator, as noted by a tendency of the readings to drift. The loss in the prestress force determined from these readings must therefore be regarded as approximate.

Subsequent loss in the prestress force, until the time of test, was determined from the Whittemore readings located on the surface of the beams at the cgs. The total percent loss and the final prestress force is given in Table 3.

The measured loss in the prestress force was less than expected, and considerably less than the 20 percent assumed in the design of bridge girders by the Pennsylvania Department of Highways.[25] Part of this may have been due to the difficulty in obtaining the strain bar readings, as previously discussed. However, it should be noted that the amount of prestress steel in the box and I-beams was 0.52 and 0.46 percent, respectively, which is about 60 percent of the steel in typical bridge girders. Furthermore the compressive stresses in the bottom fibers of the beams after release were only approximately 30 percent of the compressive strength of the concrete, compared to 60 percent allowed by the Pennsylvania Department of Highways.

2.6 HANDLING AND STORAGE

The beams were stored in the prestressing plant for approximately 3 weeks after fabrication. They were subsequently stored outdoors. All of the cylinders were stored with the beams.

The beams were shipped by truck to Fritz Engineering Laboratory. Beams G-1 and G-2 were shipped together, and G-3 and G-4 separately. Cylinders were packed in straw alongside the beams during shipment. The beams were stored in a simply supported position on the laboratory floor until tested.

Each beam was carefully examined after arrival at the laboratory. Tension cracks were observed in the top flanges of the box beams. The cracks in G-1 were located approximately 10-in. apart in the end regions of the beam, and extended to a depth of about 10-in. near the junction of the void and end block. The only cracks observed in G-3 were at the junction of the void and end block, and extended to a depth of about 5-in.

A horizontal crack was observed in both ends of the long I-beam, G-4. These cracks occurred at the junction of the web and bottom flange and extended approximately 2-in. into the beam, to the location of the first stirrup. There were no cracks observed in G-2.

3. METHOD OF TESTING

3.1 TEST SETUP

Two or three tests were conducted on each beam, using the loading arrangement shown in Fig. 12. These tests were conducted in a 5 million pound Baldwin universal testing machine. Two steel loading beams were required to transmit the load from the testing machine head to the two load points in the first test setup on all of the beams except the short I-beam. Loading Beam 2 was used alone for the short I-beam. The end reactions were transmitted through rigid pedestals to the floor. The second and third test setup was simplified by elimination of the steel loading beams.

The test beams and the two steel loading beams were carefully aligned and centered in the testing machine. Hydro-stone grout, manufactured by U. S. Gypsum Co., was used between the 2-in. steel plates and the beams. A level was used to set the plates located at the load points.

Figure 13a and b shows views of beams G-4 and G-3, respectively, prior to the first test. Figure 13c shows beam G-1 during the second test. Figure 13d shows beam G-4 during the third test. External reinforcement composed of 1-in. diameter rods and steel plates were used to reinforce the cracked shear span so that a test could be conducted on the other shear span.

When reference is made to the left and right sides of the beams, these sides may be established by standing at the B end of the beam and looking toward the A end.

3.2 TEST PROCEDURE

Before the test was started, vertical lines were marked on the sides of each test beam to show the location of the stirrups. Initial

readings were also taken on all of the instrumentation. Load was applied in increments of approximately 5 percent of the predicted failure load. Deflection readings, internal strain bar readings, and external SR-4 gage readings were taken at each load increment after the deflection stabilized. Whittemore readings were taken at selected loads. The load causing flexural cracking and inclined cracking was carefully noted and recorded, along with the ultimate load and various observations made during the test. Felt tipped pens were used to mark the crack patterns. Photographs were taken during and after the test.

If an inclined crack developed suddenly during loading, the load indicated on the testing machine would decrease. When this happened, the loading valve was closed in order to maintain the deflection, until the load stabilized. Some readings would be taken at this load. Then the load was increased to the next increment before additional readings were taken.

After the first test, each beam was separated at the failure region. The remaining part of the beam was examined and reset under the testing machine for a second test. Second tests were conducted on all beams; however, the effect of the first test on G-3 was so severe that the second test was influenced by the damage incurred during the first test. A third test was conducted on only one beam, G-4.

Cracks developing during the second or third tests were marked with dashed lines. Fewer readings were taken during these tests. Photographs were again taken during and after the test.

The tests were carried out on the dates indicated in Table 2. In general 8 to 10 hours were required to conduct the first test on a beam. The cylinder tests were conducted at the end of the first test. The second and third tests required 3 to 4 hours to complete.

4. I - B E A M T E S T S

4.1 TEST RESULTS

Five tests were conducted on the two I-beams, G-2 and G-4, as shown in Table 4. In the first test on G-2, the beam failed in shear in region B. This was the shear span with the least amount of web reinforcement, as indicated by the values of $rf_y/100$. When a second test was conducted on the other shear span, the beam failed in flexure. G-4 failed in flexure in the first test. A second and third test were conducted on the half of region B and Region A, respectively, which were adjacent to the support in the first test. The beam failed in shear in both of these tests.

The principal results of the I-beam tests are presented in Table 4. V_{cr} is the applied load shear causing flexural cracking. The region of maximum moment in the second and third test on G-4 was not cracked during the first test, and consequently values of V_{cr} were obtained for these tests. V_{ic} is the applied load shear causing significant inclined cracking. In the first test on G-2, inclined diagonal tension cracking formed in both shear spans. Inclined flexure shear cracks formed in both shear spans of G-4 during the first test, but these cracks were not significant as far as the behavior of the member was concerned. Inclined diagonal tension cracking formed in both the second and third test on G-4. V_f is the applied load shear causing failure.

Sketches of the cracking in the beams at V_{ic} are presented in the Appendix. These sketches are explained and considered in more detail in Section 6.3. The mid-span deflection during testing is shown in Fig. 14. The results of strain measurements on the compression flange during testing are shown in Fig. 15. In Fig. 15 the designations s and t refer to side and top respectively. The designations 1, r, and c refer to the left side, right side, and center, respectively. The strain over the depth of G-4, at the mid-span section, is shown in Fig. 16. The first and last observations of the widths of selected inclined

cracks are tabulated in Table 6. The growth in width of some of these inclined cracks is shown in Fig. 17. Photographs taken during and after testing are shown in Figs. 18 through 22. In the photographs, the vertical lines on the sides of the beam indicate the locations of the stirrups. The irregular lines mark the crack patterns. The cross marks indicate the extent of development and the shear when the crack was first observed. These data are discussed in Sections 4.2 and 4.3 along with a description of the behavior and mode of failure of the I-beams. All reference to load on the member is in terms of applied load shear.

4.2 BEHAVIOR AND MODE OF FAILURE OF BEAM G-2

4.2.1 First Test

A flexural crack was first observed in region C at a shear of 72 kips. The mid-span deflection in the beam at this time was 0.338-in. The flexural crack started on the right side of the bottom of the beam, and did not progress across the bottom to the left side until additional load had been applied. Diagonal tension inclined cracking occurred suddenly in region A while the shear was being held constant at 104 kips. When the inclined cracking occurred, the load shown on the testing machine decreased to about 100 kips. Figure 18a shows the resulting inclined cracking in region A. Diagonal tension inclined cracking occurred suddenly in region B after the shear had been increased again to 104 kips and held for approximately 15 minutes. With the deflection maintained, the shear decreased to about 98 kips. Figure 18b shows the resulting inclined cracking in region B. The deflection in the beam after the shear had been increased again to 104 kips was 1.53-in.

A sudden shear failure occurred in region B when the shear was increased to 110 kips. The first indication of failure was spalling of the extreme compression fibers adjacent to the load point bearing plate. This was followed by the sudden extension of an inclined crack through the compression flange, intersecting the location of the spalling, as shown in Fig. 18c. No stirrups were broken during the failure.

The strain measurements plotted in Fig. 15 show the change in behavior in the shear span when diagonal tension cracking occurred. At shears of 60 and 100 kips, strains in the top fibers had increased with load. However, the higher strain on the left side, along with the observation that the flexural cracking started on the right side, indicates that the load may have been applied somewhat eccentrically. After inclined cracking the strain decreased at locations along the centerline greater than a distance d/2 from the load point. In region B, the strains at 1.5d and 2d from the load point changed from compression to tension. In region A, the strain decreased but remained in compression, at least up to a shear of 108 kips. Therefore, the change in behavior due to diagonal tension cracking was more pronounced in the shear span with the least amount of web reinforcement.

The Whittemore targets in the web were used to determine the initial width and subsequent growth of the diagonal tension cracks. As may be seen in Fig. 18a and b, there were 3 cracks in both shear spans on which data were obtained. The data on crack widths shown in Fig. 17a is for the widest crack which in both shear spans was the crack closest to the load point. Initial readings were obtained at a lower shear than the shear which caused the cracks to form, since the load indicated on the testing machine decreased when the cracks formed. The last measurement in region B, obtained at 98.2 percent of the load causing failure, showed that the crack had grown to a width of 0.174-in. This was nearly 3 times greater than the width of the widest crack in region A, showing that the greater amount of web reinforcement in region A restricted the development of the cracks.

No appreciable strand slip was measured at the A end of the beam, but all 4 top strands at the B end slipped approximately 3/32-in. As may be seen in Fig. 18b, diagonal tension cracking had extended within a few inches of the end of the beam at the level of these 4 strands.

4.2.2 Second Test

After the B end had been removed, G-2 was reset under the testing machine and examined. Cracks in the top fibers of region A, shown in Fig. 19, apparently developed concurrently with the failure, since these cracks were not observed during the first test. However, these cracks appeared to be completely closed. Strain readings at the level of the cgs indicated that the flexural cracks were almost completely closed and that the prestress force was fully effective in region A.

Flexural cracks, which had formed during the first test, reopened in the region below the load point at a shear of approximately 60 kips. At a shear of 100 kips, inclined cracks developed across the existing flexural cracks in region C.

The beam held its maximum load for approximately 15 minutes before a slow flexural failure occurred at a shear of 118 kips. The failure was characterized by crushing of the concrete in the compression flange adjacent to the load point, as shown in Fig. 19b and 19c. However, the failure was influenced to some extent by shear, since the failure occurred above the top of an inclined crack in the shear span with the least amount of web reinforcement. Cracks parallel to the direction of the compressive stress were observed in the region in which crushing occurred prior to failure.

The width of the widest crack in region A after the first test was 0.038-in. Figure 17b shows the increase in width of this crack during the second test. The last measurement of 0.106-in. was obtained at 98.4 percent of the load causing failure.

The slip measurements at the A end of the beam after the second test gave no indication of any strand slip, despite the extension of an inclined crack to within a few inches of the end of the beam, as shown in Fig. 19b.

4.3 BEHAVIOR AND MODE OF FAILURE OF BEAM G-4.

4.3.1 First Test

Flexural cracking was first observed when the applied load shear was 34 kips and the deflection was 0.72-in. Figure 20a shows the beam when the shear was 62 kips, or 94 percent of the ultimate load. The deflection was approximately 4½-in. at this time. The beam failed in flexure, as shown in Fig. 20b, after it had held a shear of 66 kips for several minutes.

Inclined flexure shear cracking had developed from flexural cracks in both shear spans prior to failure, as shown in Fig. 20c and d. These flexure shear cracks had formed over distances approximately 1.7d from the load point. At no time did it appear that these cracks would cause failure, and additional cracking would probably have had to form further from the load point before shear would have been critical. Flexure shear crack widths of 0.032-in. and 0.027-in. were measured in regions A and B, respectively, while the load was held at 97 percent of the load causing failure. These widths were obtained using the targets in the web of the beam.

The flexural failure occurred almost exactly in the center of the beam. The two No. 6 bars used as reinforcement in the top flange buckled when the failure occurred, as shown in Fig. 20b. Spalling and cracking parallel to the direction of the compressive stress was observed prior to failure.

Figure 15 shows that the strains in the compression flange were affected very little by the flexure shear cracking. Figure 16 shows the strain history at mid-span. After release, the strain varied from 0.00003-in. per in. tension in the top fiber to 0.00032 in. per in. compression in the bottom fibers. From after release until the time of test, all of the fibers shortened by approximately 0.00017-in. per in., as shown by the dashed line. The variation in strain during the test is shown at shears of 34, 50, and 60 kips. A maximum strain of 0.0023 was measured in the extreme fiber in compression at the ultimate shear of 66 kips, approximately 2 minutes before failure.

4.3.2 Second Test

After G-4 had been separated at mid-span, a second test was conducted on a shear span which was the half of region B adjacent to the support in the first test. External reinforcement was used to strengthen the other half of region B, which was cracked during the first test.

Flexural cracking was first observed at a shear of 76 kips on one edge of the bottom of the beam directly below the load point. This crack did not progress to the other edge of the bottom until the shear had reached 100 kips. Inclined cracking occurred in the reinforced shear span at a shear of 112 kips. With the deflection maintained at what it was when the inclined cracking occurred, the shear decreased to 101 kips. During reloading, diagonal tension inclined cracking, shown in Fig. 21a, occurred in the test region at a shear of 110.5 kips, causing the shear to decrease to 97.5 kips.

Failure occurred at a shear of 114 kips, when the inclined crack suddenly sheared through the compression flange, as shown in Fig. 21b and c. The beam had held the ultimate load for approximately 10 minutes before the shear failure occurred. The maximum moment was 79 percent of the moment causing failure in the first test. No stirrups were fractured in the failure.

Figure 17c shows the growth in width of the critical diagonal tension crack in region B. The first measurement was not taken until the shear had been increased from 97.5 kips to the shear which had caused the crack to form. The last measured width of 0.131-in. was obtained at the failure load.

4.3.3 Third Test

The third test on G-4 was conducted on a shear span which was half of region A. External reinforcement was used to strengthen the other half of region A.

The first flexural crack appeared at one edge of the bottom of the beam at a shear of 76 kips. This crack, as in the preceding test, did not progress across the bottom until the shear had reached

104 kips. Inclined cracking occurred in the reinforced region at a shear of 116 kips, after which the shear decreased to 112.5 kips. Diagonal tension cracking occurred in the test region at a shear of 119 kips, after which the shear decreased to 109 kips.

The beam failed at a shear of 136 kips due to crushing in the compression flange adjacent to the load point, as seen in Fig. 22a and b. Prior to failure cracks were observed in this region parallel to the direction of the compressive stress. The shear failure occurred at 94 percent of the moment causing the flexural failure in the first test. None of the stirrups were broken during the failure.

Figure 17c shows the growth in width of the diagonal tension crack in region A. It is evident that the greater amount of web reinforcement in region A restrained the width of the crack.

5. BOX BEAM TESTS

5.1 TEST RESULTS

Four tests were conducted on the two box beams, G-1 and G-3, as shown in Table 5. G-1 failed in shear in region A in the first test. This was the shear span with the greatest amount of web reinforcement. When a second test was conducted on the other shear span, the beam again failed in shear. In the first test on G-3, the beam failed in shear in region B. A second test was conducted on region A, but the failure was influenced by damage sustained during the first test.

Flexural cracking, inclined cracking, and failure occurred at the values of V_{cr}, V_{ic}, and V_u given in Table 5. During the first test on G-1, inclined diagonal tension cracking occurred in the web on the right side of region B, then on the left side of region A, and then on the right side of Region A. Diagonal tension cracking did not develop in the web on the left side of region B until the second test. Inclined flexure shear cracking occurred in both shear spans during the first test on G-3. Sketches of the cracking in the beams at V_{ic} are contained in the Appendix.

The mid-span deflection of the beams during the tests is shown in Fig. 14. Data on strain in the compression flange are presented in Figs. 23 and 24. Information on inclined crack widths is given in Table 6 and in Fig. 25. Photographs taken during and after the testing of the beams are shown in Figs. 26 through 29. These data are discussed in Sections 5.2 and 5.3, along with a description of the behavior and the mode of failure of the box beams.

5.2 BEHAVIOR AND MODE OF FAILURE OF BEAM G-1

5.2.1 First Test

G-1 was subjected to a shear of 120 kips before flexural cracks were observed. At this shear the deflection was 0.322-in. Diagonal

tension inclined cracking occurred on the right side of region B at a shear of 136 kips. The Appendix contains a sketch showing this crack. When the crack formed, the shear decreased to 130.5 kips. Inclined cracking subsequently occurred on the left side of region A at a shear of 152 kips. This crack formed well back from the load point and extended up to and partially through the top flange, as shown in the sketch in the Appendix. This crack had an initial width of 0.035-in., and its subsequent growth is shown in Fig. 25. Diagonal tension inclined cracking next occurred on the right side of region A at a shear of 192 kips, causing the shear to decrease to 185 kips. This crack is also shown in the Appendix.

The beam failed suddenly in region A at a shear of 198.5 kips. The shear failure appeared to start at the apex of the inclined crack on the right side of the beam, as shown in Fig. 26a. Failure was due to crushing and shearing of the concrete in the compression flange. Figure 26b shows the left side of the beam after the failure. The unusual appearance of this side of the beam was probably due to twisting in the beam as a result of the start of the failure in the other web. There were no stirrups broken in this failure. However, in the right side of the beam, some of the stirrups were pulled out of the concrete in the region where the inclined crack crossed the lapped splice.

The strain in the compression flange during the first test on G-1 is shown in Fig. 23. The effect of the diagonal tension cracking, which occurred in the right side of region B at a shear of 136 kips, and on the left side of region A at a shear of 152 kips, is shown very clearly. On the right side of region A, strain readings were obtained, at a shear of 192 kips, both before and after the diagonal tension crack formed. The sudden decrease in strain in the top fibers on the right side, as a result of the cracking, is very evident. The left side of region B did not develop any inclined cracking during the first test, and this is reflected in the uniform strains in the shear span.

5.2.2 Second Test

Figure 27a and b shows the right and left side of region B, respectively, at the start of the second test. Deep cracks extending downward into the compression flange may be seen on both sides of the beam. These cracks formed concurrently with the failure in the first test in the other end of the beam. However, these cracks were completely closed at the start of the second test. Full recovery of the prestress force was evident since the strain along the cgs was the same at the start of the second test as at the start of the first test.

Flexural cracks, which had formed during the first test in region C, reopened in the region beneath the load point at a shear of approximately 104 kips. Inclined cracks also formed in region C across the existing flexural cracks at this load. Inclined cracking occurred on the left side of region B at a shear of 206.5 kips. This crack, shown dashed in the sketch in the Appendix, formed high in the web and near the support. It developed suddenly, extending into the compression flange and forward toward the load point.

A sudden shear failure occurred at a shear of 215.5 kips, due to crushing of the compression flange adjacent to the load point on the left side of the beam. The failure was apparently triggered by a flexural crack, shown dotted in Fig. 27c, which formed at a section approximately 2d from the load point. This crack precipitated the inclined crack above it, which ran toward the load point. This region was already affected by the crack in the compression flange of the beam, and when the inclined crack formed, the beam failed. Figure 27d is a view of the failure region in the top of the beam showing the two cracks which caused the compression failure adjacent to the load point. Figure 27e shows the right side of the beam. The cracking over the support was due to the failure on the other side of the beam. None of the stirrups were fractured during the failure.

The width of the inclined crack on the right side of region B was measured during this test. Since Whittemore targets had not been placed on this side of the beam, the width was measured with a micro-

scope and a scale graduated to 0.01-in. at the three locations shown in Fig. 27a which are circled and numbered 1 to 3. At the start of the test, the width at locations 1, 2, and 3 was 0.05-in., 0.06-in., and 0.04-in., respectively. At a load which was 97 percent of the load causing failure, the widths were 0.06-in., 0.17-in., and 0.08-in. The variation in the width of the crack with load, as measured at location 2, is shown in Fig. 25a.

A large amount of strand slip was measured at the end of the beam after the second test. The slip was due to the cracking which formed back toward the support on the right side of the beam, as shown in Fig. 27e. However, since this cracking was not directly responsible for the failure, the slip apparently occurred as a consequence rather than a cause of the failure.

5.3 BEHAVIOR AND MODE OF FAILURE OF BEAM G-3

5.3.1 First Test

Flexural cracks were observed at a shear of 68 kips. The deflection in the beam at this time was 0.76-in. Figure 28a shows the beam carrying a shear of 116 kips, which was 91 percent of the ultimate load. The deflection was 5.5-in. at the time this picture was taken.

In region B, flexure shear cracks which subsequently caused the failure had developed at a shear of 116 kips. These cracks, shown in the sketches in the Appendix, had formed at a distance of approximately 1.9d from the load point. The failure occurred very suddenly at a shear of 127.5 kips. An overall view of the beam after failure is shown in Fig. 28b, and close-up views of the failure region are shown in Fig. 28c and d. Two stirrups were fractured on each side of the beam, where they were crossed by the critical flexure shear crack. Fig. 28e and f show views of the left and right side of region A near the load point after failure. A flexure shear crack on the left side of region A may be observed at a distance of approximately 2.3d from the load point.

Measurements of the width of the flexure shear cracks were obtained after they had extended to the mid-depth of the beam. In both

the A and B end, a flexure shear crack crossed between the Whittemore targets at a horizontal distance of approximately 30 inches from the load point. Initial measurements were obtained at a shear of 112 kips in the B end, and 116 kips in the A end, and the subsequent growth in width of these cracks is shown in Fig. 25b. It is evident that the different amount of web reinforcement in the A and B end did not affect the width of the cracks as much as in some of the preceding tests.

5.3.2 Second Test

This test was conducted with a 15-ft span consisting of the part of the beam which had been region A. Cracking developed in an unusual manner, and the beam failed in shear at approximately 80 percent of the expected capacity. Figure 29a and b shows the cracking which developed on each side of the beam. The behavior of the beam indicated that the test was affected by damage from the failure in the first test.

6. STRENGTH OF TEST BEAMS

6.1 GENERAL

Any structural member must have sufficient strength to safely carry its intended load. The degree of safety is the ratio of the load causing any response which is incompatible with the serviceability of the member to the load for which the member is designed. The limiting response may be either a static or a fatigue failure, a condition of instability, or excessive deflection.

For typical prestressed concrete bridge girders, the degree of safety generally depends on the static ultimate strength of the member. The static strength in turn depends on the capacity to resist moment shear, and torsion. Procedures for determining the flexural strength, based upon a rational concept of the behavior of the beam, are well established. Bridge girders are generally not designed for torsion.

Previous research has shown that before shear is critical, significant inclined cracking must have developed. In a beam without web reinforcement, the shear causing significant inclined cracking is the ultimate shear strength. The addition of web reinforcement increases the shear strength of the beam, by an amount approximately equal to the shear carried by the stirrups crossed by the inclined cracking. Therefore an analysis of shear strength must begin with the inclined cracking strength. However, inclined cracking is either caused by high diagonal tension stresses in the web, or by flexural cracking which either turns and becomes inclined in the direction of increasing moment or which precipitates inclined cracking above it. In the latter case the flexural cracking strength is important. Furthermore, the maximum shear that any beam must carry is limited by the ultimate flexural strength of the member.

This investigation was to determine if the shear strength of the F Series I-beams,[16] which was summarized in Section 1.1, was

comparable to the shear strength of full-sized bridge beams. In particular the investigation was to determine if the specification for design of web reinforcement in Section 1.1.1 would satisfactorily predict the shear strength observed in the full-sized beam tests described in the preceding chapters. In the following sections, the strength of the test beams will be evaluated by considering first their flexural cracking, inclined cracking, and ultimate flexural strength, and then their ultimate shear strength.

6.2 FLEXURAL CRACKING STRENGTH

The applied load shear causing flexural cracking, V_{cr}, marked the first significant change in the action of the beam during testing. Up to this point, the response of the beam to load had been essentially linear, as indicated by the load-deflection curves in Fig. 14. Since all of the beams were symmetrically loaded, the maximum applied load moment causing flexural cracking was related to V_{cr} by:

$$M_{cr} = V_{cr}\, a \tag{5}$$

Values of V_{cr} and M_{cr} for the first test on each beam are listed in Table 7.

The flexural cracking moment, M_{fc}, is generally calculated from the equation:

$$M_{fc} = M_{cr} + M_d = Z_b \left(f'_r + \frac{F}{A} + \frac{Fe}{Z^b}\right) \tag{6}$$

Solving for the flexural tensile strength of the concrete gives:

$$f'_r = \frac{M_{cr} + M_d}{Z^b} - F\left(\frac{1}{A} + \frac{e}{Z^b}\right) \tag{7}$$

Equation 7 was used to calculate values of f'_r for each test listed in Table 7, using the section properties in Fig. 3. M_d was assumed equal to the maximum dead load moment in the beam. The values of f'_t are listed in Table 7, and ranged from 289 to 659 psi, with an average of 395 psi. The values of f'_r are also compared to $\sqrt{f'_c}$ and

f'_{sp}, where these properties of the concrete were determined from tests on vibrated cylinders cast in metal molds. The average ratios of f'_r/f'_c and f'_r/f'_{sp} were 4.59 and 0.64, respectively.

For the F Series tests, these same ratios of $f'_r/\sqrt{f'_c}$ and f'_r/f'_{sp} were 9.5 and 1.33, respectively. This considerable difference may be due to two reasons. First, in several tests flexural cracking was initially observed at one edge of the bottom flange. This cracking did not progress across the bottom to the other edge until additional load was applied. Therefore there must have either been some eccentricity in the prestress force, possibly due to the manner in which the prestress force was released into the beam, or there must have been some torsional moment from the load being applied eccentrically. Second, as discussed in Section 2.5, considerable difficulty was experienced in obtaining the strain readings on which the determination of the prestress loss was based. If the prestress loss was greater than determined, the calculated values of f'_r would be increased. In fact, if the prestress loss was assumed equal to 20 percent, the ratios of $f'_r/\sqrt{f'_c}$ and $f'_r/\sqrt{f'_{sp}}$ would be 9.4 and 1.2, respectively.

6.3 INCLINED CRACKING STRENGTH

Significant inclined cracking occurred in the test beams at the values of V_{ic} given in Tables 4 and 5. Sketches of the cracking at these shears are presented in the Appendix. These sketches were drawn from photographs taken during testing. Cracking which occurred in the first test on a beam is shown by wide solid lines, while cracking which occurred in subsequent tests is shown by wide dashed lines. The shear at which flexural cracks or inclined flexure shear cracks were first observed is written directly below the crack. Inclined cracks which extended downward to the bottom fibers have nothing written below them. The stirrup locations are shown by vertical narrow broken lines.

The magnitude of the principal tensile stresses in the web at inclined cracking were calculated at the intersection of the grid lines and the top of the web, the cg in the box beams and the mid-height

of the web in the I-beams, and the bottom of the web for each sketch in the Appendix. The state of stress in the shear span was assumed to be defined by a horizontal normal stress, f, and a shearing stress, v. The normal stress was calculated from:

$$f = F\left(\frac{ey}{I} - \frac{1}{A}\right) - \frac{y}{I}\left(V_{ic}x + M_d\right) \tag{8}$$

The origin of the coordinate system was taken at the intersection of the grid line through the support and the cg of the section, x being positive when measured along the cg in the direction toward the centerline of the beam, and y being positive upwards. The shearing stress was calculated from:

$$v = \frac{Q\left(V_{ic} + V_d\right)}{Ib} \tag{9}$$

The principal tensile stress was determined from the relationship:

$$f_{pt} = \frac{f}{2} + \sqrt{\left(\frac{f}{2}\right)^2 + v^2} \tag{10}$$

The direction of the compressive stress trajectory was calculated from:

$$\theta = \tfrac{1}{2} \tan^{-1}\left(-\frac{2v}{f}\right) \tag{11}$$

The compressive stress trajectories were drawn as light dashed lines through the intersection of each grid line and the cg of the box beam or mid-height of the web of the I-beam. Flexural stresses were also calculated from Eq. 8 at the intersection of the grid lines and the bottom fibers.

The tests on G-1 and G-2 were conducted on shear spans with a length of 9'-0", corresponding to a/d ratios of 3.34 and 3.49, respectively. The second and third test on G-4 were conducted on a 7'-6" shear span, corresponding to an a/d ratio of 2.92. It is evident from the sketches in the Appendix that the inclined cracking in all of these tests developed largely in an uncracked region, and was due to high principal tensile stresses in the web of the beams. Furthermore, the sketches indicate that the f_{pt} causing the inclined cracking is near the cg in the box beams and the junction of the web and the bottom flange in

the I-beams.

In G-1, diagonal tension cracking first occurred on the right side of region B at a principal tensile stress of approximately 230 psi. Cracking next occurred on the left side of region A at about 280 psi, and then on the right side of region A at about 390 psi. In this latter case the sketch in the Appendix shows four flexural cracks in the vicinity of grid line 4, which were first observed at the same shear of 192 kips that caused the diagonal tension cracking. However, the flexural tensile stresses in this region are not great enough to have caused flexural cracking except possibly for the crack adjacent to grid line 5. It therefore appears that this latter crack formed when the shear was increased from 184 to 192 kips. The diagonal tension crack subsequently formed due to the high stresses in the web. This caused the formation of the three other flexural cracks due to the sudden increase in the stress in the strand. Diagonal tension cracking did not occur in the left side of region B until the second test, at about 430 psi.

Both the crack on the left side of region A, in the first test, and the crack on the left side of region B, in the second test, formed close to the support, and extended up into the compression flange. From there the cracks ran forward to the load point, as shown for the left side of region B in Fig. 27d. There is the possibility that these cracks may have been influenced by torsion due to the cracking on the other side of the beam. While there is a spherical head between the testing machine and the top loading beam, as shown in Fig. 12, any rotation about this point would be resisted by the horizontal stiffness of the box beam. Therefore, any decrease in vertical stiffness on one side of the beam, due to inclined cracking, would tend to make the applied load eccentric, and would introduce a torsional moment into the shear span.

Diagonal tension cracking occurred at the same shear in both ends of G-2, at a principal tensile stress of about 400 psi. It is probable that the crack closest to the load point was the first to form. In the second and third tests on G-4, diagonal tension cracking formed at critical stresses of about 400 and 470 psi, respectively.

In the F Series beams,[16] diagonal tension cracking occurred in tests on a/d ratios of less than approximately 4.5. This cracking was related to a principal tensile stress of $(8 - 0.78 \frac{a}{d})\sqrt{f'_c}$ at the cg of the section at the mid-point of the shear span. The location of the section, however, was not critical because of the negligible dead weight of the beams. It is not exactly correct to compare the critical stress of $(8 - 0.78 \frac{a}{d})\sqrt{f'_c}$ to the stresses which caused the cracking in the test beams. However, assuming that a comparison can be made, the value of $(8 - 0.78 \frac{a}{d})\sqrt{f'_c}$ for the tests on G-1, G-2, and G-4 is 479, 431, and 497 psi, respectively. Thus diagonal tension cracking occurred at lower web stresses in the test beams than in the F Series beams. As noted in Section 6.2, this difference may be due to eccentric loading, or to an over-estimation of the prestress force in the test beams.

The test on G-3 was conducted on an a/d ratio of 5.56. Significant inclined cracking occurred in region B at a shear of 116 kips. The cracking in both sides of region B is shown in the Appendix. There are several cracks which start from high flexural tensile stresses and then turn and become inclined in the direction of increasing moment. The flexure shear crack which was first observed at a shear of 116 kips was considered to be significant because this crack subsequently caused the shear failure, as shown in Fig. 28c and d. The crack is located at a distance from the load point equal to approximately 1.8d, and formed at a stress in the bottom fibers of approximately 600 psi.

In the F Series beams, flexure shear cracking was related to a stress of $9.5\sqrt{f'_c}$ occurring in the bottom fibers at a distance $[-31.6 + 15.6\ (a/d) - 0.88\ (a/d)^2]$ in inches from the load point. For an a/d ratio of 5.56, the critical crack would be located 27.7-in., or 1.95d, from the load point. Applying this criteria to G-3, significant flexure shear cracking would be expected when a stress of 845 psi is reached at a distance of 1.95d from the load point. Thus flexure shear cracking occurred sooner in G-3 than expected by comparison to the F Series beams.

6.4 ULTIMATE FLEXURAL STRENGTH

The calculation of the ultimate flexural strength of the test beams was based on the strain and stress distribution shown in Fig. 30. From equilibrium of internal forces:

$$T = C + C' \tag{12}$$

$$M_{fu} = Td_r - Cd_c - C'd'_r \tag{13}$$

where T = resultant tensile force in the prestress steel

C = resultant compressive force in the concrete

C' = resultant compressive force in the non-prestressed steel

M_{fu} = ultimate flexural moment

d_r = distance from the extreme fiber in compression to T

d_c = distance from the extreme fiber in compression to C

d'_r = distance from the extreme fiber in compression to C'

The resultant tensile force in the prestressed steel and the resultant compressive force in the non-prestressed steel and in the concrete are equal to:

$$T = \sum_{i=1}^{n} A_{s_i} f_{s_i} \tag{14}$$

$$C = k_3 f'_c \left(A_c - \sum_{i=1}^{n'} A'_{s_i}\right) \tag{15}$$

$$C' = \sum_{i=1}^{n'} A'_{s_i} f'_{s_i} \tag{16}$$

where A_{s_i} = cross sectional area of prestressed steel at a particular level, i

A'_{s_i} = cross sectional area of non-prestressed steel at a particular level, i

A_c = cross sectional area of beam above a distance $k_1 c$ below the extreme fiber in compression

f_{s_i} = tensile stress in prestressed steel at a particular level, i

f'_{s_i} = compressive stress in non-prestressed steel at a particular level, i.

n = number of levels of prestressed steel

n' = number of levels of non-prestressed steel

c = distance from the extreme fiber in compression to neutral axis at failure

k_1 = ratio of maximum concrete compressive stress to average concrete compressive stress

k_3 = ratio of maximum concrete compressive stress to f'_c

Since the strain distribution remains linear to failure:

$$\epsilon_{cu_i} = \left(\frac{d_i - c}{c}\right) \epsilon_u \tag{17}$$

$$\epsilon'_{cu_i} = \left(\frac{c - d'_i}{c}\right) \epsilon_u \tag{18}$$

where ϵ_{cu_i} = tensile concrete strain at a particular level, i

ϵ'_{cu_i} = compressive concrete strain at a particular level, i

d_i = distance from extreme fiber in compression to a particular level, i, of prestressed steel

d'_i = distance from the extreme fiber in compression to a particular level, i, of non-prestressed steel

ϵ_u = ultimate concrete compressive strain

Assuming that the change in steel strain during loading to failure is equal to the change in strain in the adjacent concrete:

$$\epsilon_{su_i} = \epsilon_{se_i} + \epsilon_{ce_i} + \epsilon_{cu_i} \tag{19}$$

$$\epsilon'_{su_i} = \epsilon'_{s1_i} + \epsilon'_{ce_i} + \epsilon'_{cu_i} \tag{20}$$

where ϵ_{su_i} = total tensile strain in prestressed steel at a particular level, i

ϵ'_{su_i} = total compressive strain in non-prestressed steel at a particular level, i

ϵ_{se_i} = tensile strain in prestressed steel at a particular level, i, at the effective prestress force

ϵ_{ce_i} = compressive strain in the concrete at a particular level, i, due to prestress

ϵ'_{sl_i} = initial compressive strain in non-prestressed steel at a particular level, i

ϵ'_{ce_i} = tensile strain in the concrete at a particular level, i

The tensile force in the prestressed steel was related to the strain by the following analytical representation of the load-strain curve in Fig. 6:

$$A_{s_i} f_{s_i} = 32.8\ \epsilon_{su_i} \qquad \text{for } 0 < \epsilon_{su_i} < 0.70\%$$

$$A_{s_i} f_{s_i} = -39.5 + 171.8\ \epsilon_{su_i} - 157.9\ \epsilon^2_{su_i} + 63.6\ \epsilon^3_{su_l} - 9.4\ \epsilon^4_{su_i} \qquad \text{for } 0.70\% < \epsilon_{su_i} < 2.0\% \tag{21}$$

$$A_{s_i} f_{s_i} = 29.3 + 0.599\ \epsilon_{su_i} \qquad \text{for } 2.0\% < \epsilon_{su_i}$$

where $A_{s_i} f_{s_i}$ has units in kips. The compressive stress in the non-prestressed steel was calculated from:

$$f'_{s_i} = E\ \epsilon'_{su_i} \qquad \text{for } \epsilon'_{su_i} < \epsilon_y \tag{22}$$

$$f'_{s_i} = f_y \qquad \text{for } \epsilon'_{su_i} > \epsilon_y$$

Equations 12 through 22 were used to calculate the ultimate flexural strength of the test beams. First a value of c was selected. Next ϵ_{cu_i} and ϵ'_{cu_i} were calculated from Eqs. 17 and 18 assuming ϵ_u

equal to 0.003. Then the total strain in the prestressed and non-prestressed steel, ϵ_{su_i} and ϵ'_{su_i}, were calculated from Eqs. 19 or 20. Values of ϵ'_{s1_i} were determined from experimental Whittemore readings, and are given in Table 8. Then the force or the stress in the steel was calculated from Eqs. 21 or 22. T, C, and C' were calculated from Eqs. 14 through 16 and substituted into Eq. 12. Values for k_1 and k_3 recommended by Mattock, Kriz, and Hognestad[26] were used in Eq. 15, as follows:

$$k_1 = 0.85 - 0.00005\ (f'_c - 4000) \qquad \text{for } f'_c \geq 4000 \text{ psi} \qquad (23)$$

$$k_3 = 0.85 \qquad (24)$$

If Eq. 12 was satisfied, the correct value of c had been selected. If not, a new value of c was selected, and the procedure repeated until Eq. 12 was satisfied. Then M_{fu} was calculated from Eq. 13. This procedure was easily performed on a computer, and the resulting calculated flexural strength of the test beams is given in Table 8.

The maximum applied load moment, M_f, and the maximum dead load moment, M_d, sustained by the test beams are also given in Table 8. The ratio of the maximum moment in the test beams at failure to the calculated flexural strength is given in the last column Table 8. Flexural failures occurred in the second test on G-2 and the first test on G-4. The ratio of test to calculated strength in these tests was 0.975 and 0.980. The shear failure in the first test on G-3 occurred at a load approximately 1 percent greater than its calculated flexural strength. The remaining shear failures occurred at loads ranging from 4.5 to 29.0 percent below the calculated flexural strength.

6.5 ULTIMATE SHEAR STRENGTH

The three basic types of shear failures in prestressed concrete beams are web crushing, shear compression, and fracture of the web reinforcement. The action causing these types of shear failures may be described by considering the free body diagram shown in Fig. 31. This free body diagram was drawn by separating a beam along the path of an inclined crack, and by a vertical cut through the concrete at the apex

of the crack. The resultant force in the prestressed steel is represented by the horizontal and vertical components, T_h and T_v. V_w is the resultant force in the vertical web reinforcement. The resultant force transmitted above the apex of the crack is represented by the horizontal compressive thrust, C_h, and a vertical shear, C_v. Forces which would exist if the inclined crack did not extend completely through the tension flange are assumed to add to T_h and T_v.

Web crushing failures occurred when the resultant thrust causes the concrete in the web to fail. These failures usually occur in the web above the inclined crack, due to eccentricity of the resultant thrust on a section above the inclined crack. Web crushing failures are often complicated by the formation of several inclined cracks in the web. These cracks divide the web into individual compressive struts. If the compressive force in a strut is eccentric with respect to the axis of the strut, crushing may occur at the intersection of the web and the top flange.

Shear compression failures occur when the resultant thrust causes the concrete in the compression flange to fail. These failures may be due to general crushing and destruction in the region above the apex of an inclined crack, or to the sudden extension of an inclined crack completely through the compression flange. Shear compression failures are influenced by the location of the load point.

Other types of shear failures may occur if the beam is not properly proportioned. Stirrups must be adequately anchored in both the tension and compression flange to prevent a pull-out failure when crossed by an inclined crack. There must also be adequate anchorage of the tension steel so that the force T_h can be developed. In beams with little or no web reinforcement, the doweling force T_v can tear the tension flange away from the web, which usually results in a web crushing failure near the support.

Two of these types of shear failures were observed in the test beams. Shear compression failures occurred in the first and second test on G-1, the first test on G-2, and the second and third

test on G-4. Stirrups were fractured in the first test on G-3, although the failure was similar to a shear compression failure. In the first test on G-2 and the second test on G-4, the shear compression failure was due to the sudden extension of an inclined crack completely through the compression flange, as shown in Figs. 18c and 21c. The other shear compression failures were due to crushing of the compression flange above the apex of an inclined crack, as shown in Figs. 22b, 26a, and 27d. The stirrup fracture failure is shown in Figs. 28c and 28d.

The pictures all show that the relatively small compression flanges of the test beams influenced their ultimate shear strength. In contrast the majority of the F Series I-beams, with relatively larger compression flanges, failed in the web.

The results of the F Series tests were summarized in Section 1.1. Based upon the results of these and other tests, recommendations were made for the design of web reinforcement in prestressed concrete bridge girders, in the form of the specification which was presented in Section 1.1.1.

For design, it was recommended that the area of web reinforcement placed perpendicular to the axis of the member at any section be not more than that given in Eq. 3. This requirement may be written as:

$$\left(\frac{rf_y}{100}\right)_{max.} = 7\sqrt{f'_c} \tag{25}$$

The average concrete strength of the test beams was approximately 7500 psi. Thus the specification recommends that $rf_y/100$ shall be less than approximately 600 for all of the web reinforcement to be effective in resisting shear. Values of $rf_y/100$ in the test beams ranged from 44 to 114.

It was also recommended that the area of web reinforcement be not less than that given by Eq. 2. This equation may be written as:

$$\left(\frac{rf_y}{100}\right)_{min.} = \frac{\lambda V_u}{b'd_s} \tag{26}$$

Since V_u varies along the length of the test beams, the minimum web reinforcement requirement also varies. However, the web reinforcement was placed at a constant spacing in all of the test regions. Therefore, the critical section would be at a distance d from the support. Assuming d_s equal to 32.5-in. in the box beams, 28-in. in the I-beams with No. 3 stirrups, and 30-in. in the I-beams with No. 2 stirrups, and V_u equal to V_f plus V_d at the critical section, values of $\frac{rf_y}{100}$ min. were calculated for each test. These values may be compared to the amount of web reinforcement provided in Table 9. In all of the tests except one, the amount of web reinforcement provided was less than that required by Eq. 2.

The shear strength of the test beams was predicted from Eq. 1 re-written as Eq. 4. For non-composite beams, the shear at inclined cracking caused by excessive principal tensile stresses in the web may be calculated from the equation:

$$V_{cd} = V_d + \frac{C_1 + \sqrt{C_1^2 - 4C_2}}{2} \tag{27}$$

where

$$C_1 = \frac{xyf_t Ib^2}{Q^2} - 2V_d$$

$$C_2 = V_d^2 - \frac{I^2 b^2}{Q^2}\left[f_t\left(f_t + \frac{F}{A} - \frac{Fey}{I} + \frac{M_d y}{I}\right)\right]$$

For the box beams, the cg is in the web. Therefore Eq. 27 reduces to

$$V_{cd} = \sqrt{\left[\frac{Ib'}{Q_{cg}}\right]^2\left[f_t\left(f_t + \frac{F}{A}\right)\right]} \tag{28}$$

However, for the I-beams, the cg lies below the junction of the web and the bottom flange. Therefore V_{cd} was calculated from Eq. 27 with y equal to $(16 - \bar{y})$. For non-composite beams, the shear at inclined cracking caused by flexural cracking may be calculated from the equation:

$$V_{cf} = \frac{\frac{I}{y}\left(\frac{F}{A} + f_r\right) + Fe - M_d}{x - d} + V_d \tag{29}$$

In all of the tests, the critical section for V_{cd} and V_{cf} was adjacent to the load point, or at x equal to a, and the calculated values of V_{cd} and V_{cf} at this section are given in Table 9. The predicted inclined cracking shear V_c is the least value of V_{cd} and V_{cf}. This is compared to the observed shear at inclined cracking in the test beams, $V_{ic} + V_d$, in Table 9. The ultimate shear V_u was calculated from Eq. 4. The resulting values of V_u are recorded in Table 9, where they are compared to the ultimate test shear, $V_f + V_d$.

Table 9 shows that the test to predicted ratios of inclined cracking shear ranged between 0.73 and 1.20, with the average equal to 1.01. The test to predicted ratios of ultimate shear strength, excluding the flexural failure, ranged from 0.91 to 1.12, with the average equal to 1.04.

It is significant to observe that the low test to predicted ratios of inclined cracking shear for G-1 did not result in proportionally low test to predicted ratios of ultimate shear strength. It is also significant to note that the test to predicted ratios of ultimate shear strength are not appreciably different for the second or third tests than for the first tests. Since these beams were severely cracked in the first test and this did not appreciably affect the subsequent tests, it follows that any shrinkage cracking that a bridge beam may sustain during fabrication would not affect its ultimate shear strength.

The test to predicted ratios of ultimate shear strength in Table 9 are lower than the similar test to predicted ratios of shear strength for previous tests shown in Fig. 1. This difference is largely due to the relatively lower inclined cracking strengths of the test beams which, as discussed previously, may have been due to experimental errors in the determination of the prestress force or to eccentrically applied loads. It is also due, at least to some extent, to the relatively small compression flanges of the test beams. However, it may be concluded that even with these differences, the proposed specification satisfactorily predicted the shear strength of the test beams.

The shear strength of the test beams was also predicted using the provisions of Section 2610 of ACI 318-63 and Section 1.13.13 of the current AASHO specifications, disregarding any minimum steel requirements. These test to predicted ratios are tabulated in Table 10.for comparison of the proposed specification to the AASHO and ACI codes. The high and widely varying test to predicted ratios obtained using the AASHO code indicates that this specification does not reflect the actual behavior of the test beams.

There is little difference between the test to predicted ratios for the proposed specification and the ACI code. If some of the tests had been conducted on a/d ratios less than 2.92, the differences would have been greater, with the proposed specification more closely but conservatively predicting the shear strength. The behavior of the test beams was not significantly affected by the small amount of web reinforcement provided, and the proposed specification requires less minimum web reinforcement than the ACI code.

7. SUMMARY AND CONCLUSIONS

The objective of this investigation was to compare the behavior and strength of full-sized prestressed concrete bridge beams with the behavior and strength of smaller F Series I-beams previously tested at Lehigh University. Four full-sized beams were selected from standard sections used for prestressed bridges in Pennsylvania. Two beams had an I-shaped cross section and two had a hollow box-shaped cross section. One beam of each cross section had a length of 47-ft., and the other had a length of 29-ft. All four beams had a depth of 36-in.

Prestress was applied with 7/16-in. diameter 270 ksi strand initially tensioned to 21.7 kips. Intermediate grade deformed No. 2 and No. 3 bars were used for vertical web reinforcement in the girders. Spacing of the stirrups was varied from 12-in. to 22½-in. The concrete strength of the test beams ranged from 6660 psi to 7930 psi; the average concrete strength at the time of test was 7520 psi. Some special studies were conducted on the effect of the type of cylinder mold on the strength of concrete. These results are summarized on pages 11 and 12.

Nine ultimate strength tests were conducted on the four test beams, on shear span to effective depth ratios ranging from 2.92 to 5.84. Diagonal tension and flexure shear inclined cracking were observed in the tests. Diagonal tension inclined cracking occurred in the tests on shear span to effective depth ratios less than approximately 3.5, and was due to high principal tensile stresses in the webs of the members. In the tests on the shorter box beam, diagonal tension cracking occurred at different loads on opposite sides of the beam in the same shear span. This unsymmetric behavior caused torsion in the shear spans, which detrimentally affected the strength and behavior of the member. Flexure shear inclined cracking was due to flexural cracks that either turned and became inclined in the direction of increasing moment, or precipitated inclined cracking in the web above the flexural crack. Similar inclined cracking, except for the unsymmetric diagonal tension cracking in the short box beam, was also observed in the F Series beams.

Six shear failures and two flexural failures were observed in the tests. Failure occurred prematurely in one other test due to damage sustained in a preceding test. Five of the six shear failures occurred in the compression flange, and were classified as shear compression failures. The other shear failure was caused by fracture of the web reinforcement. Both of these types of shear failure were also observed in the F Series beams.

It was found that both the inclined cracking strength and the ultimate shear strength of the full-sized test beams was somewhat less than the F Series beams. The inclined cracking strength may have been less than expected because of difficulties encountered in experimentally determining the prestress loss. If the prestress loss had been assumed equal to 20 percent, the inclined cracking strength of the test beams would have been comparable to the inclined cracking strength of the F Series beams.

However, it was found that the proposed specification for the design of web reinforcement, which was conservatively based on the results of the F Series beams, satisfactorily predicted the ultimate shear strength of the test beams. It is therefore recommended that this specification be used for design of web reinforcement in bridge beams.

8. ACKNOWLEDGMENTS

This work was conducted in the Department of Civil Engineering at Fritz Engineering Laboratory, under the auspices of the Institute of Research of Lehigh University, as part of a research investigation sponsorec by: the Pennsylvania Department of Highways; the U. S. Department of Commerce, Bureau of Public Roads; and the Reinforced Concrete Research Council.

Completion of this work was facilitated by the capable help of the Fritz Engineering Laboratory staff and technicians. The cooperation and assistance of Mr. Joseph Nagle and Schuylkill Products, Inc. in fabricating the test beams is gratefully acknowledged. The authors wish to thank Dr. D. A. VanHorn and Mr. R. H. R. Tide for their assistance in preparation of this report. The authors also wish to thank Mrs. Valerie Yarimci for typing the manuscript.

9. NOTATION

a	Length of shear span
A	Cross-sectional area of beam
A_s	Cross-sectional area of prestressed steel
A'_s	Cross-sectional area of non-prestressed steel
A_y	Cross-sectional area of one stirrup placed perpendicular to the longitudinal axis of the member
b	Width of beam at the horizontal section under investigation
b'	Width of web
cg	Center of gravity of beam cross-section
cgs	Center of gravity of prestressed steel
C_h	Horizontal component of the resultant compressive force above the apex of an inclined crack
C_v	Vertical component of the resultant compressive force above the apex of an inclined crack, i.e., the shear carried by the concrete
d	Distance from the extreme fiber in compression to the cgs, i.e., the effective depth of the member
d_s	Distance from the extreme fiber in compression (in composite sections from the top of the girder alone) to the lowest level at which the stirrups are effective
e	Eccentricity of prestress force, i.e., distance from cg to cgs
E	Modulus of elasticity of non-prestressed reinforcing bars
E_c	Modulus of elasticity of concrete
f	Normal stress
f'_c	Compressive strength of concrete
f'_{ci}	Compressive strength of concrete at release
f_{pt}	Principal tensile stress
f_r	$8\sqrt{f'_c}$
f'_r	Flexural tensile strength of concrete
f'_{sp}	Splitting tensile strength of concrete
f_t	$(6 - 0.6\,\frac{x}{d})\sqrt{f'_c}$, but not less than $2\sqrt{f'_c}$

f_y	Yield point of non-prestressed steel
F	Prestress force at time of test
F_i	Prestress force before release
i	Particular level of steel
I	Moment of inertia about the cg of the cross-section
L	Span length
M	Moment
M_{cr}	Applied load moment causing flexural cracking
M_d	Dead load moment
M_{fc}	Flexural cracking moment
M_{fu}	Ultimate flexural moment
M_f	Applied load moment causing failure
Q	Moment, about the cg, of the area of the cross-section on one side of the horizontal section under investigation
Q^{bf}	Q for a section taken at the junction of the web and bottom flange
Q^{cg}	Q for a section taken at the cg
Q^{mw}	Q for a section taken at the mid-height of the web
Q^{tf}	Q for a section taken at the junction of the web and top flange
r	Web reinforcement ratio in percent, equal to 100 $A_v/b's$
s	Spacing of stirrups
T_h	Horizontal component of the resultant force in the prestressed steel
T_v	Vertical component of the resultant force in the prestressed steel
v	Shear stress
V	Shear
V_c	Shear at inclined cracking
V_{cd}	Shear at inclined cracking caused by excessive principal tensile stress in the web
V_{cf}	Shear at inclined cracking caused by flexural cracking
V_{cr}	Applied load shear causing flexural cracking
V_d	Dead load shear
V_f	Applied load shear causing failure
V_{ic}	Applied load shear causing significant inclined cracking

V_u	Ultimate shear
V_w	Resultant force in web reinforcement
x	Distance from the vertical section under investigation to the closest support
y	Distance from the cg of the cross-section to the horizontal section under investigation, positive upwards
$\bar{y}$	Distance from bottom fibers to the cg of the cross-section
Z^b	Section modulus with respect to stress in the bottom fibers
Z^t	Section modulus with respect to stress in the top fibers
ϵ	Strain
θ	Angle, with respect to the horizontal, of the compressive stress trajectory, positive counterclockwise

10. TABLES

Table 1 Properties of the Concrete

BEAM	AT TRANSFER				AT TEST							
	METAL MOLD		CARDBOARD MOLD		METAL MOLD				CARDBOARD MOLD			
	VIBRATED		VIBRATED		VIBRATED			RODDED	VIBRATED			RODDED
	f'_c	E_c	f'_c	E_c	f'_c	E_c	f'_{sp}	f'_c	f'_c	E_c	f'_{sp}	f'_c
	psi	ksi x10^{-3}	psi	ksi x10^{-3}	psi	ksi x10^{-3}	psi	psi	psi	ksi x10^{-3}	psi	psi
G-1	6370		6190		8240*		505		7830*		540	
3 Days**	6900*		6610*		7760*		660*		7250*		670*	
46 Days	6790*		5870*		7600*		690*		7800*	5.3*	615*	
	6740	5.0	6210	4.7	7520*		585*	7690*	7300*	5.0*	520*	6840*
	7340*	5.0*	6980*	4.7*	8710*	5.2*	580*	7850*	7290*	4.9*	540*	7410*
	6760*	5.0*	6690*	4.9*	7660*	5.3*	580*	7680*	8260*	5.1*	610*	7210*
AVE.	6820	5.0	6430	4.8	7920	5.3	600	7740	7620	5.1	585	7150
G-2									6430			
3 Days	5660		5480		6910		620		6190*		570	
32 Days	5550*		5380*		6720*		605		6310*		540	
	5480*		5730*				555*		6540*		600*	
	6210	4.9	5850		6530	4.6	575*	6790*	7160	5.1	615*	6570*
	6440*	4.9*	5620*		6300*	5.0*	600*	6880*	6280*	4.8*	580*	6420*
	6140*	4.8*	6200*		6840*	5.0*	560*	6980*	6740*	4.9*	505*	6910*
AVE.	5910	4.9	5710		6660	4.8	585	6880	6520	4.9	570	6630
G-3	5770		5910		7650		695		7270		665	
2 Days	7000*		5800*		8180*		670*		6990*		545*	
42 Days	6120*		5220		8360*		580*		6210		650*	
	6130	5.0	6000	4.6	7560	5.0	705*	7460*	7360	4.7	675*	6800*
	7290*	5.0*	6810*	4.7*	7790*	5.5*	580*	7600*	7530*	4.8*	535*	7070*
	7090*	4.6*	5180	5.4	8020*	5.2*	660	7410*	7000*	4.9*	590*	6860*
AVE.	6570	4.9	5820	4.9	7930	5.2	650	7490	7060	4.8	610	6910
G-4	6150		6150		7500*		645		7550*		680	
2 Days	6120*		5770*		8180*		645		7760*		605	
36 Days	6260*		6010*		7890*		565*		7370*		675*	
	6250	4.8	6420	4.5	7620	4.7	580*	7850	7620	4.5	610*	7160
	5990*	4.6*	6660*	5.0*	6810	4.9	730*	7820	7360	4.8	640*	7640
	6440*	4.8*	6460*	4.9*	7480*	4.8*	570*	7600*	7790*	5.1*	635*	7320*
AVE.	6200	4.7	6250	4.8	7580	4.8	625	7760	7580	4.8	640	7370

* Strength of cylinders representative of concrete in the web and compression flange of the test beams.

** Age of cylinders at transfer and at test

Table 2 Dates of Operations

Beam	Date				
	Cast	Prestress Release	1st Test	2nd Test	3rd Test
G-1	4/24/64	4/27/64	6/ 9/64	6/10/64	-
G-2	4/17/64	4/20/64	5/19/64	5/20/64	-
G-3	4/22/64	4/24/64	6/ 3/64	6/ 5/64	-
G-4	4/20/64	4/22/64	5/26/64	5/27/64	5/29/64

Table 3 Prestress Data

Beam	F_i (kips)	Total Percent Loss	F (kips)
G-1	563.8	8	518.7
G-2	345.6	6	324.9
G-3	558.6	8	513.9
G-3	344.8	6	324.1

Table 4 I-Beam Test Results

Beam	Test	Test Setup	$\frac{a}{d}$	V_{cr} (kips)	V_{ic} (kips)	V_f (kips)	Failure
G-2	1	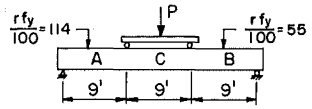	3.49	72	A End 104 B End 104	110	B End Shear
	2	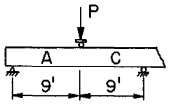	3.49	—	—	118	Flexure
G-4	1	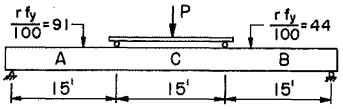	5.84	34	—	66	Flexure
	2	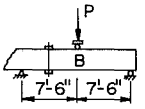	2.92	76	110.5	114	Shear
	3	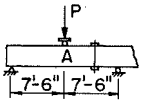	2.92	76	119	136	Shear

Table 5 Box Beam Test Results

Beam	Test	Test Setup	$\frac{a}{d}$	V_{cr} (kips)	V_{ic} (kips)	V_f (kips)	Failure
G-1	1	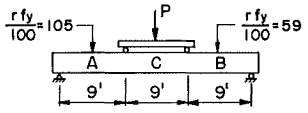	3.34	120	(B Right) 136 (A Left) 152 (A Right) 192	198.5	A End Shear
	2	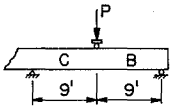	3.34	—	B(Left) 206.5	215.5	B End Shear
G-3	1	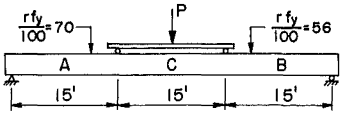	5.56	68	B End 116	127.5	B End Shear
	2	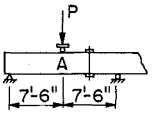	2.78	—	—	192	—

Table 6 Inclined Crack Widths

Beam	Test	End	$\frac{rf_y}{100}$ (psi)	First Observation		Last Observation	
				Crack Width (in.)	Percent of Ult. Load	Crack Width (in.)	Percent of Ult. Load
G-1	1	A(left)	105	0.030	76	0.05	88.6
	2	B(right)	59	-	-	0.17	97.0
G-2	1	A	114	0.030	91	0.065	98.2
	1	B	55	0.064	89	0.174	98.2
	2	A	114	-	-	0.106	98.4
G-3	1	A(left)	70	-	-	0.104	97.2
	1	B(left)	56	-	-	0.132	97.2
G-4	1	A	91	-	-	0.032	97.0
	1	B	44	-	-	0.027	97.0
	2	B	44	0.079	97	0.131	100.0
	3	A	91	0.029	80	0.098	98.5

Table 7 Flexural Cracking Strength

Beam	Test	V_{cr} (kips)	M_{cr} (kip-ft)	M_d (kip-ft)	f'_r (psi)	$\frac{f'_r}{\sqrt{f'_c}}$	$\frac{f'_r}{f'_{sp}}$	Test/Spec
G-1	1	120	1080	53	307	3.45	0.51	0.85
G-2	1	72	648	38	659	8.06	1.13	1.00
G-3	1	68	1020	154	415	4.67	0.64	0.88
G-4	1	34	510	106	411	4.72	0.66	0.87
G-4	2	76	570	12	289	3.32	0.46	0.83
G-4	3	76	570	12	289	3.32	0.46	0.83
Ave.						4.59	0.64	0.88

Table 8 Ultimate Flexural Strength

Beam	ϵ'_{sl_i} * (%)	M_{fu} (kip-ft)	Test	M_f (kip-ft)	M_d (kip-ft)	$\frac{M_f+M_d}{M_{fu}}$
G-1	0.0076	2055	1	1786	52.9	0.895
	0.0082		2	1940	23.3	0.955
G-2	0.0095	1106	1	990	38.0	0.929
			2	1062	16.8	0.975
G-3	0.0125	2053	1	1914	154.2	1.007
	0.0129		2	1440	16.9	0.710
G-4	0.0165	1119	1	990	106.3	0.980
			2	855	11.6	0.774
			3	1020	11.6	0.922

*G-1 and G-3 have two levels of non-prestressed steel.
The upper value is for the upper level steel.

Table 9 Ultimate Shear Strength

Beam	Test	$\frac{rf_y}{100}$	$\frac{rf_y}{100}$ min	V_{cd} (kips)	V_{cf} (kips)	$\frac{V_{ic}+V_d}{V_c}$	V_u (kips)	$\frac{V_f+V_d}{V_u}$
G-1	1	105	126	185.8	205.4	0.83	219.9	0.91
	2	59	135	185.8	206.6	0.73	205.0	1.05
G-2	1	55	95	97.1	103.4	1.09	107.0	1.04
	2*	114	107	97.1	104.1	1.07	116.2	1.01
G-3	1	56	85	144.2	100.6	1.20	118.8	1.11
	2**	70	117	195.0	271.0	-	201.3	-
G-4	1*	44	62	79.3	51.7	-	59.6	1.16
	2	44	96	106.1	139.1	1.04	114.0	1.00
	3	91	123	106.1	139.1	1.12	121.4	1.12

* Flexural failures. Shear strength calculations based on shear span with least amount of web reinforcement.

** Premature failure affected by the first test.

Table 10 Test to Predicted Shear Strength Ratios

Beam	Test	$\frac{a}{d}$	V_u Test/V_u Pred.		
			Proposed Specification	AASHO Code	ACI Code 318-63
G-1	1	3.34	0.91	1.9	0.96
	2	3.34	1.05	2.8	1.10
G-2	1	3.49	1.04	2.5	1.12
G-3	1	5.56	1.11	1.8	1.09
G-4	2	2.92	1.00	3.2	1.08
	3	2.92	1.12	2.6	1.19
Ave.			1.04	2.5	1.09

11. F I G U R E S

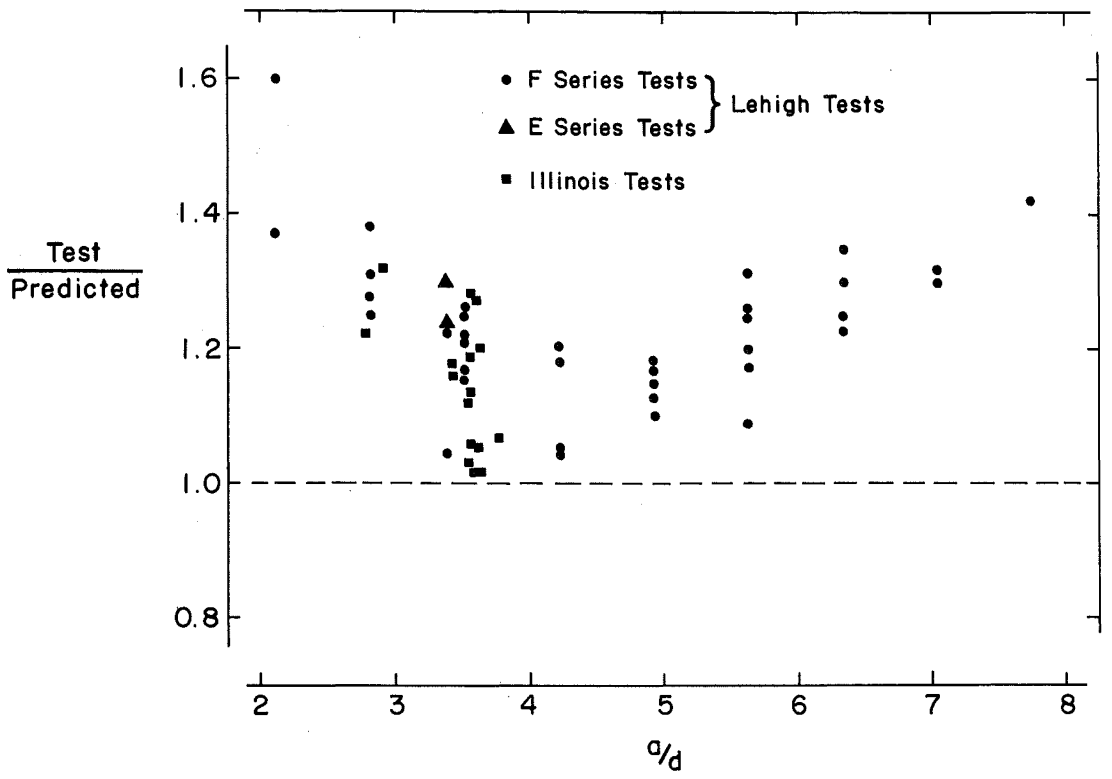

Fig. 1 Shear Strength Predicted by Eq. 4

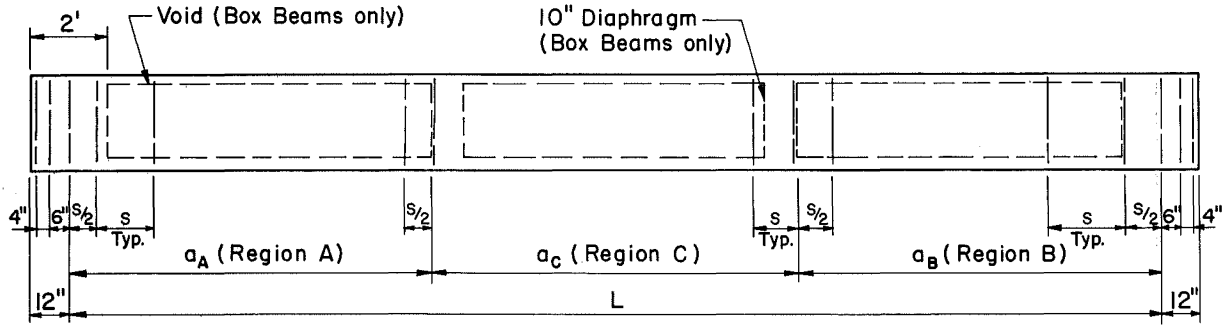

Elevation of Test Beams

Beam	Dimensions			Web Reinforcement								
				Region A			Region C			Region B		
	$a_A=a_B$	a_C	L	Size	s	$rf_y/100$	Size	s	$rf_y/100$	Size	s	$rf_y/100$
	(ft)	(ft)	(ft)	(No.)	(in.)	(psi)	(No.)	(in.)	(psi)	(No.)	(in.)	(psi)
G-1	9	9	27	3	12	105	5	12	247	3	21.6	59
G-2	9	9	27	3	18	114	5	12	412	2	18	55
G-3	15	15	45	3	18	70	5	12	247	3	22.5	56
G-4	15	15	45	3	22.5	91	5	12	412	2	22.5	44

Fig. 2 Elevation and Details of G Series Beams

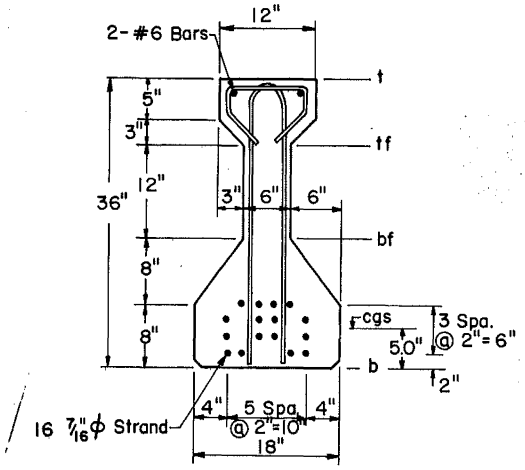

I Beams G-2 and G-4

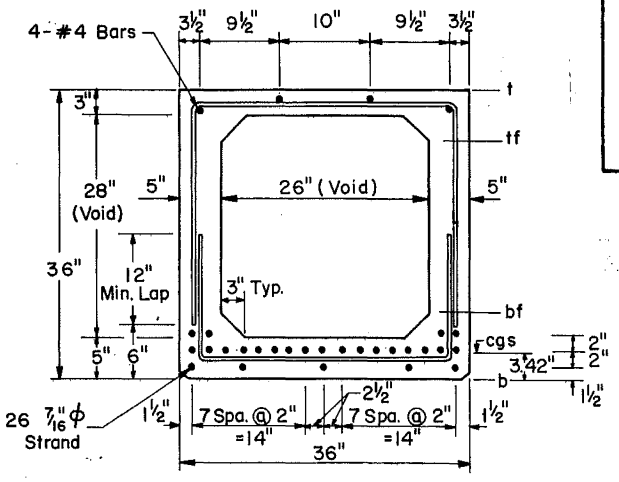

Box Beams G-1 and G-3

Section Property	I Beams	Box Beams
A	398.4-in.^{2}	585.4-in.^{2}
$\bar{y}$	15.21-in.	16.80-in.
I	50,690-in.^{4}	93,730-in.^{4}
Z^t	2438-in.^{3}	4882-in.^{3}
Z^b	3334-in.^{3}	5579-in.^{3}
Q^{tf}	1488-in.^{3}	2489-in.^{3}
Q^{cg}	-	3361-in.^{3}
Q^{mw}	1840-in.^{3}	-
Q^{bf}	1977-in.^{3}	2973-in.^{3}

Fig. 3 Cross-Sections of G Series Beams

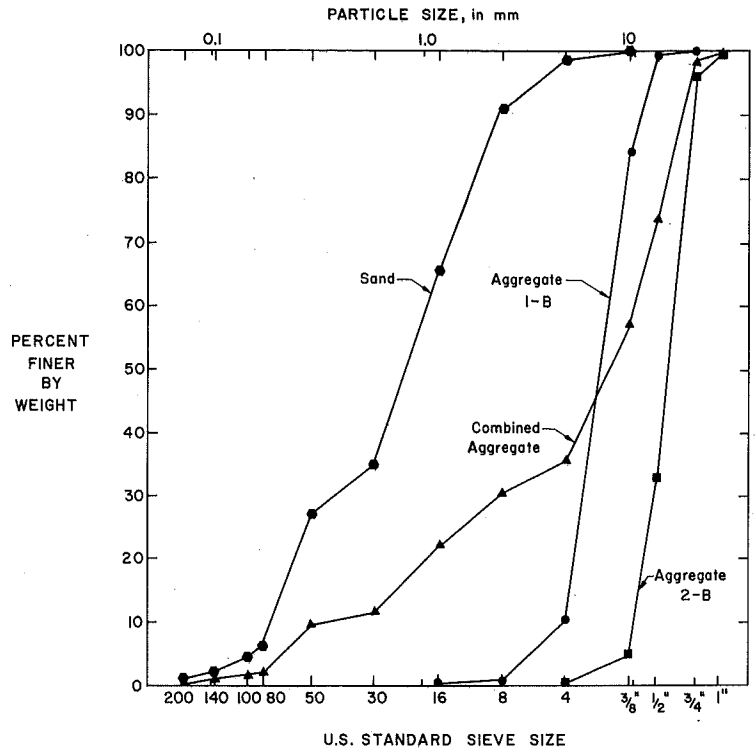

Fig. 4 Gradation of Fine and Coarse Aggregate

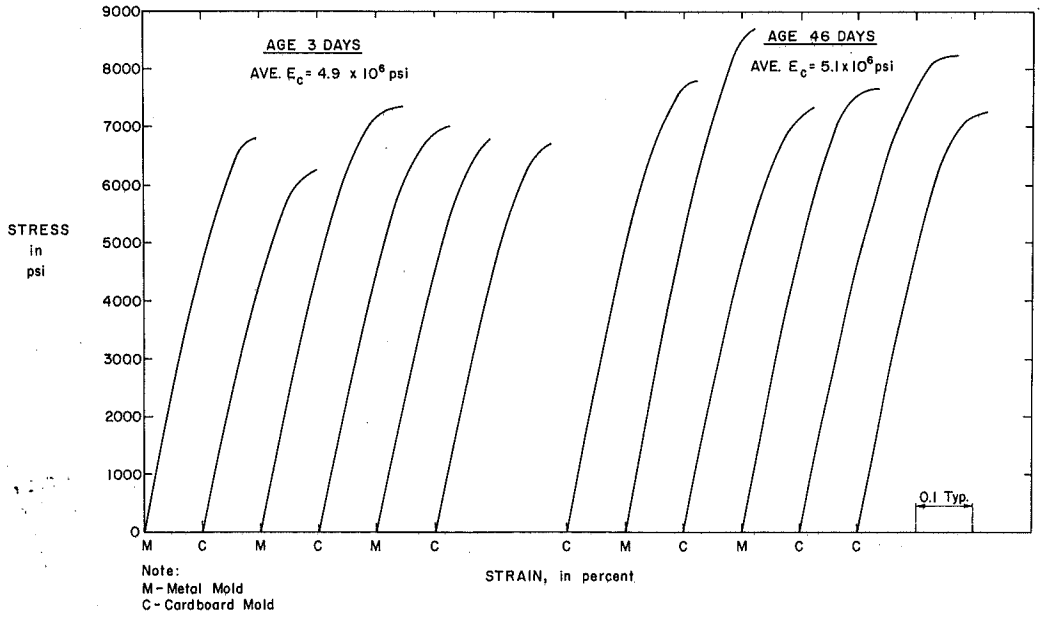

Fig. 5 Cylinder Tests for G-1

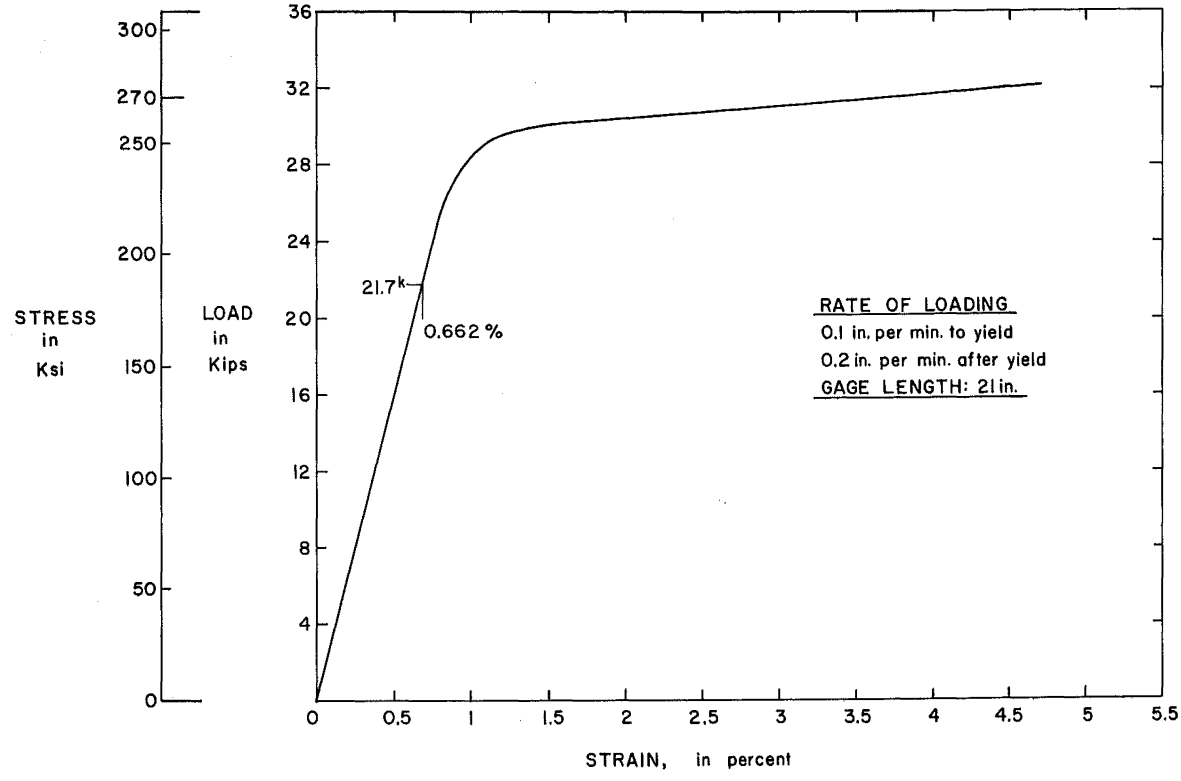

Fig. 6 Load-Strain Curve for Prestressing Strand

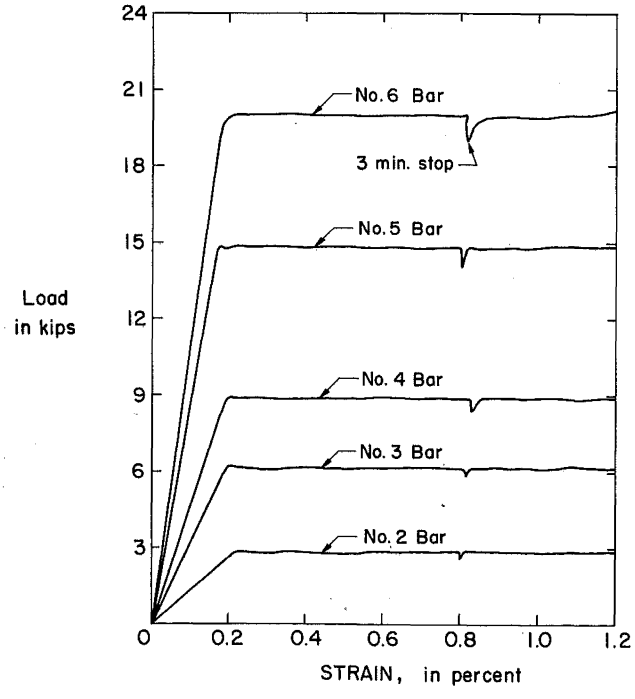

Bar Size		2	3	4	5	6
Yield Point	ksi	60.1	57.3	44.8	47.8	46.0
Tensile Strength	ksi	84.4	84.0	72.1	76.4	75.3
Elongation	%	17.2	21.3	25.1	24.9	23.9

RATE OF LOADING
0.1 in. per min. to Yield
0.2 in. per min. after Yield

Fig. 7 Load-Strain Curves for Non-Prestressed Steel

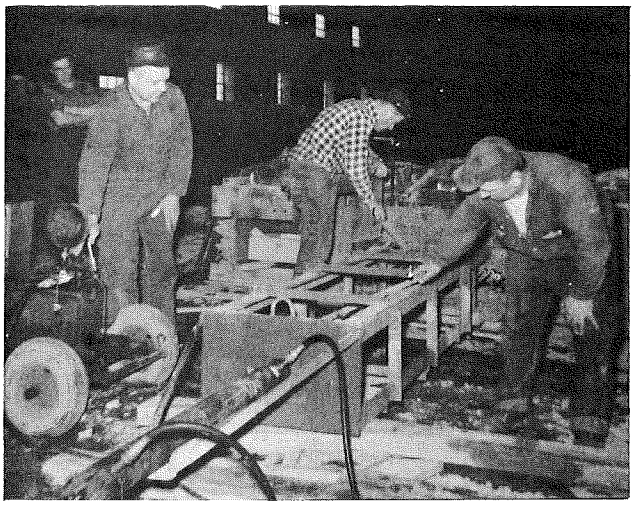

Fig. 8 Stressing of Individual Strands

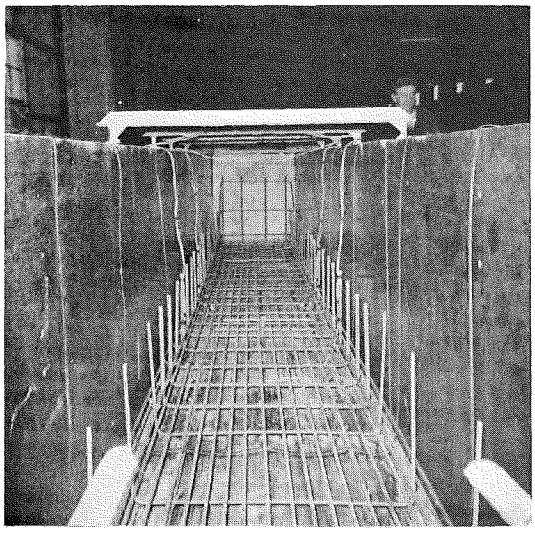

a. View from End

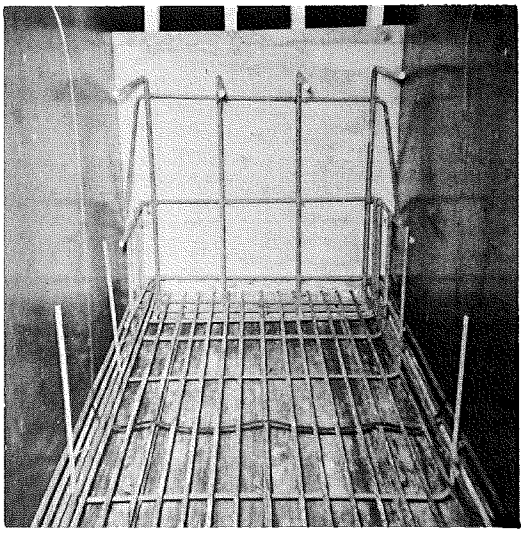

b. View of End Region

Fig. 9 Box Beams before Placing Concrete

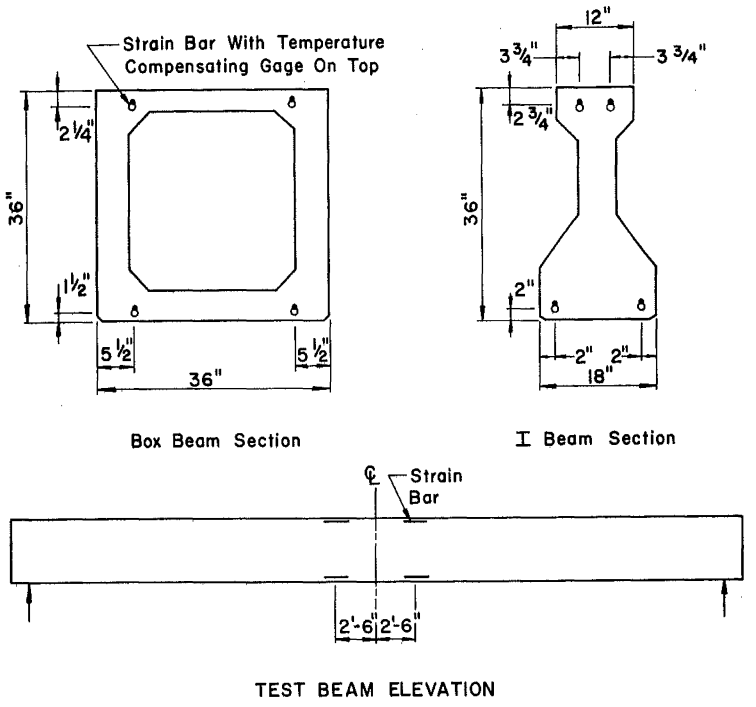

Fig. 10 Location of Internal Strain Bars

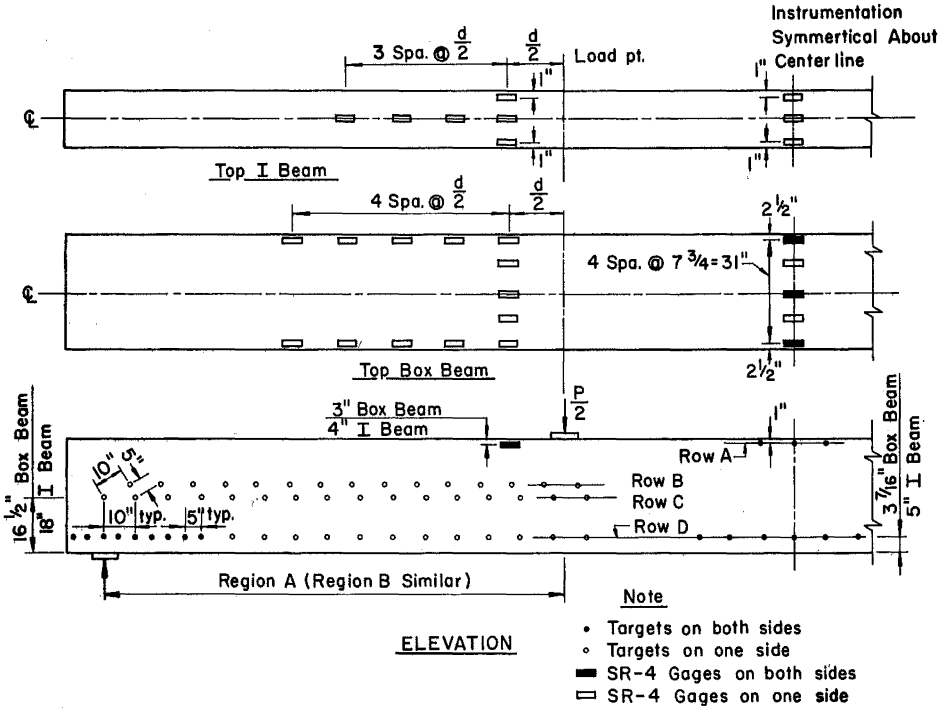

Fig. 11 Location of Whittemore Targets and SR-4 Gages

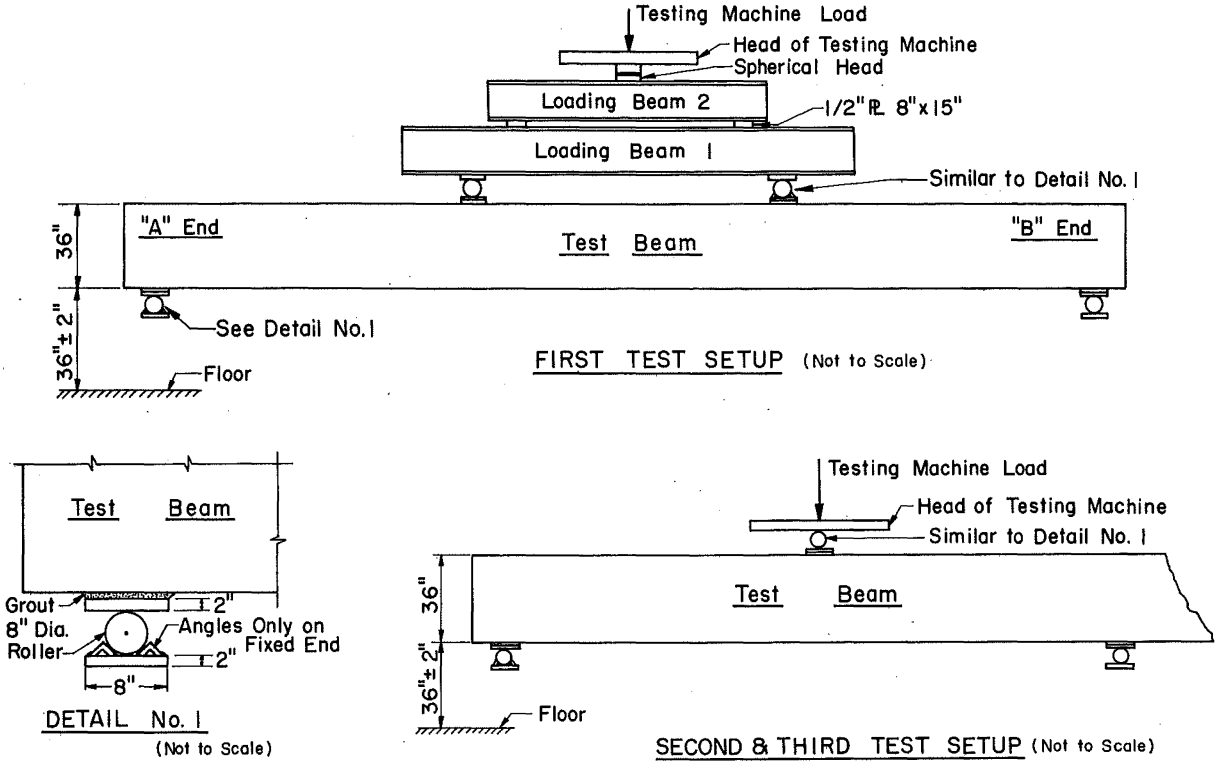

Fig. 12 Testing Arrangement

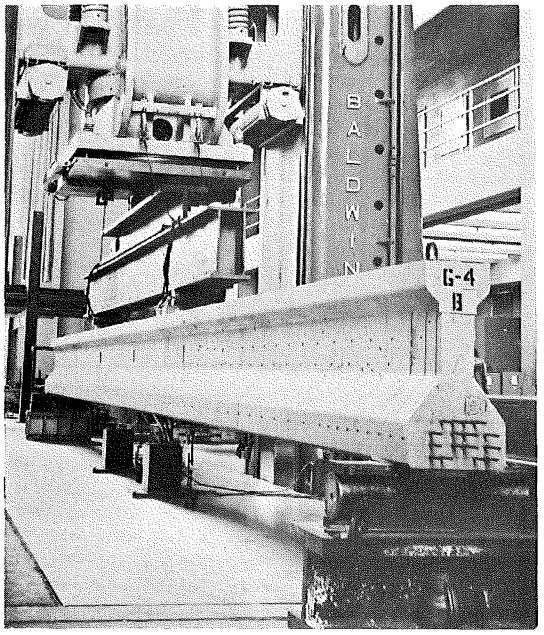

a. First Test on G-4

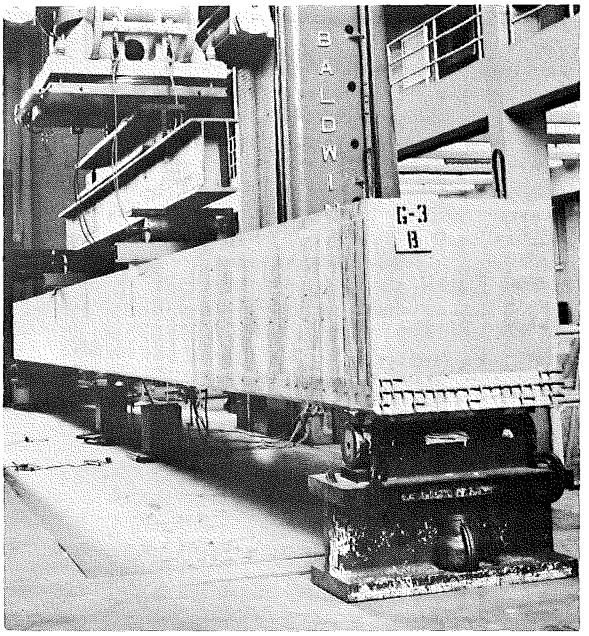

b. First Test on G-3

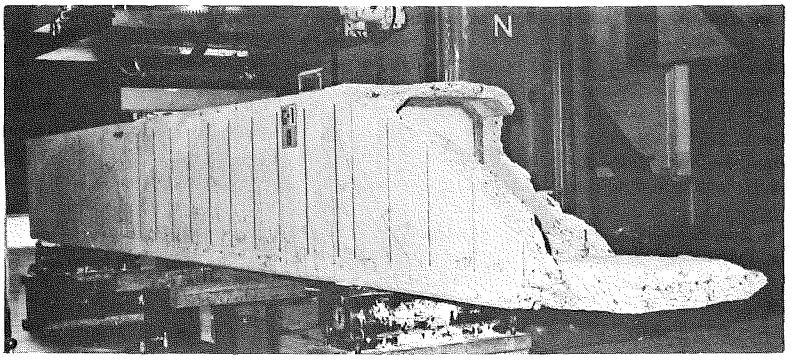

c. Second Test on G-1

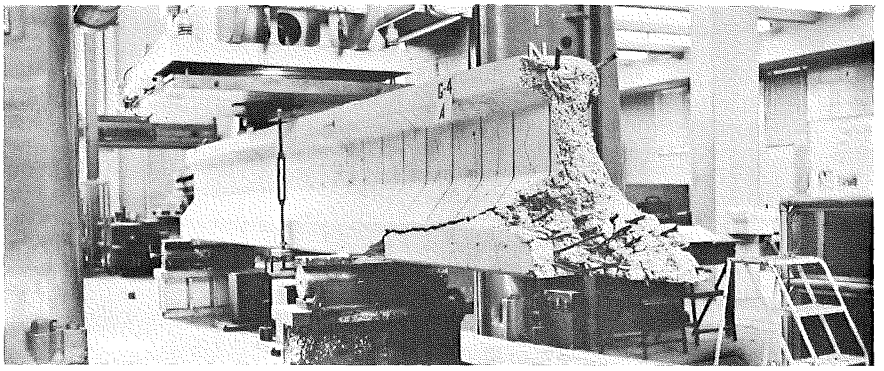

d. Third Test on G-4

Fig. 13 Views of Beams Prior to Test

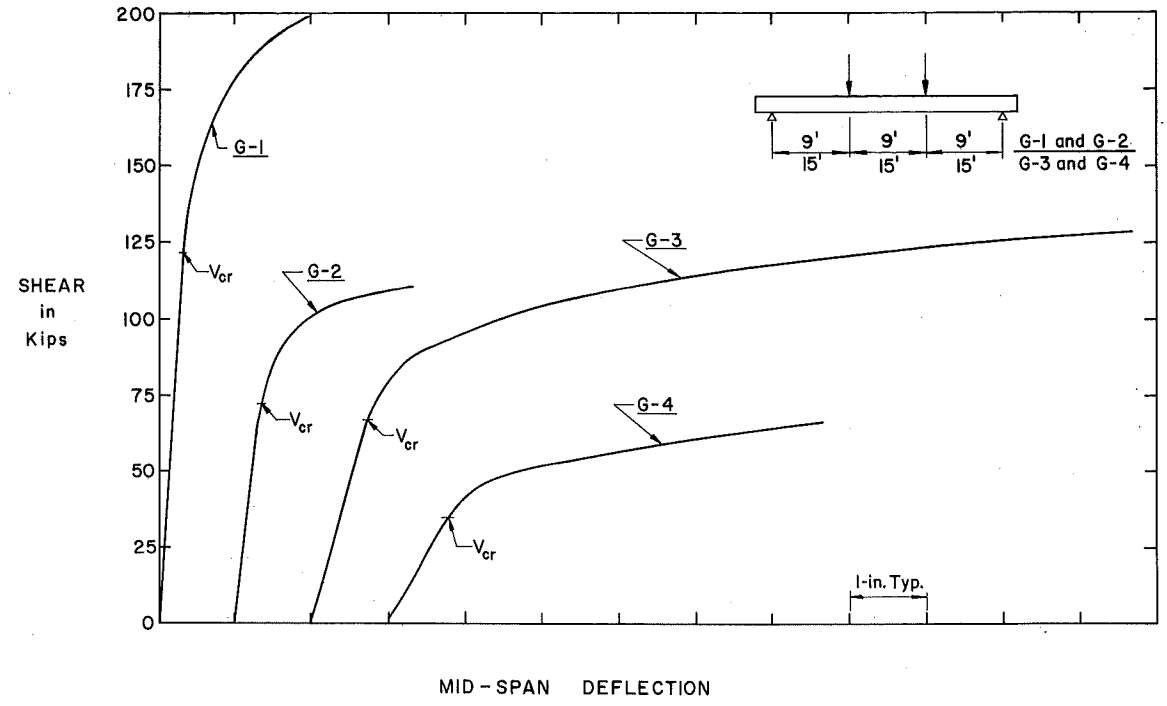

a. First Test

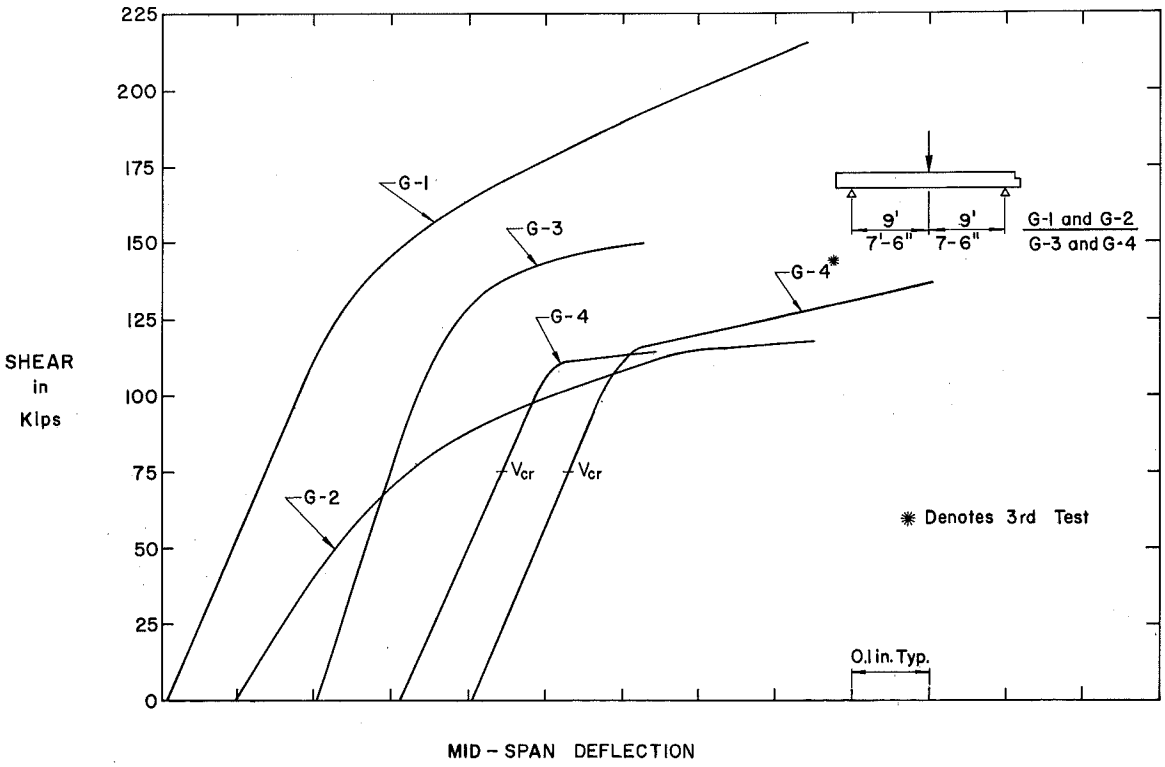

b. Second Test

Fig. 14 Load-Deflection Curves

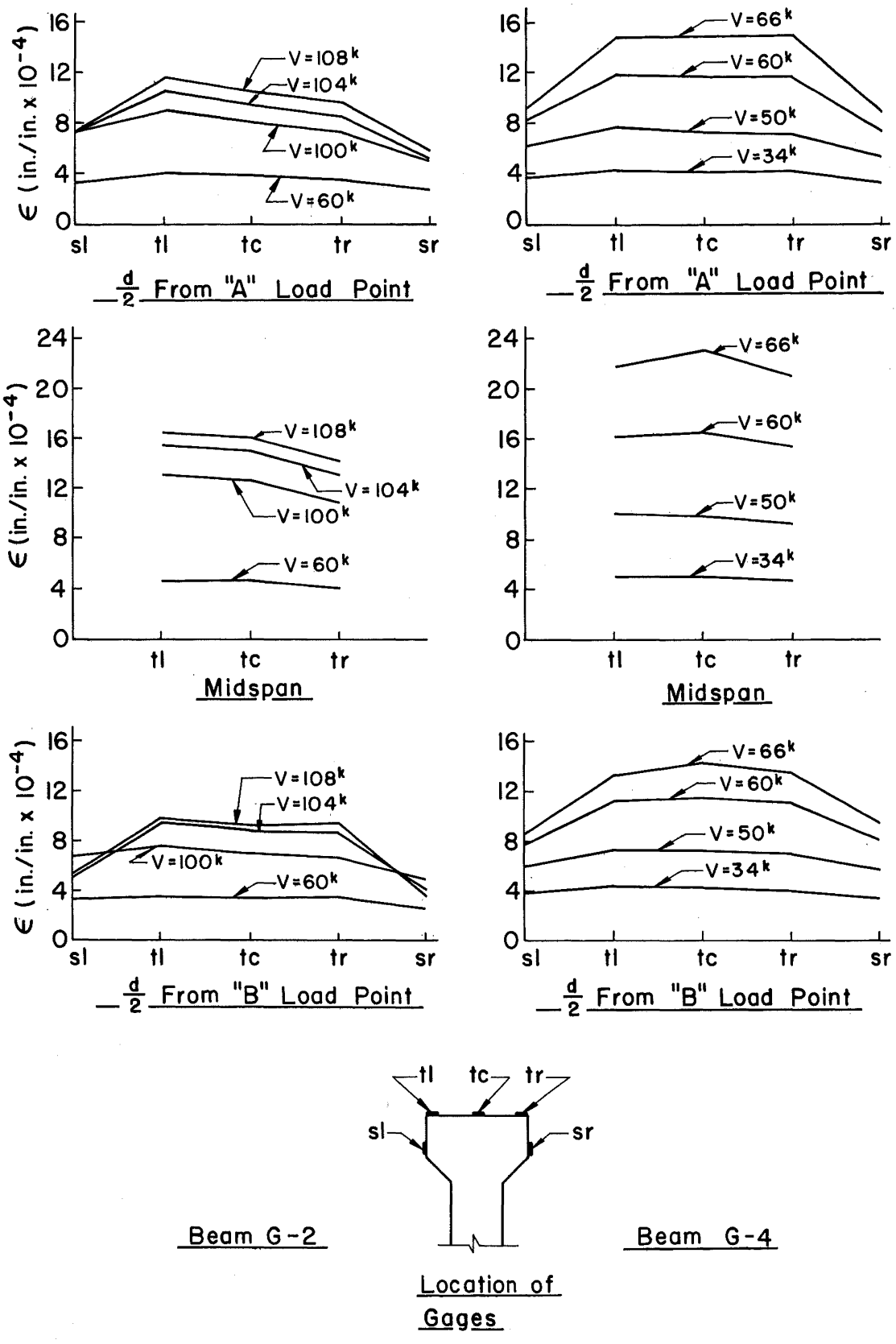

Fig. 15 Strain Measurements during the First Test on G-2 and G-4

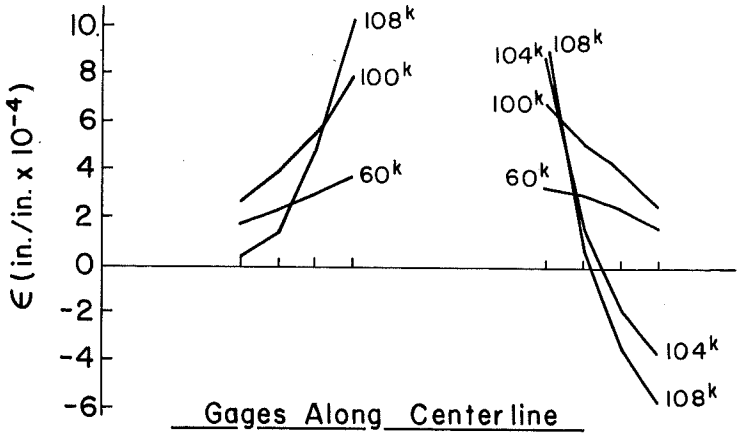

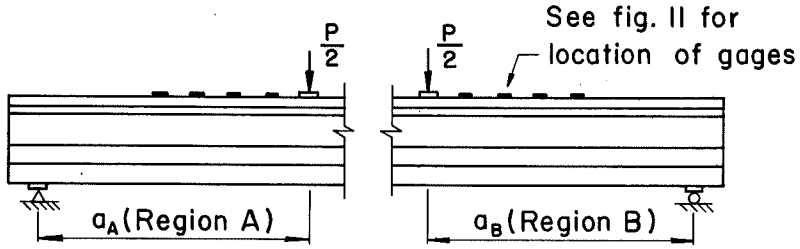

Beam G-2

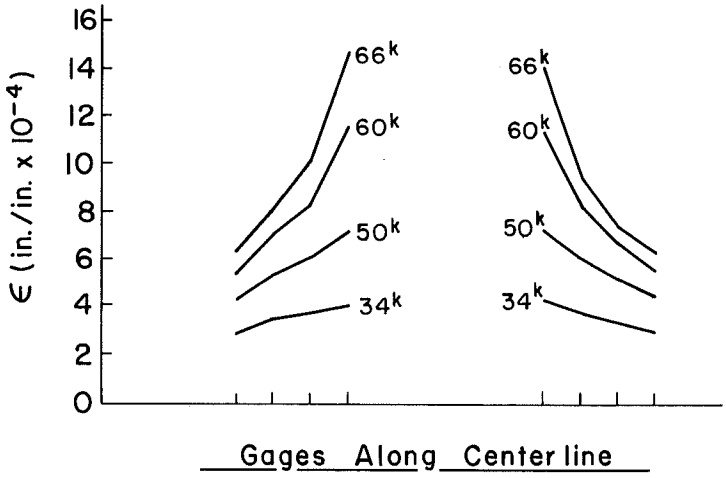

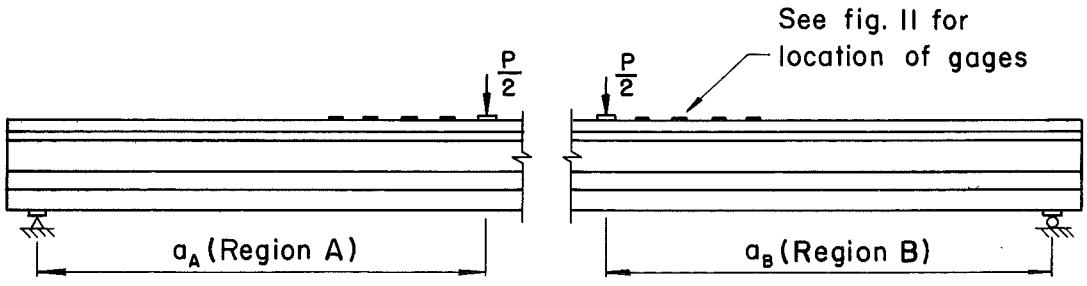

Beam G-4

Fig. 15 Cont.

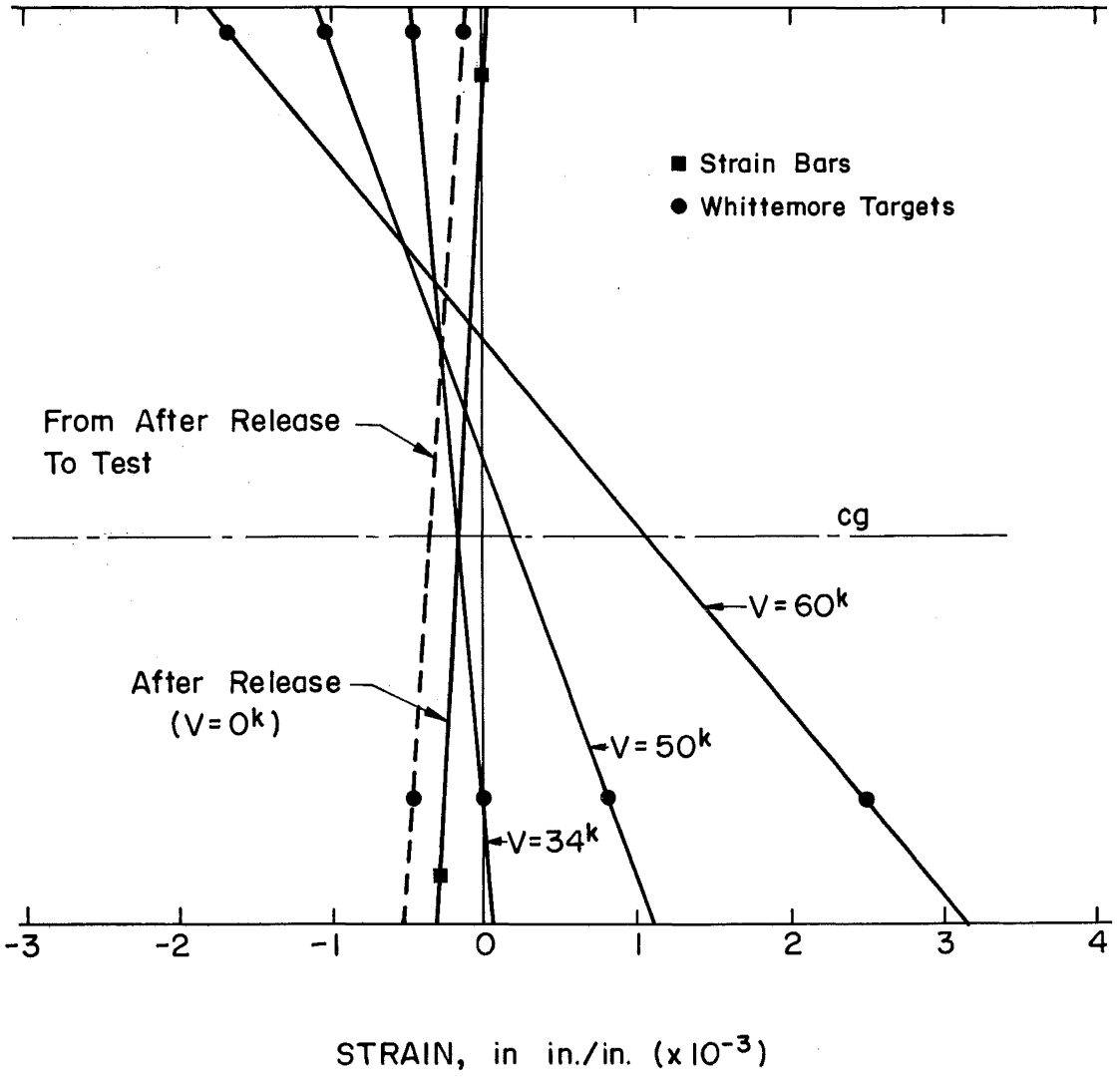

Fig. 16 Strain at Mid-Span of G-4

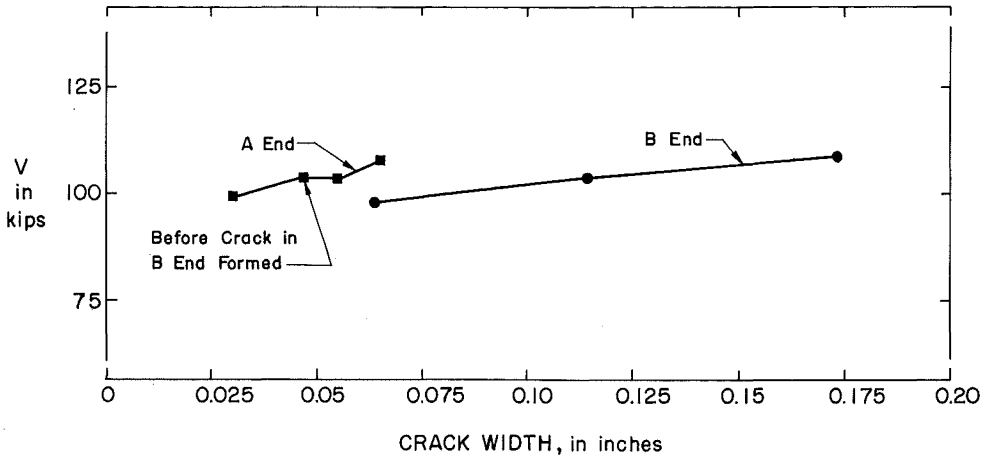

a. First Test on G-2

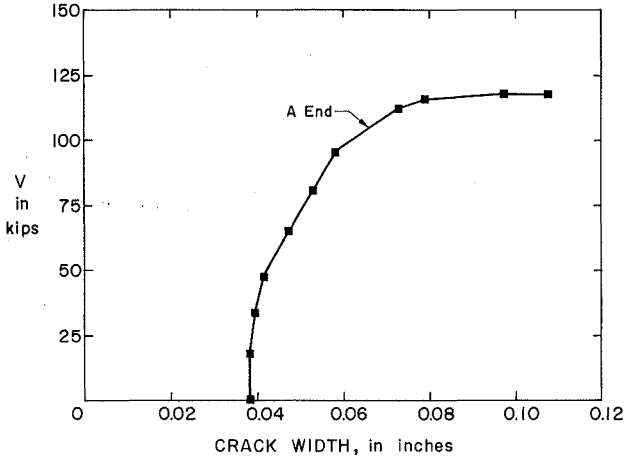

b. Second Test on G-2

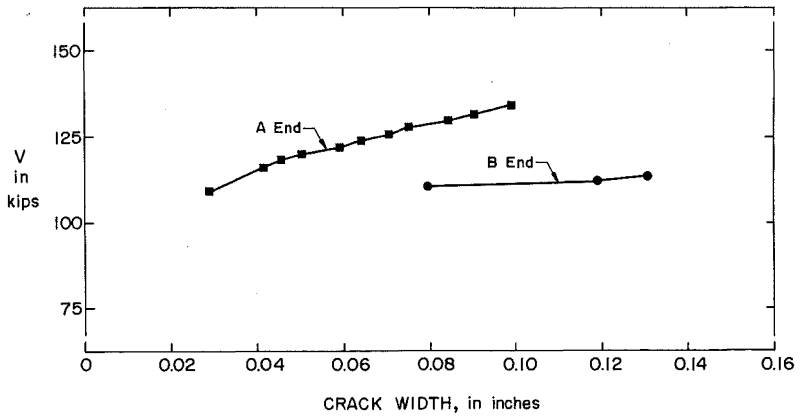

c. Second and Third Tests on G-4

Fig. 17 Inclined Crack Widths in G-2 and G-4

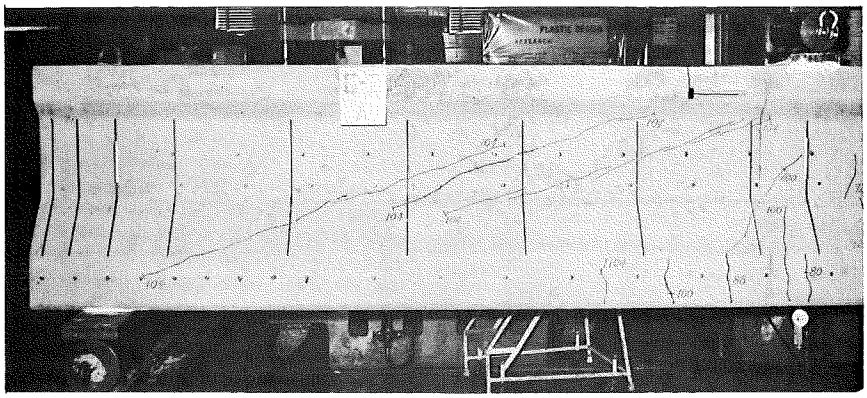

a. Region A after Inclined Cracking

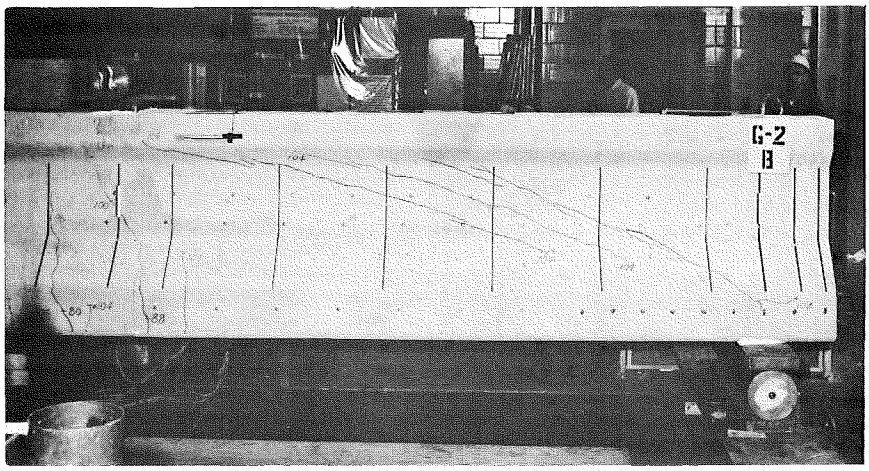

b. Region B after Inclined Cracking

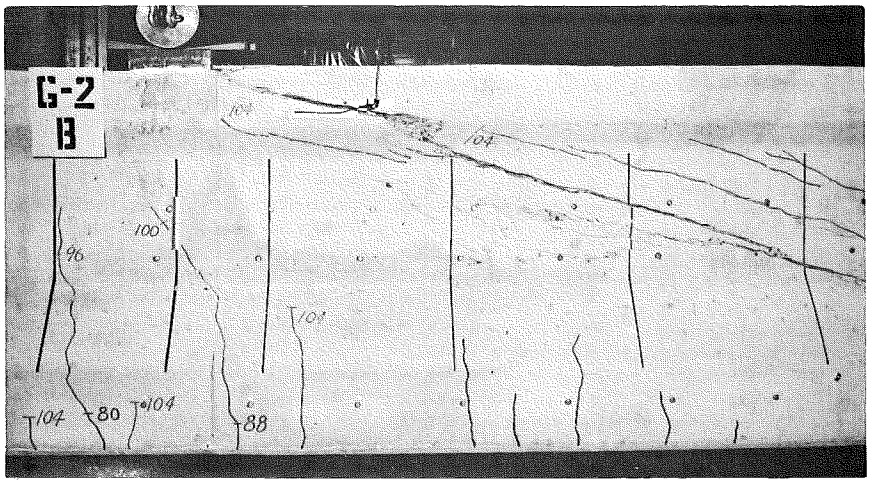

c. Region B after Failure

Fig. 18 First Test on G-2

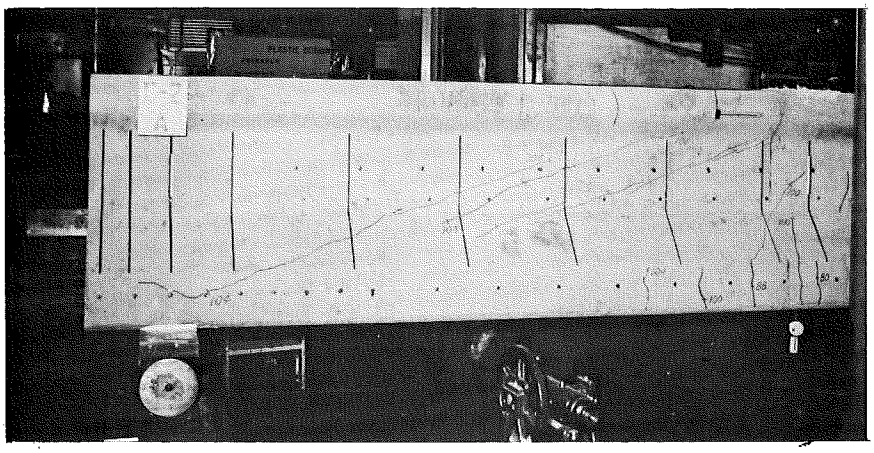

a. Condition of Region A at Start of Test

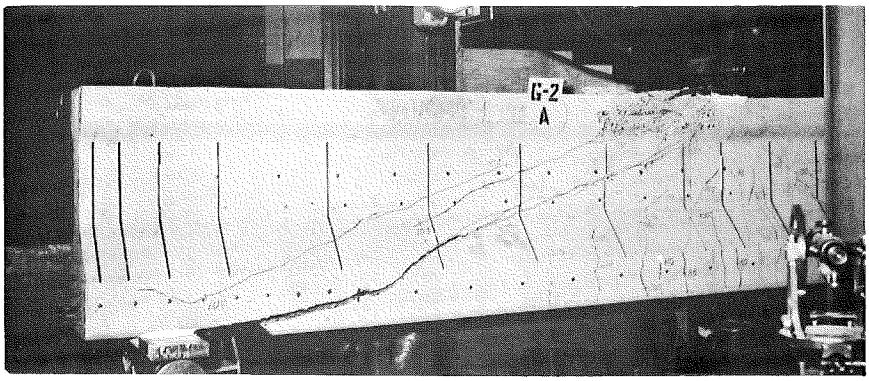

b. Region A after Failure

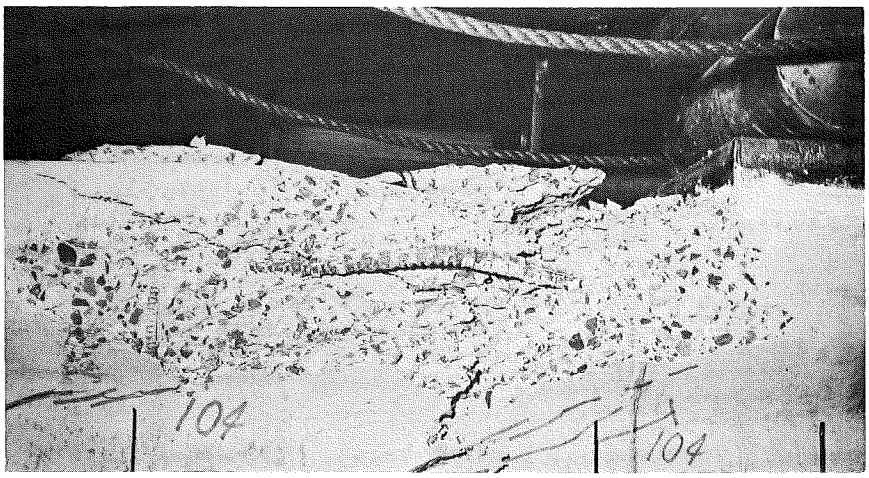

c. View of Failure Region

Fig. 19 Second Test on G-2

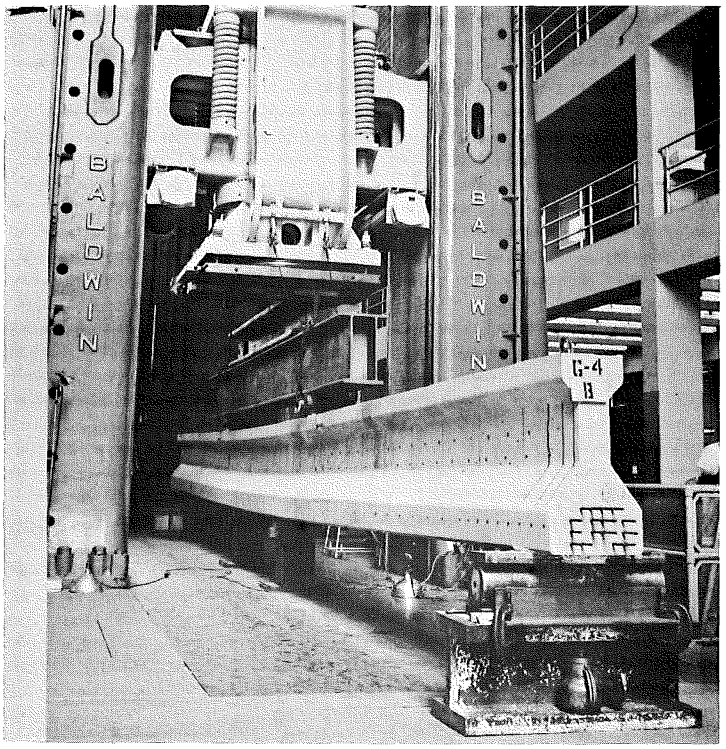

a. During Loading Near Ultimate Capacity

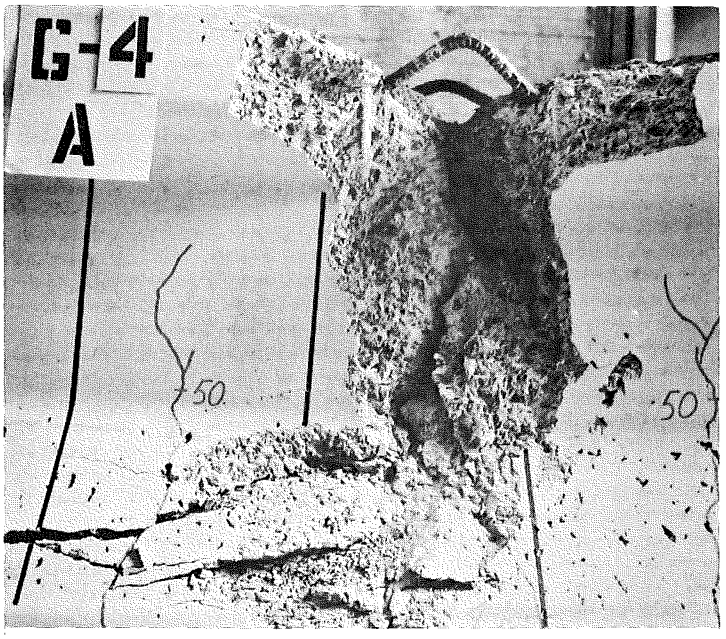

b. View of Flexural Failure Region

Fig. 20 First Test on G-4

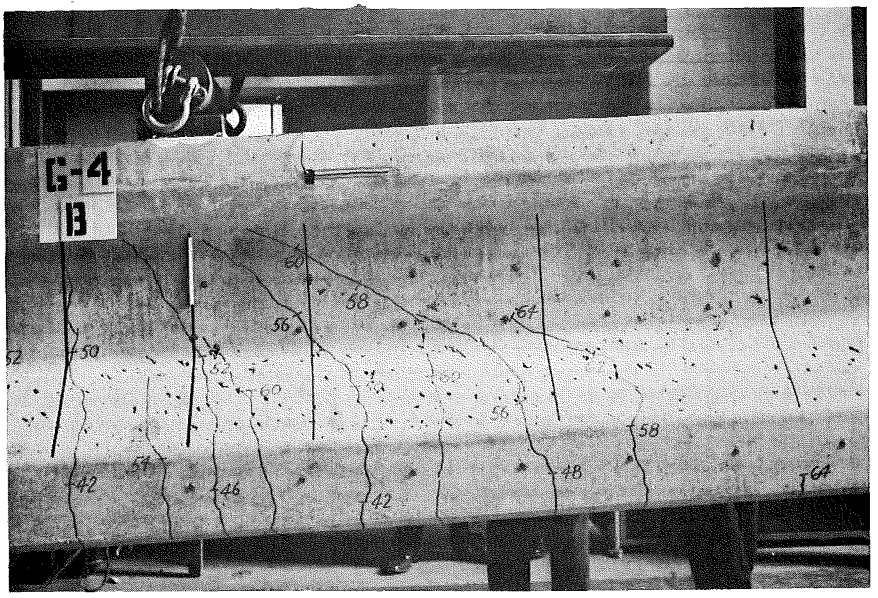

c. Region B Near Load Point

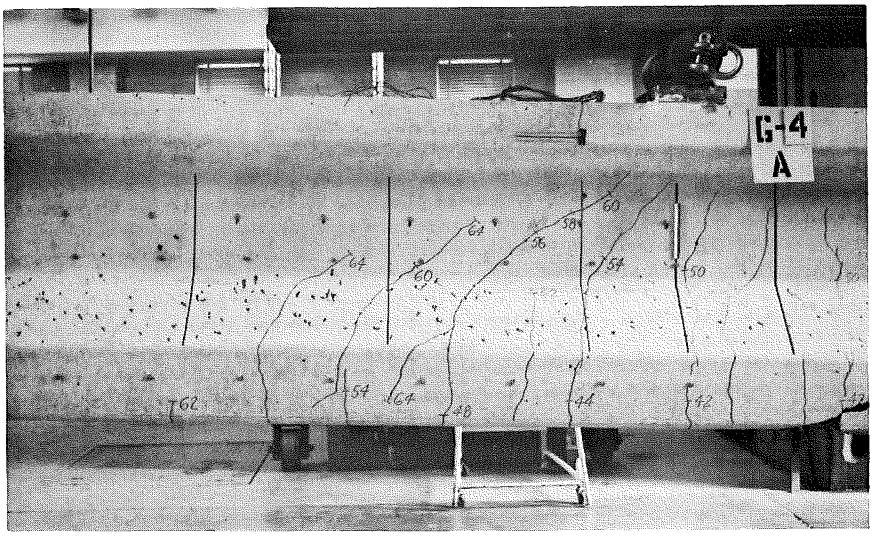

d. Region A Near Load Point

Fig. 20 Cont.

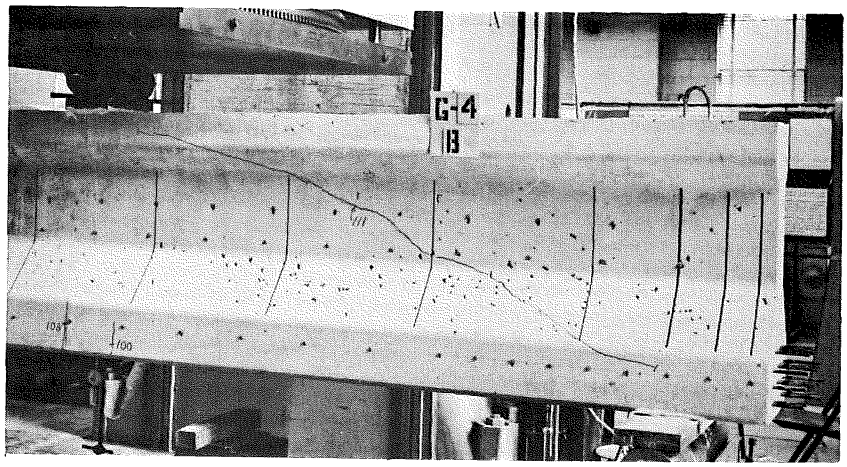

a. Region B after Inclined Cracking

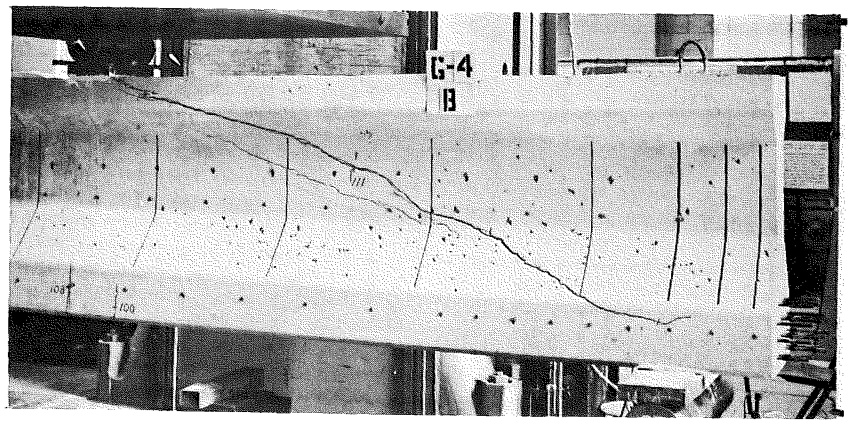

b. Region B after Failure

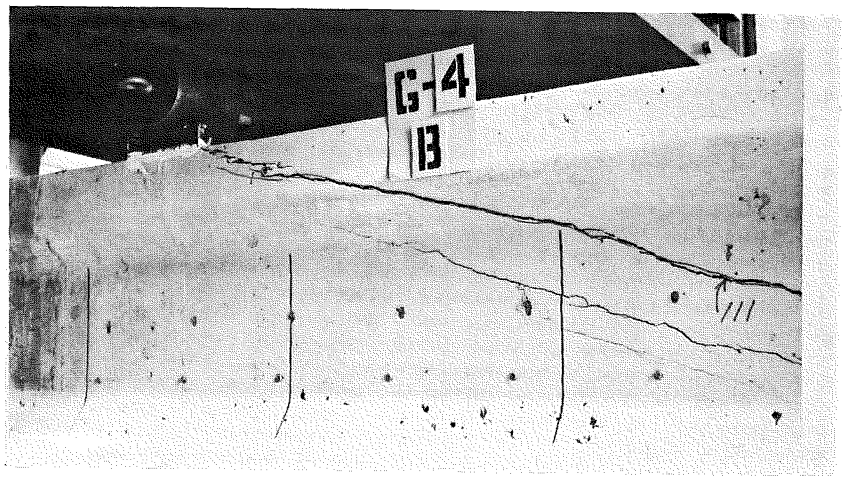

c. View of Failure Region

Fig. 21 Second Test on G-4

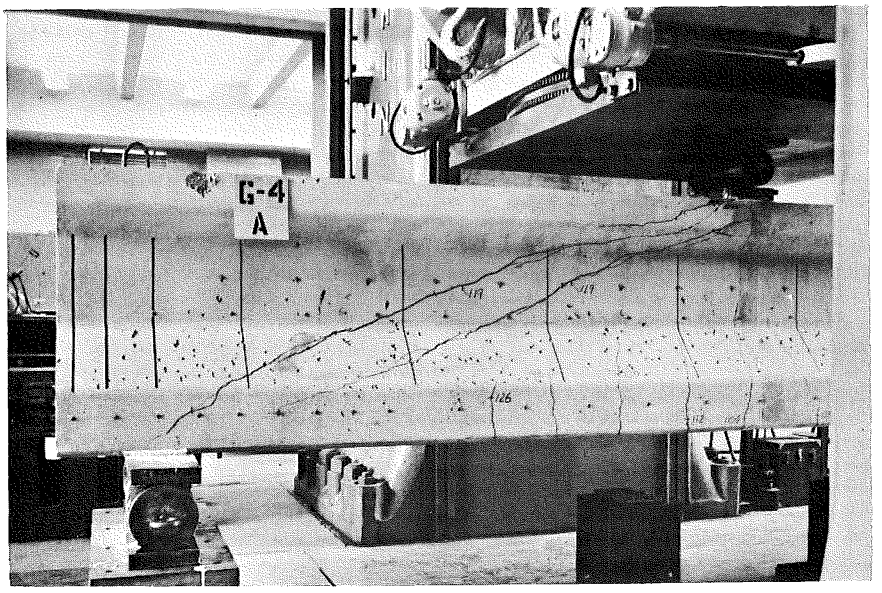

a. Region A after Failure

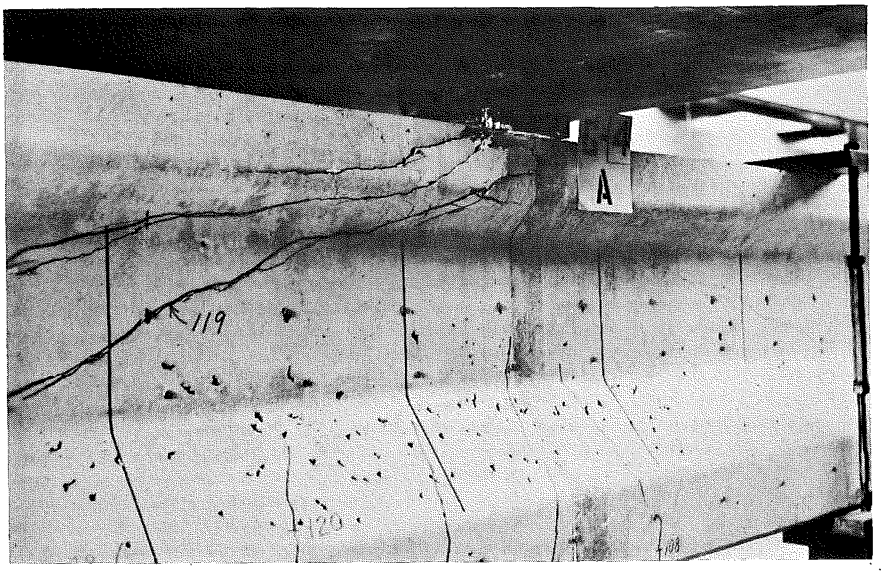

b. Close-up of Failure

Fig. 22 Third Test on G-4

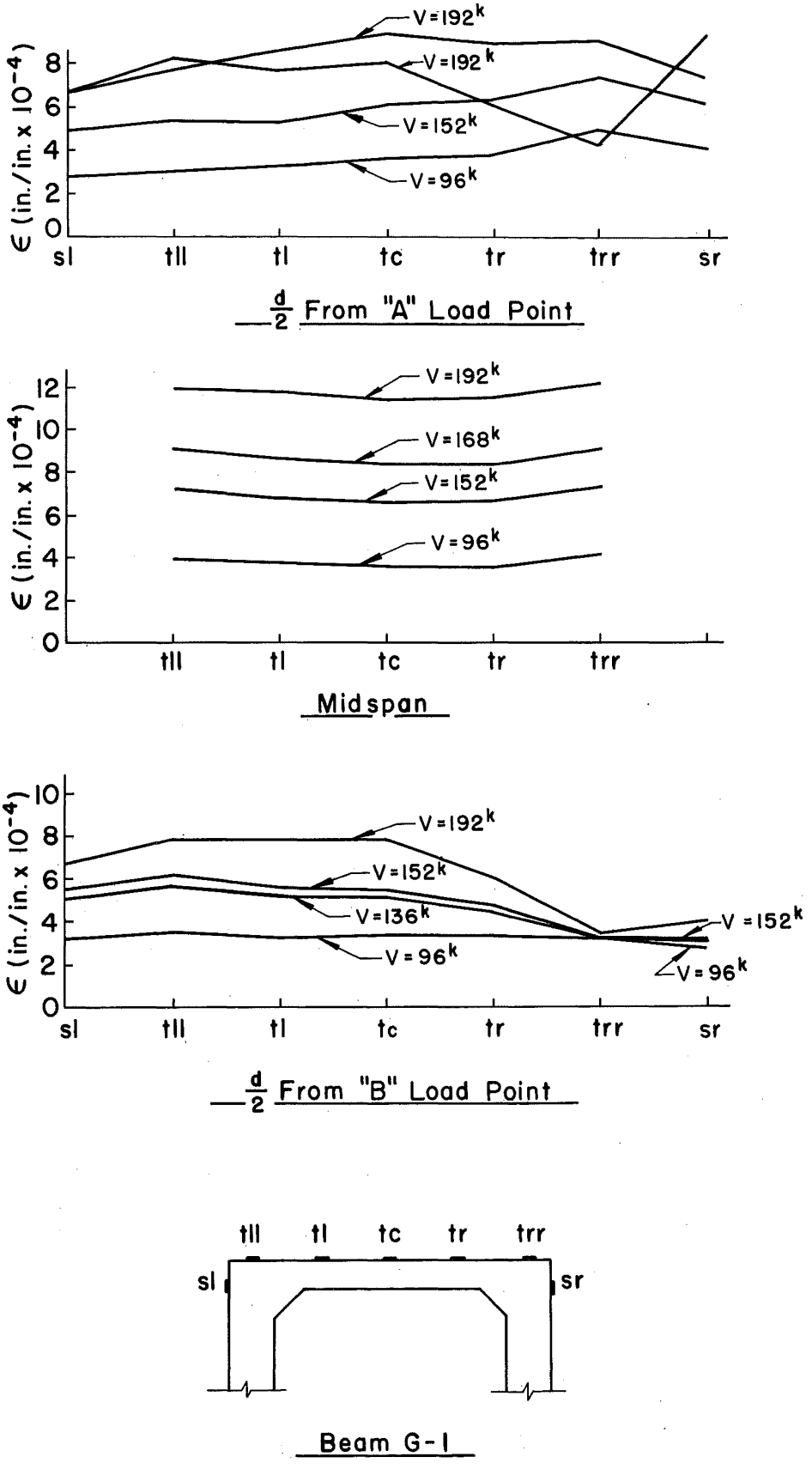

Fig. 23 Strain Measurements during the First Test on G-1

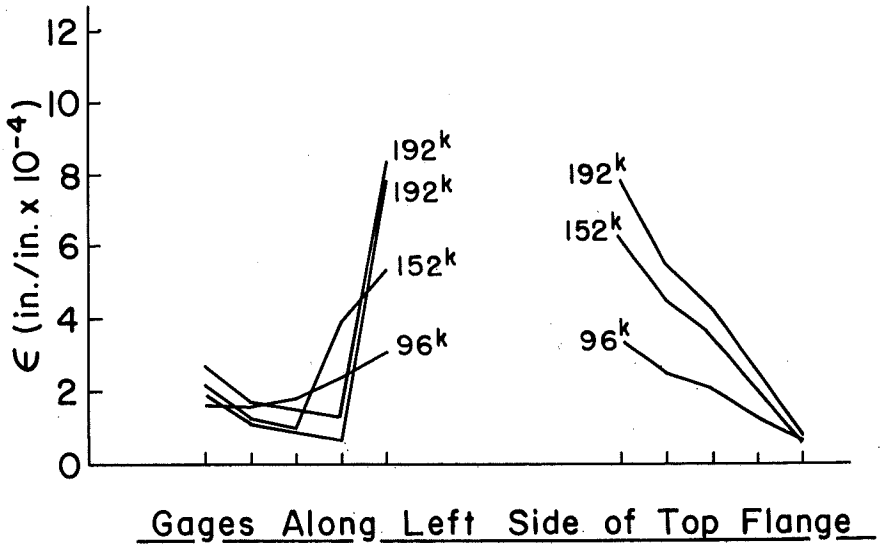

Gages Along Left Side of Top Flange

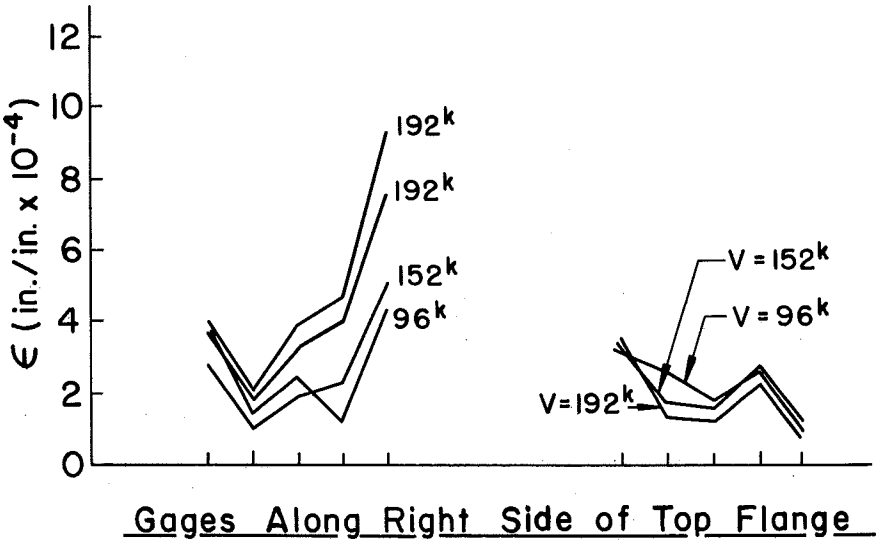

Gages Along Right Side of Top Flange

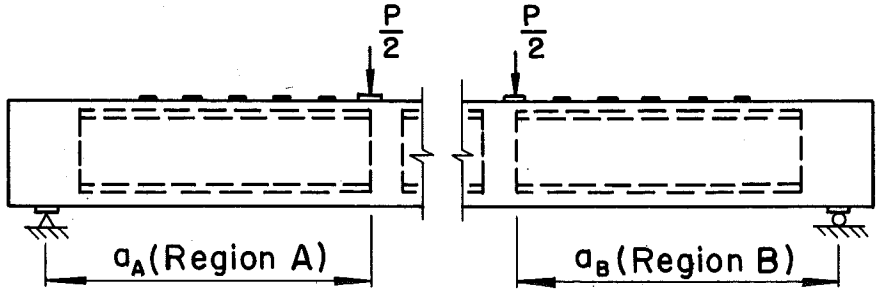

Beam G-1

Fig. 23 Cont.

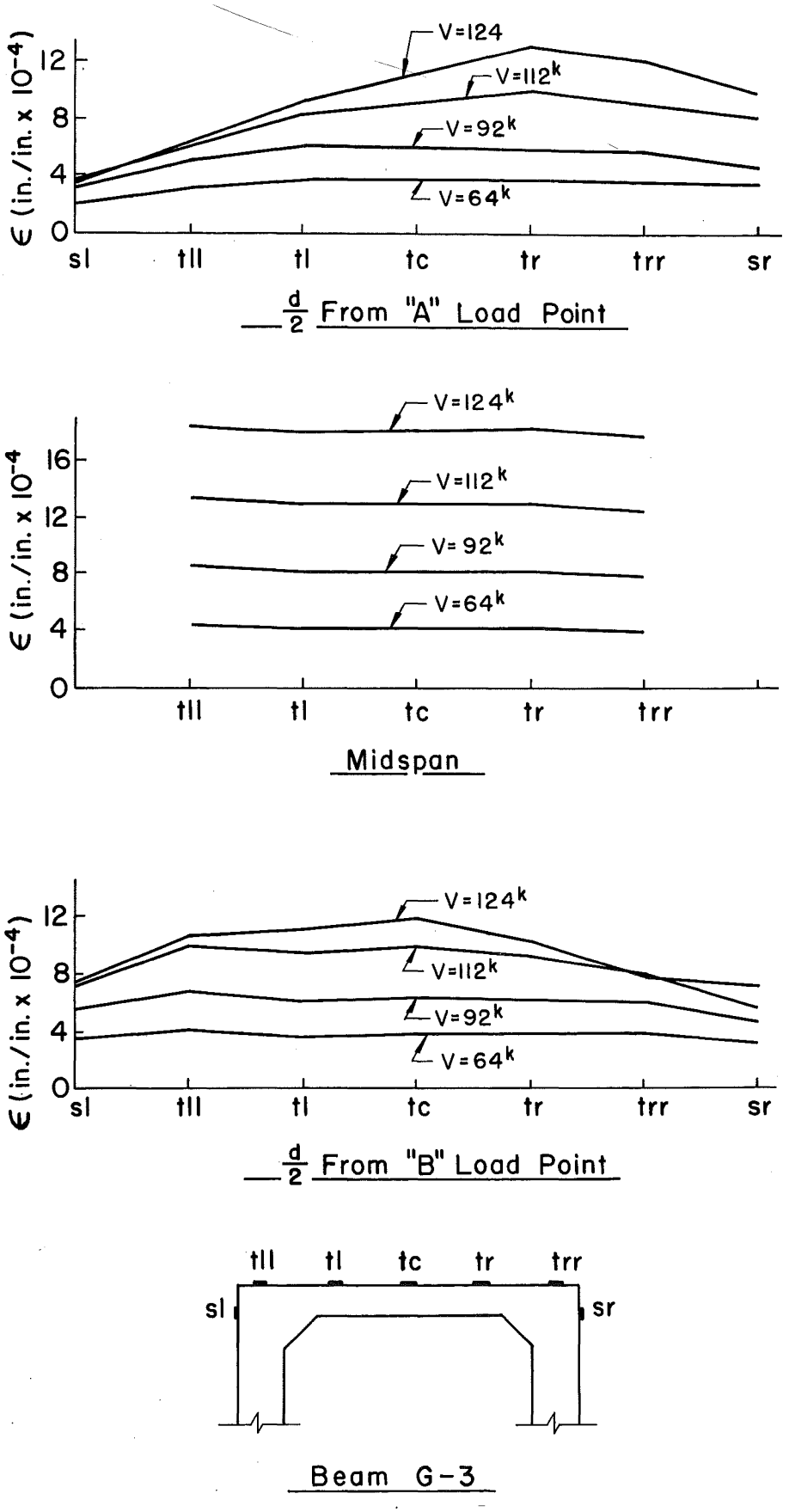

Fig. 24 Strain Measurements during the First Test on G-3

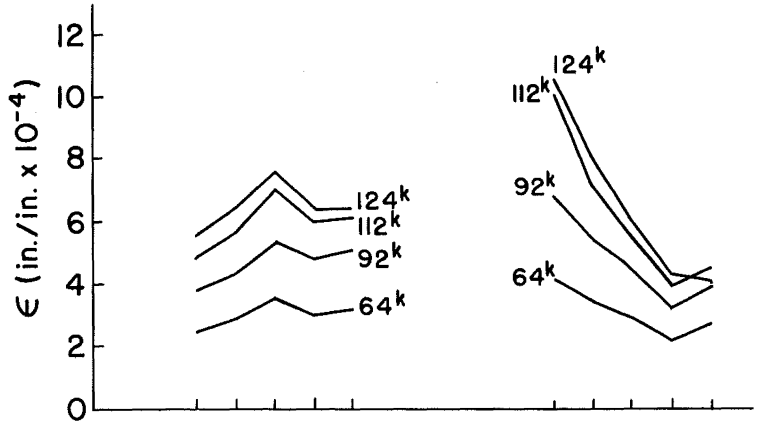

Gages Along Left Side of Top Flange

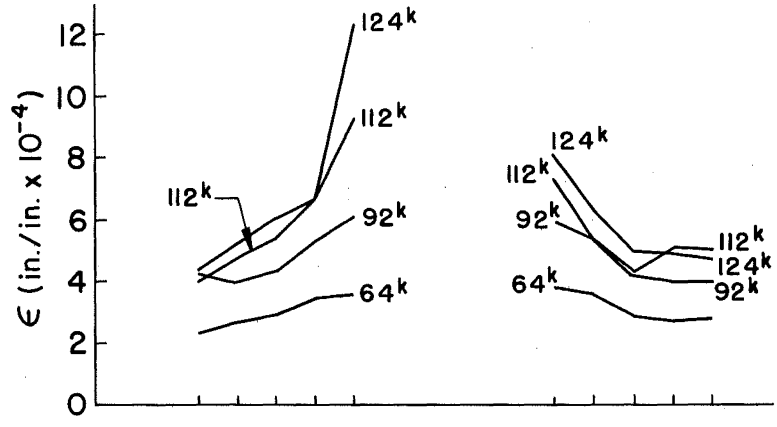

Gages Along Right Side of Top Flange

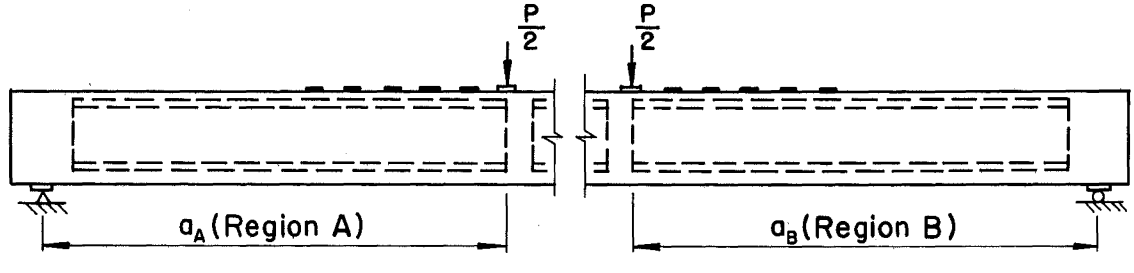

Beam G-3

Fig. 24 Cont.

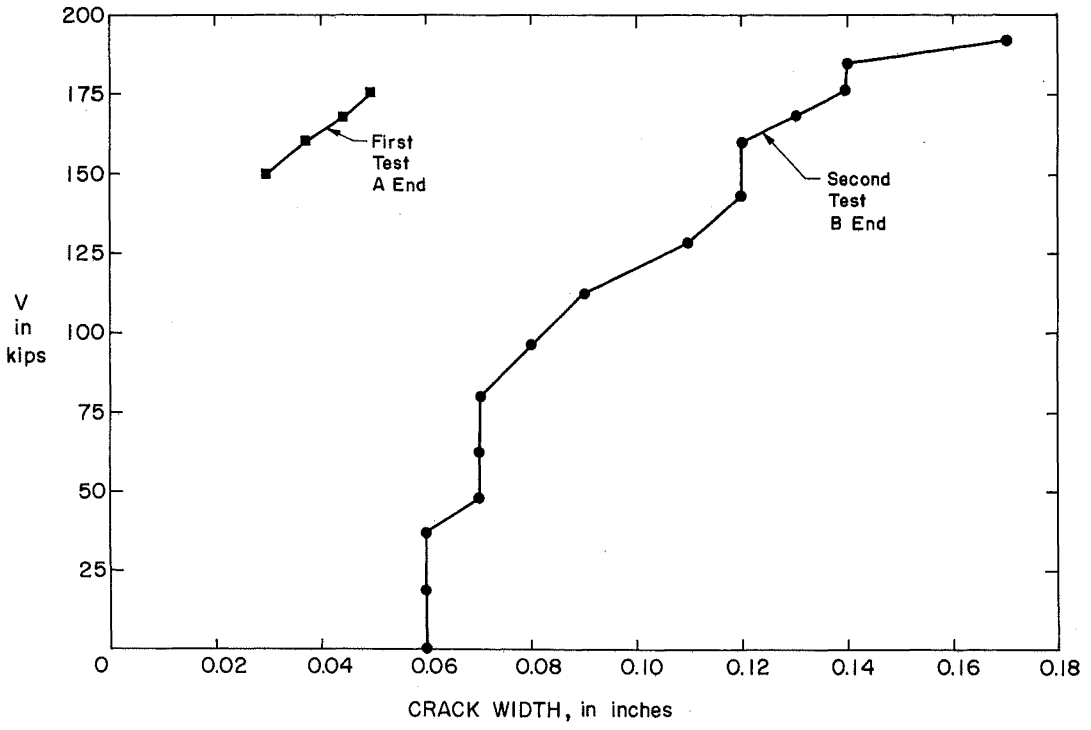

a. First and Second Test on G-1

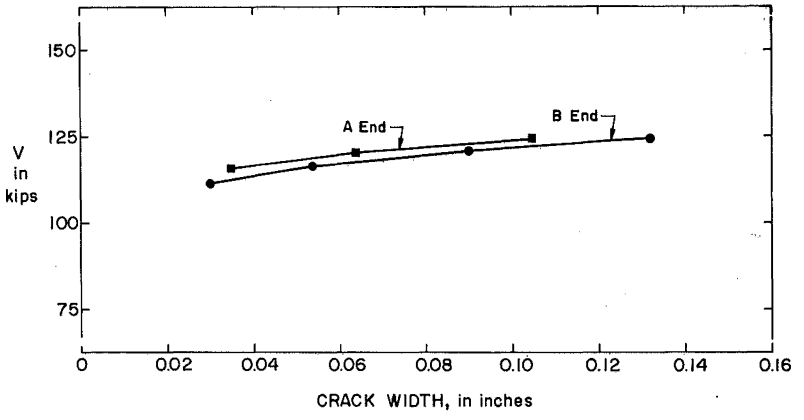

b. First Test on G-3

Fig. 25 Inclined Crack Widths in G-1 and G-3

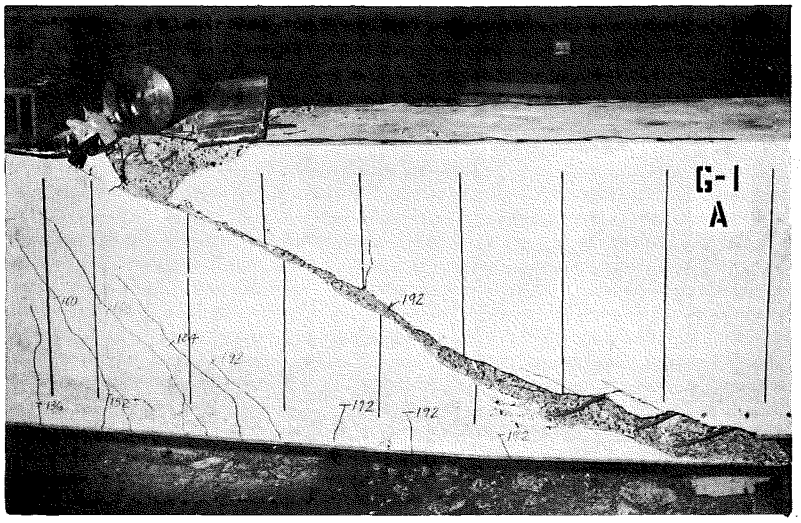

a. Right Side of Region A after Failure

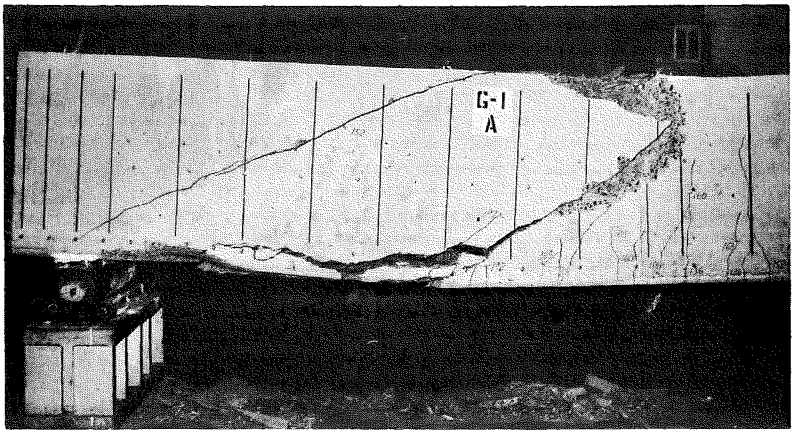

b. Left Side of Region A after Failure

Fig. 26 First Test on G-1

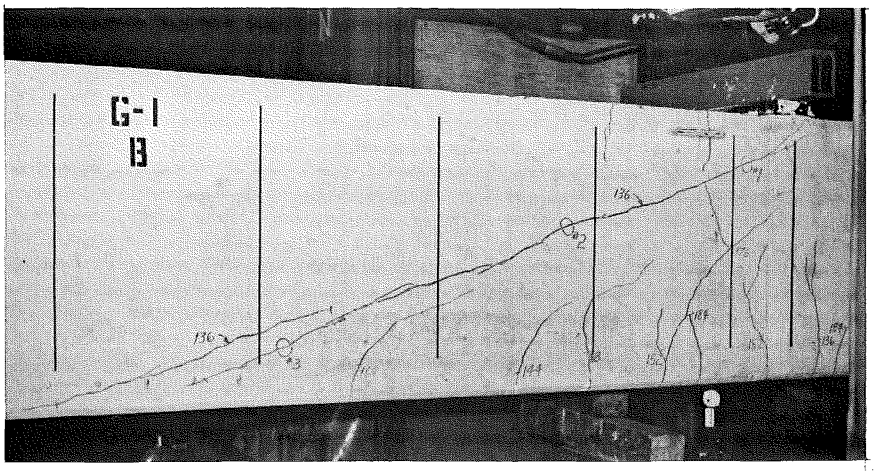

a. Right Side of Region B at Start of Test

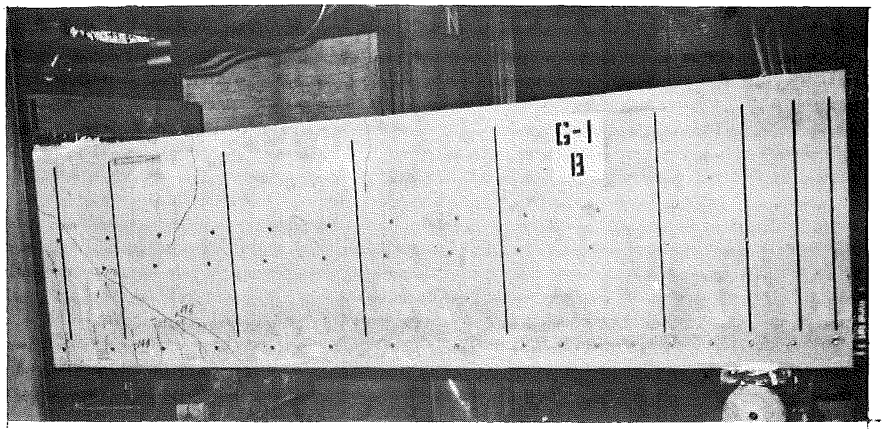

b. Left Side of Region B at Start of Test

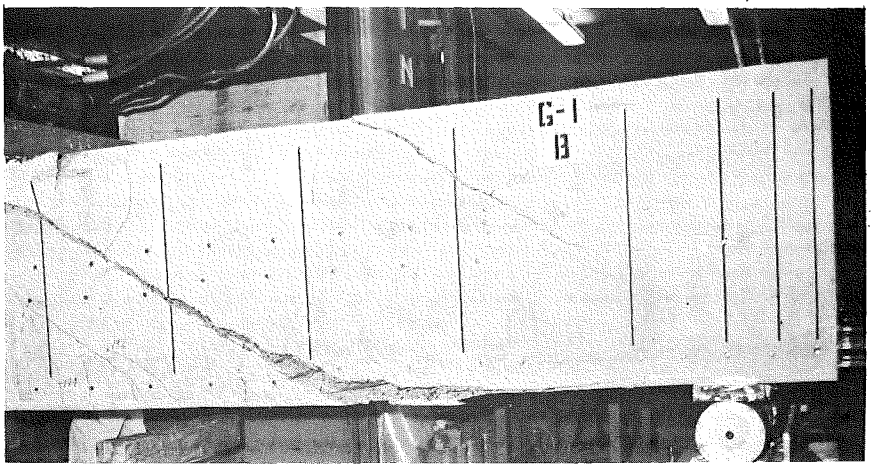

c. Left Side of Region B after Failure

Fig. 27 Second Test on G-1

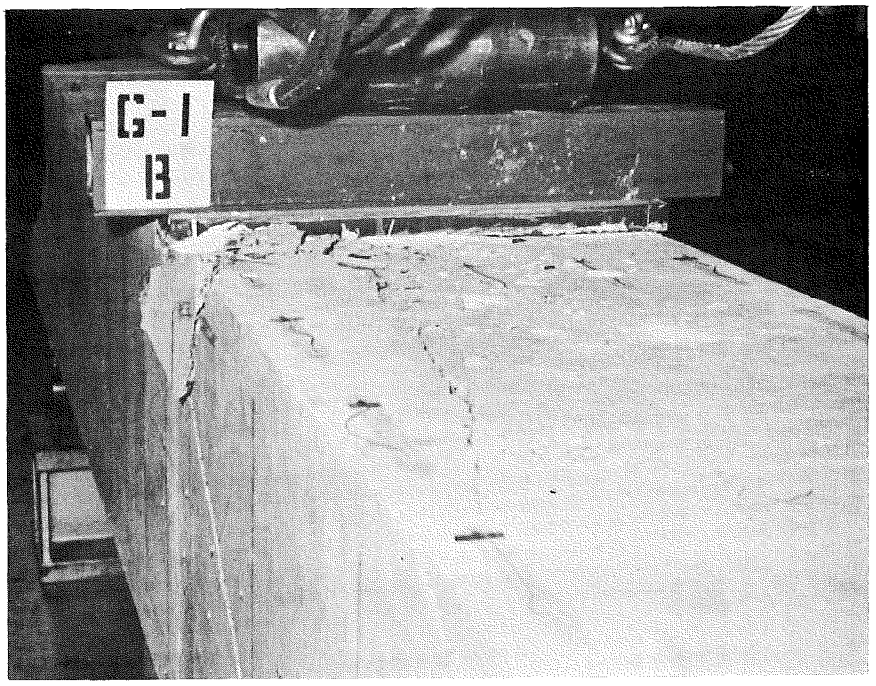

d. Left Side and Top of Region B after Failure

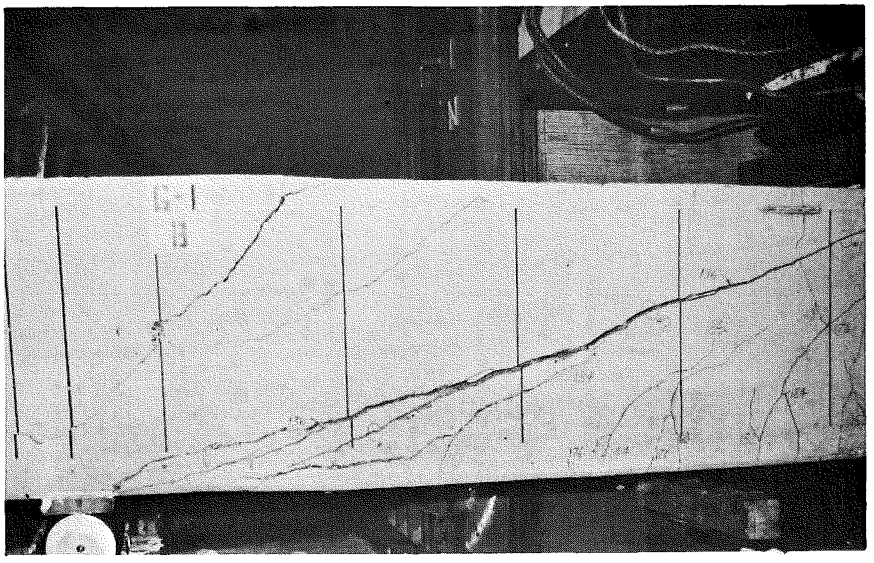

e. Right Side of Region B after Failure

Fig. 27 Cont.

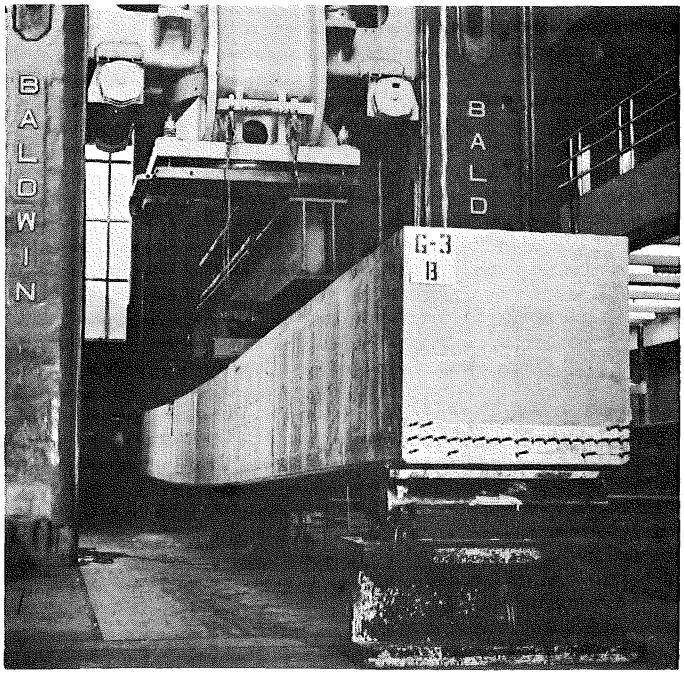

a. During Loading Near Ultimate Capacity

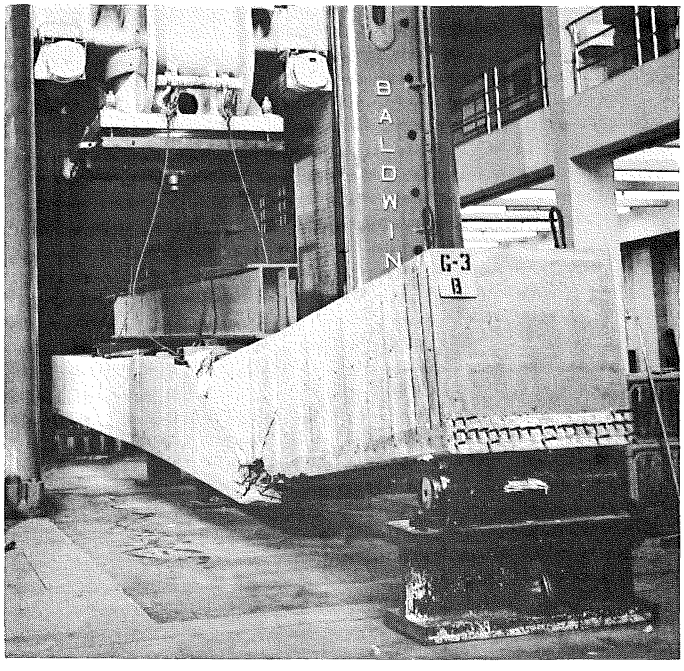

b. After Failure

Fig. 28 First Test on G-3

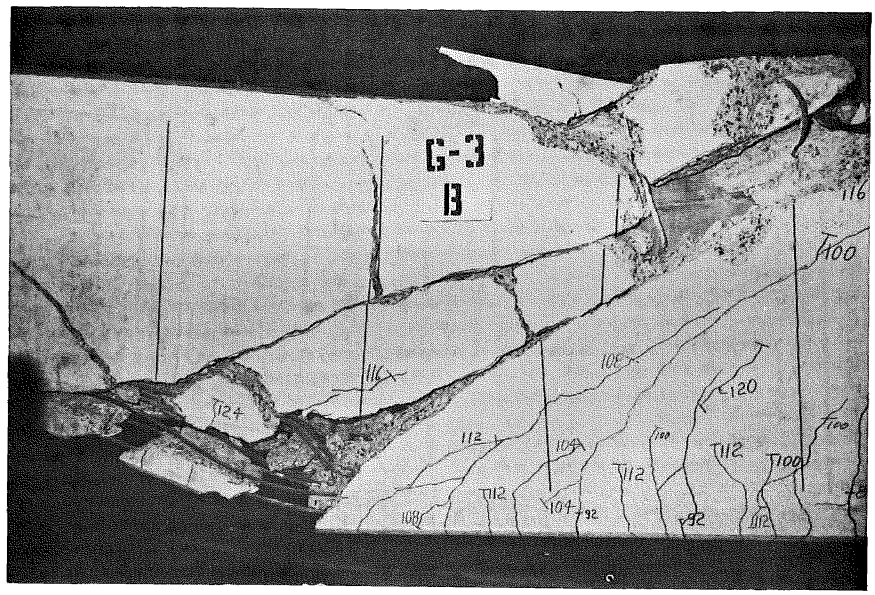

c. Right Side of Region B after Failure

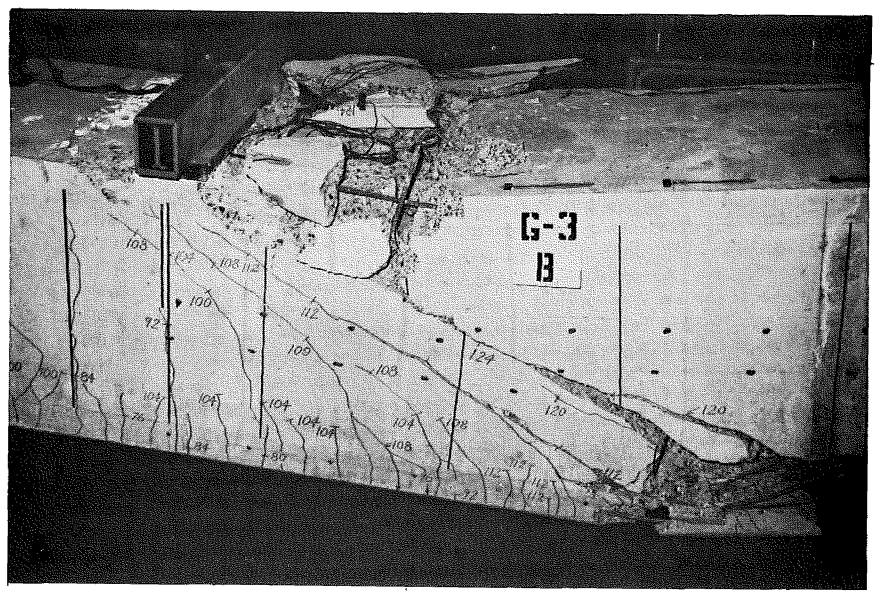

d. Left Side and Top of Region B after Failure

Fig. 28 Cont.

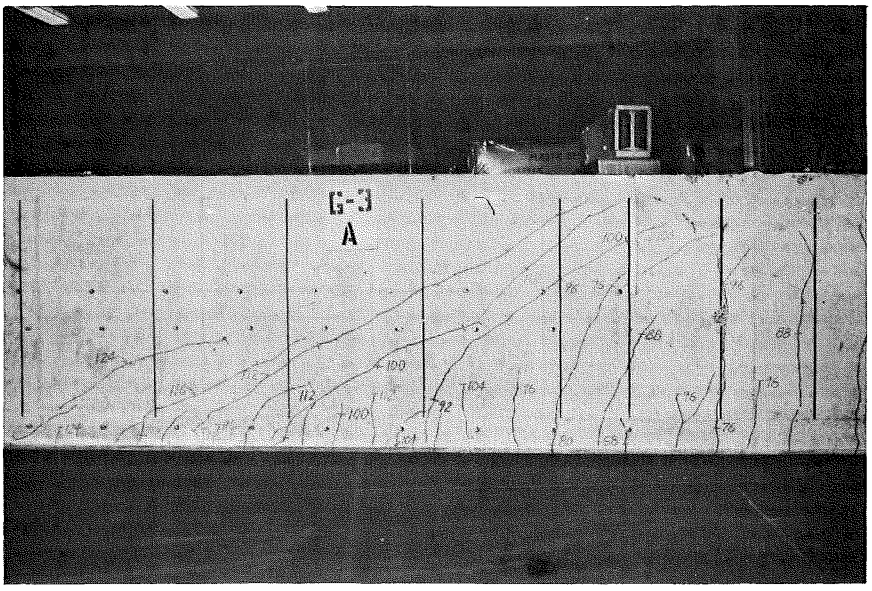

e. Left Side of Region A Near Load Point

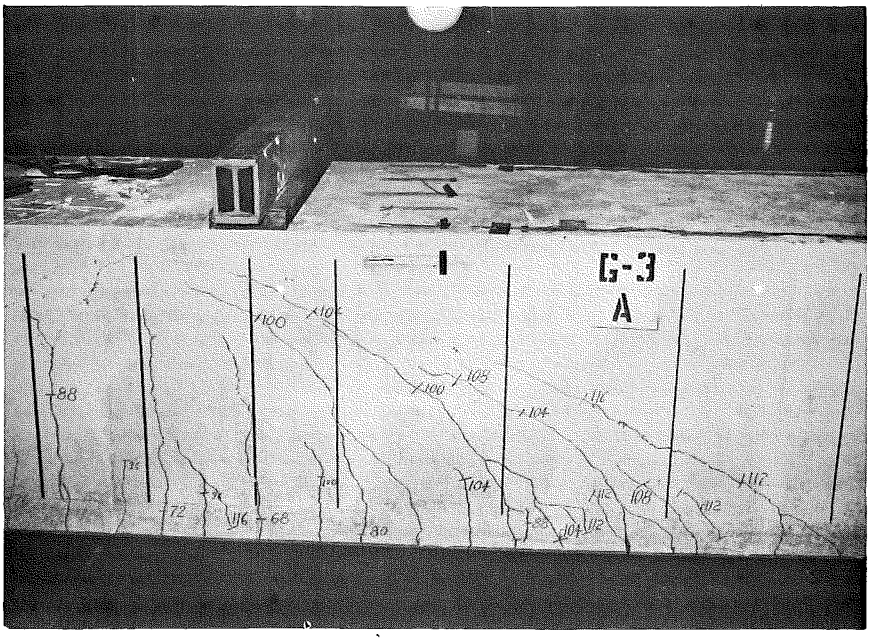

f. Right Side of Region A Near Load Point

Fig. 28 Cont.

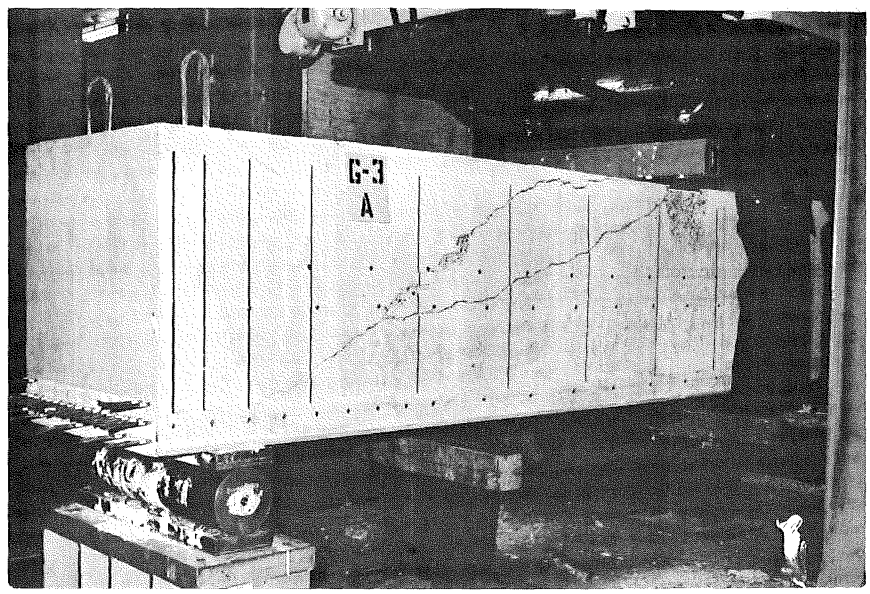

a. Left Side of Region A after Failure

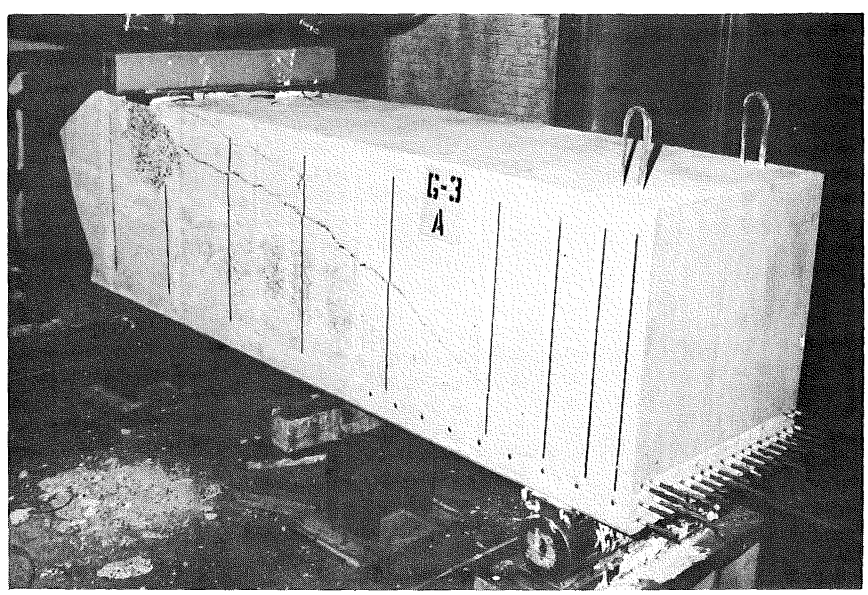

b. Right Side of Region A after Failure

Fig. 29 Second Test on G-3

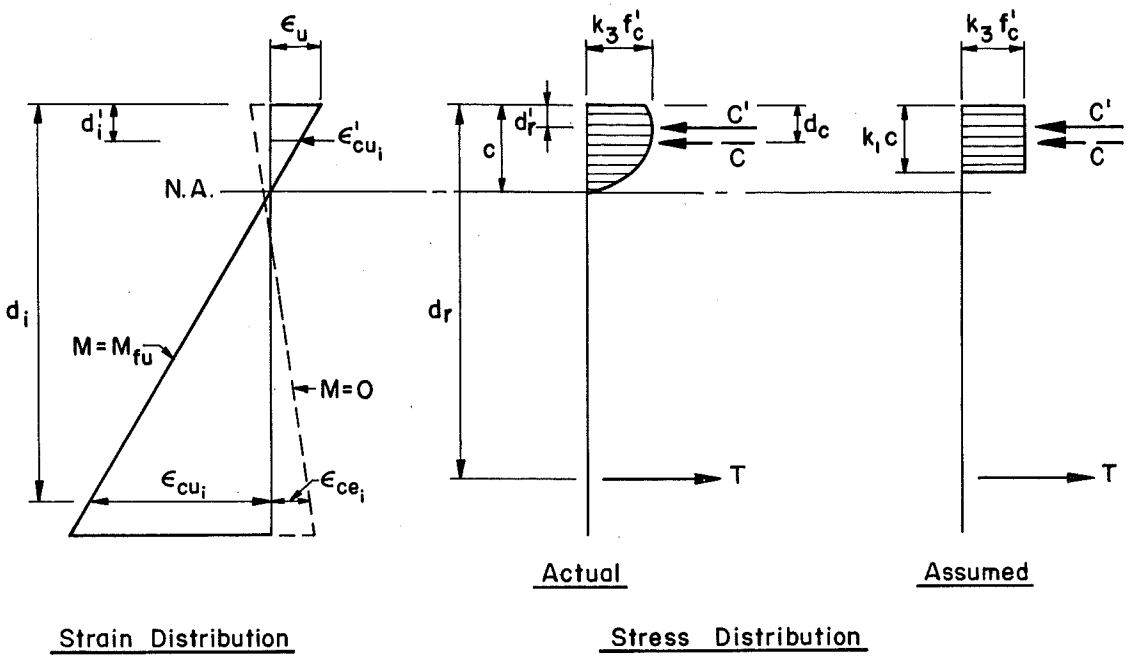

Fig. 30 Strain and Stress Distribution at Flexural Failure

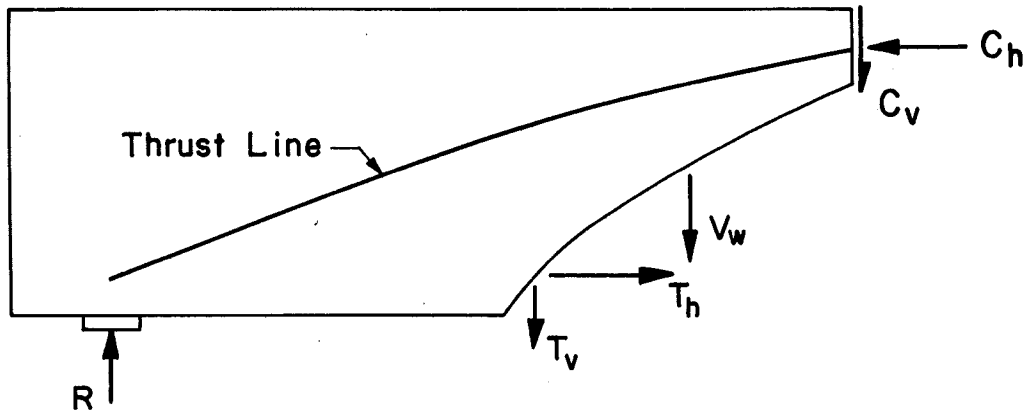

Fig. 31 Forces Acting after Inclined cracking

12. A P P E N D I X

CRACK PATTERNS

(See Section 6.3
for discussion)

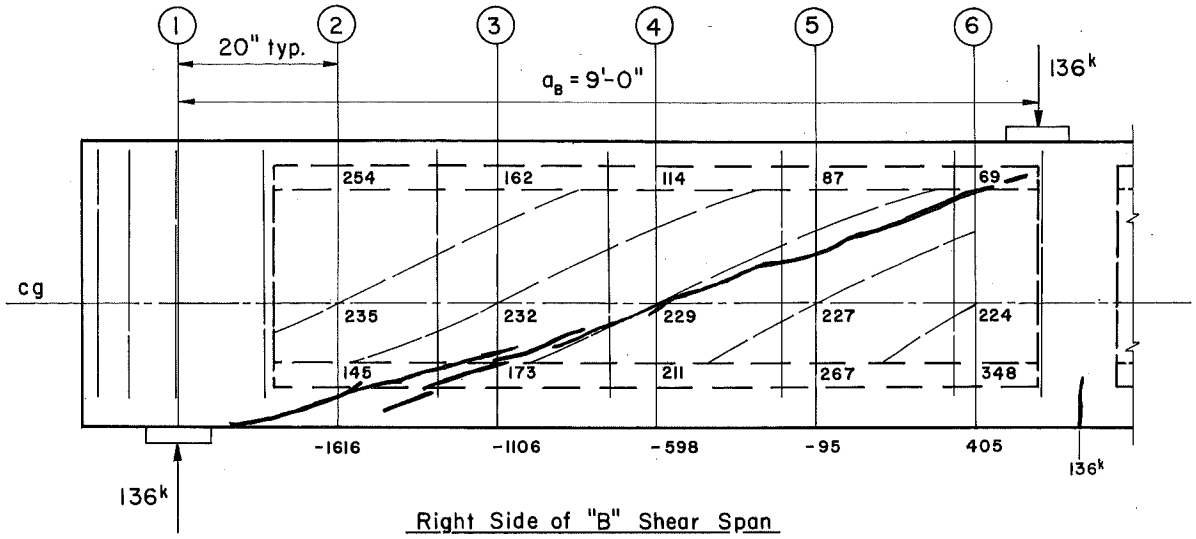

Right Side of "B" Shear Span

Beam G-1 1st. Test

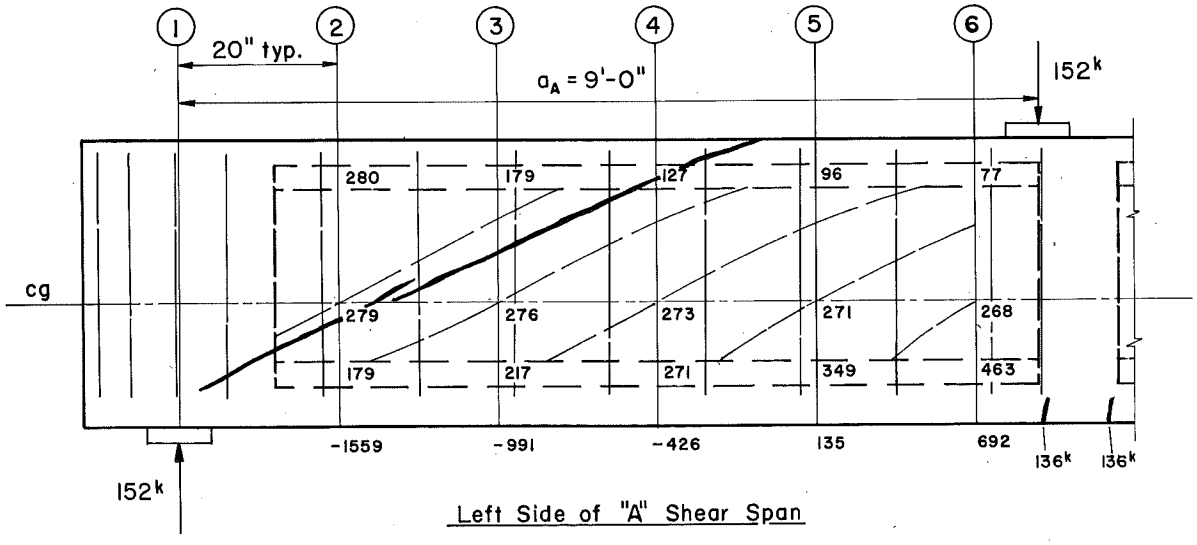

Left Side of "A" Shear Span

Beam G-1 1st. Test

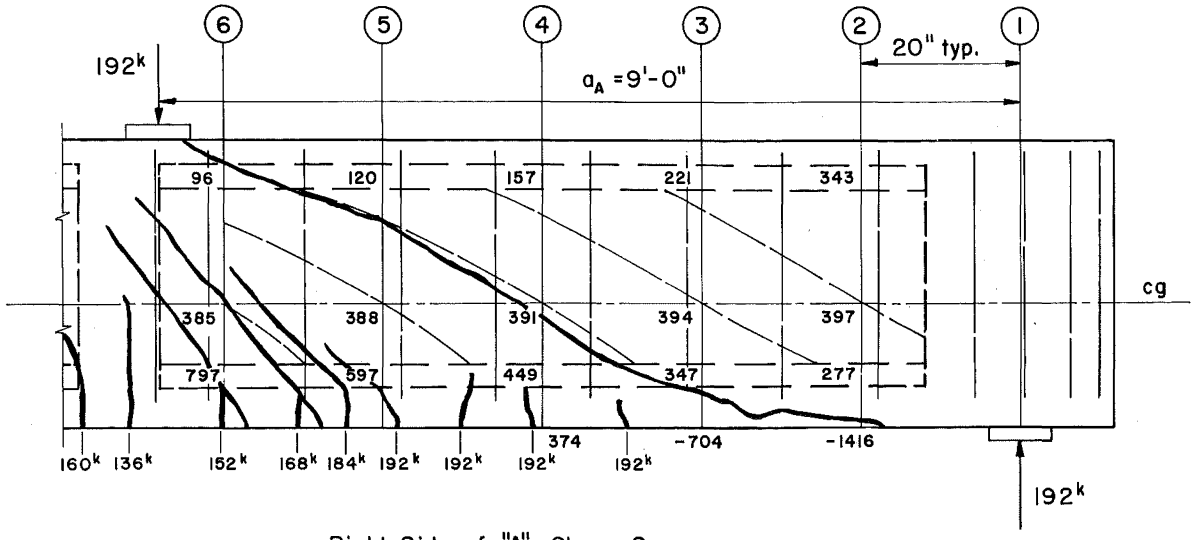

Right Side of "A" Shear Span

Beam G-1 1st. Test

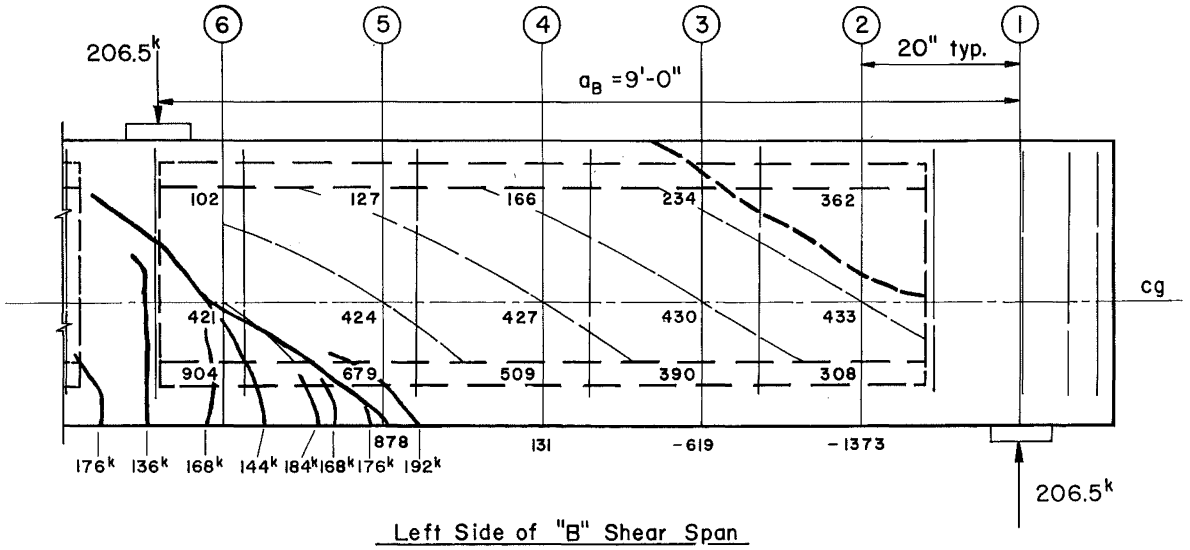

Left Side of "B" Shear Span

Beam G-1 2nd. Test

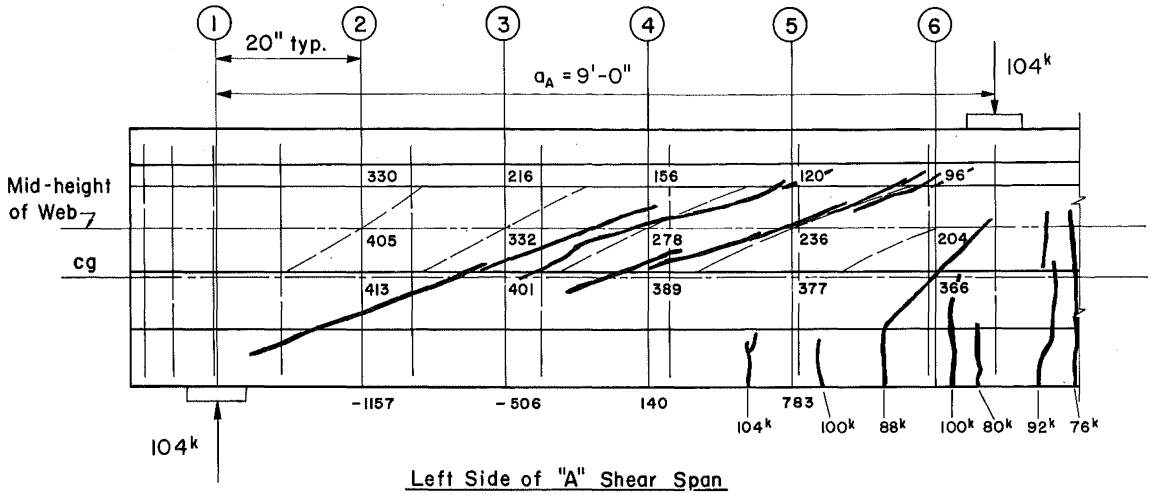

Left Side of "A" Shear Span

Beam G-2 1st. Test

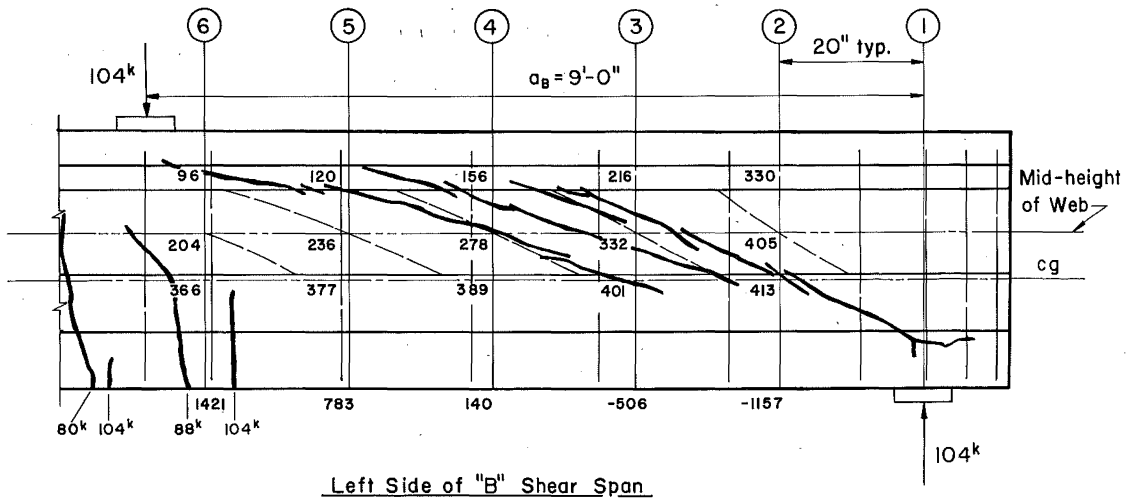

Left Side of "B" Shear Span

Beam G-2 1st. Test

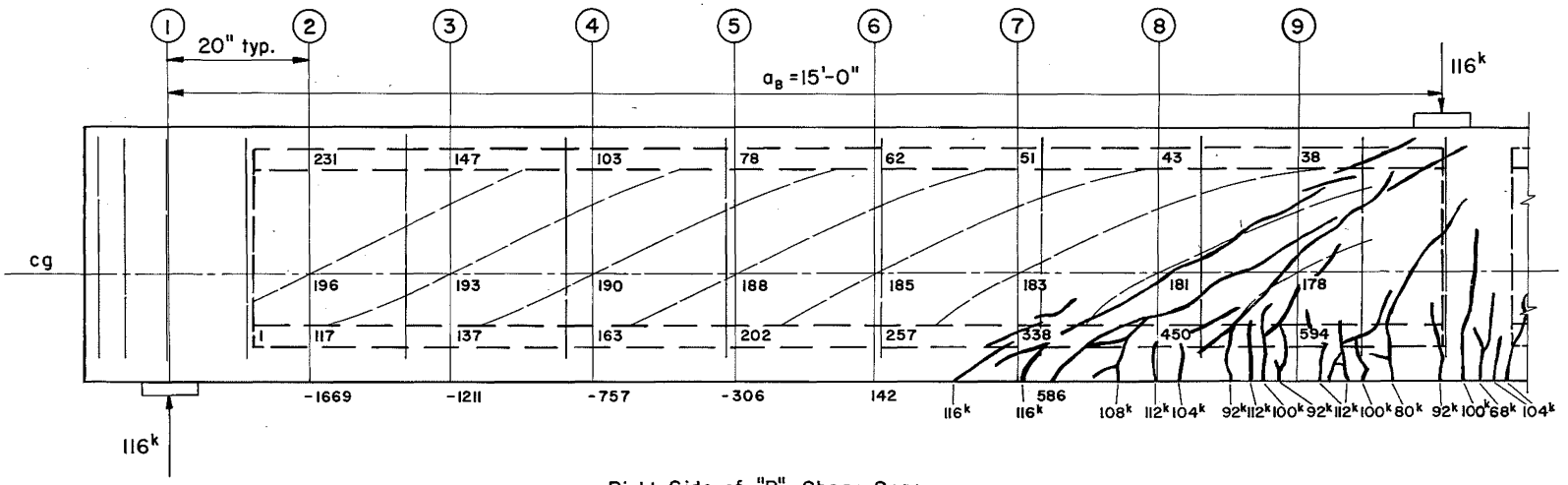

Right Side of "B" Shear Span

Beam G-3 1st. Test

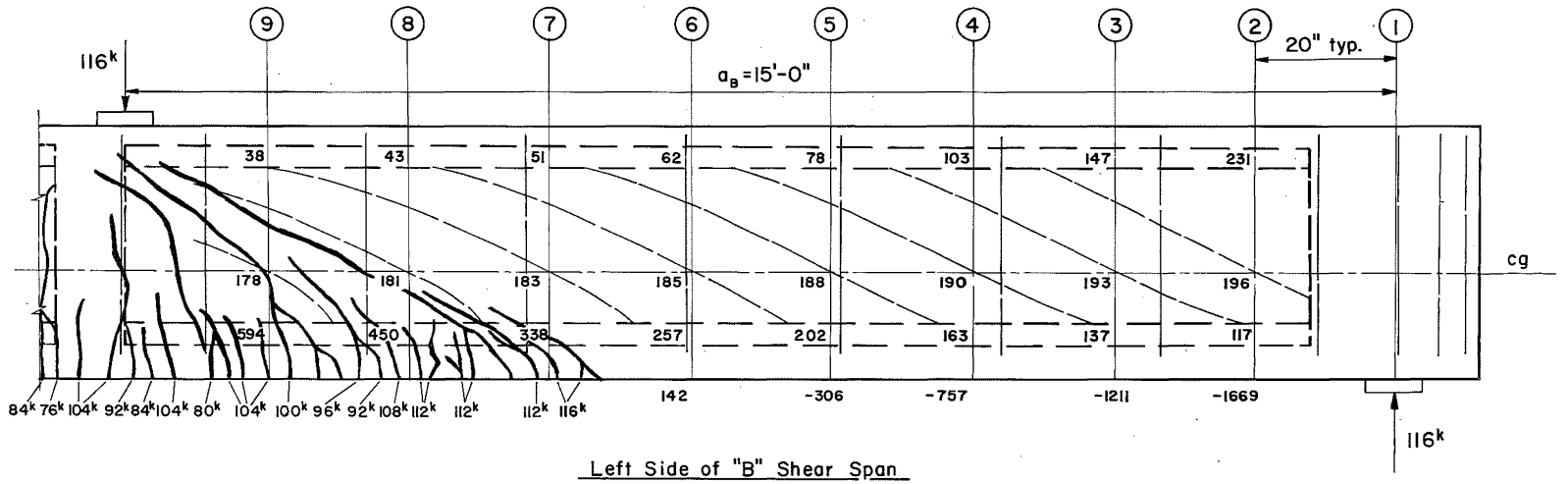

Left Side of "B" Shear Span

Beam G-3 1st. Test

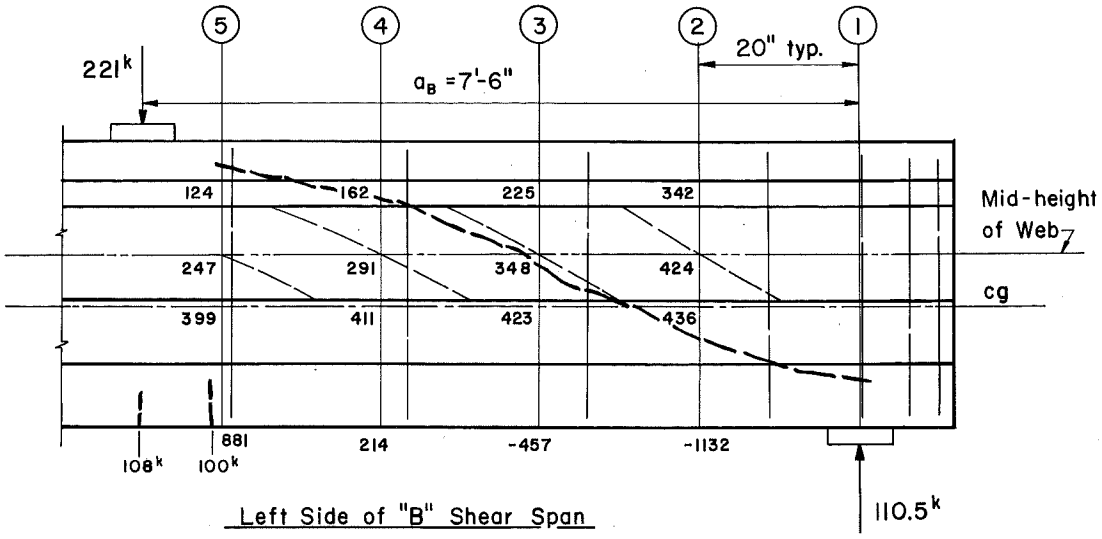

Beam G-4 2nd. Test

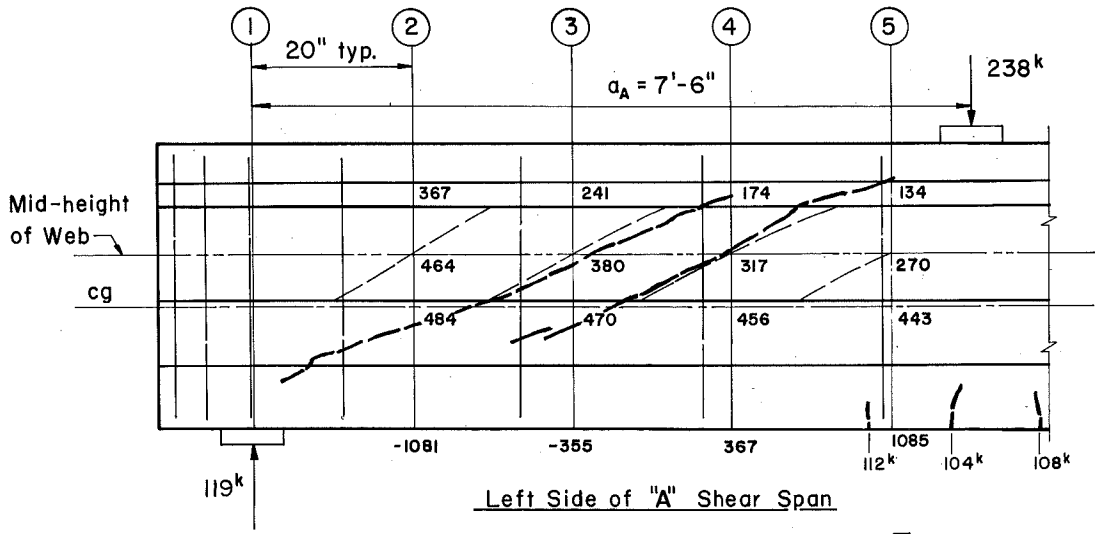

Beam G-4 3rd. Test

13. REFERENCES

1. Knudsen, K. E., Eney, W. J.
   ENDURANCE OF A FULL-SCALE PRETENSIONED CONCRETE BEAM
   Fritz Engineering Laboratory Report 223.5, Lehigh University, April 1953

2. Smislova, A., Roesli, A., Brown, D. H. Jr., Eney, W. J.
   ENDURANCE OF A FULL-SCALE POST-TENSIONED CONCRETE MEMBER
   Fritz Engineering Laboratory Report No. 223.6, Lehigh University, May 1954

3. Dinsmore, G. A., Deutsch, P. L.
   ANCHORAGE CHARACTERISTICS OF STRAND IN PRETENSIONED PRESTRESSED CONCRETE
   Fritz Engineering Laboratory Report No. 223.16, Lehigh University, July 1957

4. Dinsmore, G. A., Deutsch, P. L., Montemayor, J. L.
   ANCHORAGE AND BOND IN PRETENSIONED PRESTRESSED CONCRETE MEMBERS
   Fritz Engineering Laboratory Report No. 223.19, Lehigh University, December 1958

5. Ekberg, C. E. Jr., Walther, R. E., Slutter, R. G.
   FATIGUE RESISTANCE OF PRESTRESSED CONCRETE BEAMS IN BENDING
   Fritz Engineering Laboratory Report No. 223.15, Lehigh University, April 1957

6. Ekberg, C. E., Jr.
   REPORT ON 70-FT BEAM TEST FOR CONCRETE PRODUCTS COMPANY OF AMERICA
   Fritz Engineering Laboratory, Lehigh University, Sept. 1956

7. Lane, Richard E., Ekberg, C. E. Jr.
   REPEATED LOAD TESTS ON 7-WIRE PRESTRESSING STRANDS
   Fritz Engineering Laboratory Report No. 223.21, Lehigh University, January 1959

8. Warner, R. F., and Hulsbos, C. L.
   PROBABLE FATIGUE LIFE OF PRESTRESSED CONCRETE FLEXURAL MEMBERS
   Fritz Engineering Laboratory Report No. 223.24A, Lehigh University, July 1962

9. Ople, F. S. Jr., Hulsbos, C. L.
   PROBABLE LIFE OF PRESTRESSED BEAMS AS LIMITED BY CONCRETE FATIGUE
   Fritz Engineering Laboratory Report No. 223.26A, Lehigh University, October 1963

10. Walther, R. E.
THE ULTIMATE STRENGTH OF PRESTRESSED AND CONVENTIONALLY REINFORCED CONCRETE UNDER THE COMBINED ACTION OF MOMENT AND SHEAR
Fritz Engineering Laboratory Report No. 223.17, Lehigh University, October 1957

11. Walther, R. E., Warner, R. F.
ULTIMATE STRENGTH TESTS OF PRESTRESSED AND CONVENTIONALLY REINFORCED CONCRETE BEAMS IN COMBINED BENDING AND SHEAR
Fritz Engineering Laboratory Report No. 223.18, Lehigh University, Sept. 1958

12. McClarnon, F. M., Wakabayashi, M., Ekberg, C. E. Jr.
FURTHER INVESTIGATION INTO THE SHEAR STRENGTH OF PRESTRESSED CONCRETE BEAMS WITHOUT WEB REINFORCEMENT
Fritz Engineering Laboratory Report No. 223.22, Lehigh University, January 1962

13. Hanson, J. M., Hulsbos, C. L.
OVERLOAD BEHAVIOR OF PRESTRESSED CONCRETE BEAMS WITH WEB REINFORCEMENT
Fritz Engineering Laboratory Report No. 223.25, Lehigh University, February 1963

14. Hanson, J. M., Hulsbos, C. L.
OVERLOAD BEHAVIOR OF PRETENSIONED PRESTRESSED CONCRETE I-BEAMS WITH WEB REINFORCEMENT
Highway Research Record Number 76, Design - Bridges and Structures, 1965, pp. 1-31

15. Hanson, J. M.
ULTIMATE SHEAR STRENGTH OF PRESTRESSED CONCRETE BEAMS WITH WEB REINFORCEMENT
Ph.D Thesis, Lehigh University, 1964

16. Hanson, J. M., Hulsbos, C. L.
ULTIMATE SHEAR STRENGTH OF PRESTRESSED CONCRETE BEAMS WITH WEB REINFORCEMENT
Fritz Engineering Laboratory Report No. 223.27, Lehigh University, May 1965

17. Hanson, J. M., Hulsbos, C. L.
ULTIMATE SHEAR TESTS OF PRESTRESSED CONCRETE I-BEAMS UNDER CONCENTRATED AND UNIFORM LOADINGS
Journal of the Prestressed Concrete Institute, Vol. 9, No. 3, June 1964, pp. 15-28

18. Zwoyer, E. M., Siess, C. P.
ULTIMATE STRENGTH IN SHEAR OF SIMPLY-SUPPORTED PRESTRESSED CONCRETE BEAMS WITHOUT WEB REINFORCEMENT
Journal of the American Concrete Institute, Proceedings V. 26, October 1954, pp. 181-200

19. Sozen, M. A., Zwoyer, E. M., Siess, C. P.
INVESTIGATION OF PRESTRESSED CONCRETE FOR HIGHWAY BRIDGES, PART I: STRENGTH IN SHEAR OF BEAMS WITHOUT WEB REINFORCEMENT
Bulletin No. 452, University of Illinois Engineering Experiment Station, April 1959

20. Hernandez, G.
STRENGTH OF PRESTRESSED CONCRETE BEAMS WITH WEB REINFORCEMENT
Ph.D Thesis, University of Illinois, May 1958

21. MacGregor, J. G.
STRENGTH AND BEHAVIOR OF PRESTRESSED CONCRETE BEAMS WITH WEB REINFORCEMENT
Ph.D Thesis, University of Illinois, August 1960

22. MacGregor, J. G., Sozen, M. A., Siess, C. P.
EFFECT OF DRAPED REINFORCEMENT ON BEHAVIOR OF PRESTRESSED CONCRETE BEAMS
Journal of the American Concrete Institute, Proceedings V. 57, December 1960, pp. 649-677

23. Hernandez, G., Sozen, M. A., Siess, C. P.
STRENGTH IN SHEAR OF PRESTRESSED CONCRETE BEAMS WITH WEB REINFORCEMENT
Presented at the Convention of the American Society of Civil Engineers, New Orleans, March 1960

24. Mattock, A. H., Kaar, P. H.
PRECAST-PRESTRESSED CONCRETE BRIDGES. 4. SHEAR TESTS OF CONTINUOUS GIRDERS
Journal of the PCA Research and Development Laboratories, V. 3, No. 1, January 1961, pp. 19-46

25. Commonwealth of Pennsylvania, Department of Highways, Bridge Unit
STANDARDS FOR PRESTRESSED CONCRETE BRIDGES
September 1960

26. Mattock, A. H., Kriz, L. S., Hognestad, E.
RECTANGULAR CONCRETE STRESS DISTRIBUTION IN ULTIMATE STRENGTH DESIGN
Journal of the American Concrete Institute, Proceedings, V. 57, No. 8, February 1961, pp. 875-928